Functional Molecular Liquids for Singlet Fission and Spintronics

by

Shashani Inesha Fernando Thammitage

A Thesis submitted to the Faculty of Graduate Studies of

The University of Manitoba

in partial fulfilment of the requirements of the degree of

MASTER OF SCIENCE

Department of Chemistry

University of Manitoba

Winnipeg, Manitoba, Canada

Abstract

Functional molecular liquids (FMLs) are an emerging field in organic research due to their distinct advantages over solid materials such as ease of handling, processability, high thermal stability, flexibility and their versatile optoelectronic properties. This thesis describes the synthesis and potential of liquid organic chromophores in two novel concepts in synthetic organic chemistry: singlet fission in FMLs and FMLs for organic spintronics.

Chapter 01 gives a fundamental overview on FMLs including their key properties, their potential applications and a comprehensive exploration of the strategies employed to achieve liquefaction. **Chapter 02** presents the role of liquidity in singlet fission from the motivation of answering the Cristopher J. Bardeen's question regarding the enhanced singlet fission efficiency of molten rubrene. The design principles, synthesis strategies and characterization of rubrene derivatives are explained in this chapter up to the rubrene in solid state unsubstituted intermediates and up to the stage of propargyl alcohols in novel substituted liquid rubrene derivatives. This chapter explains the design principles, synthesis strategies and characterization of rubrene derivatives starting from solid-state unsubstituted intermediates and progressing to the formation of novel substituted liquid rubrene derivatives, specifically up to the stage involving propargyl alcohols. **Chapter 03** extends the concept of FMLs into the organic spintronics by exploring how liquidity impacts the spin transport and stability of radicals and merge the two concepts inspired by the recent studies of Takahashi Nakanishi's spin hydrodynamic

generation. The chapter explains the synthesis of stable, solid state organic radicals with propensity to liquefaction is described in this chapter.

Overall, this thesis demonstrates that introducing liquidity into functional organic materials can be used to control electronic, photophysical and spin dependent properties which opens new pathways in next generation of optoelectronic, photovoltaics and spintronic devices.

Acknowledgement

I am grateful to my supervisor, Dr. Joshua Walsh, for his support, patience and mentorship over the past two years. His calm presence and thoughtful guidance made even more difficult moments manageable. His guidance from the beginning of my journey in synthetic chemistry has deepened my passion for synthesis. Then I would like to thank my supervisory committee Dr. Rebecca Davis and Dr. David Herbert for their support. A special thank goes to my friend, Samuel Awuku. I am so grateful to work with you in the Walsh Lab.

I would like to thank my loving husband Eranga Perera, for his constant support, care and encouragement. A special thank to ELF, my furry friend, who kept company during thesis writing. Finally, my loving parents, Paul and Neela Fernando for their love and belief in me.

Table of Contents

Chapter 03 – Organic Spintronics and Functional Molecular Liquids

List of Figures

List of Schemes

List of Tables

List of Abbreviations

AcOH	Acetic acid
BDE	bond dissociation energy
b.p.	boiling point
BPA	9,10-bis(phenylethynyl)anthracene
C	Celsius
cP	Centipoise
DDQ	2,3-Dichloro-5,6-dicyano-1,4-benzaquinone
DMF	Dimethylformamide
DPA	9,10-diphenylanthracene
DPT	5,12-diphenyltetracene
E	Energy
EET	excitation energy transfer
EHC	9-(2-ethylhexyl)carbazole
EPR	electron paramagnetic resonance
EQE	External Quantum Efficiency
ESI-MS	Electrospray ionization mass spectrometry
Et_2O	Diethyl ether
EUC	Europium Complex
F	Fluorescence
FML	Functional Molecular Liquids
GMR	Giant magnetoresistance

Ga	Gallium
Hg	Mercury
HOMO	highest occupied molecular orbital
h	Hours
ITO	Indium Tin Oxide
ISC	Inter System Crossing
IC	Internal Conversion
LUMO	lowest unoccupied molecular orbital
T_m	Melting temperature
Hg	Mercury
nm	nanometers
NBS	N-bromosuccinimide
n-BuLi	*n*-butyllithium
NEt_3	Triethylamine
NMR	Nuclear Magnetic Resonance
OFET	organic field-effect transistors
OLED	Organic Light Emitting Diodes
OP	Optoelectronics
OPV	oligo(*p*-phenylene vinylene)
OSC	Organic Solar Cells
PAH	Polyaromatic hydrocarbon

Pas	Pascal-seconds
PCBM	phenyl-C_{61}-butyric acid methyl ester
PDI	Perylene diimide
PET	polyethylene terephthalate
PH	Phosphorescence
PhMgBr	Phenyl magnesium bromide
PV	Photovoltaics
PLQ	Photoluminescence Quantum Yield
PVK	Poly(*N*-vinylcarbazole)
rt	room temperature
S_1	Singlet excited state
SF	Singlet Fission
SHDG	Spin Hydrodynamic Generation
SOC	Spin orbit coupling
SOMO	Singly Occupied Molecular Orbital
T_1	triplet excited state
TBAHFP	tetrabutylammoniumhexafluorophosphate
*t*BuOK	potassium tert-butoxide

TEMPO	2,2,6,6-tetramethyl-1-piperidinyloxy
T_g	Glass transition temperature
TIPS	bis(triisopropylsilylethynyl)
THF	tetrahydrofuran
T_m	melting temperature
TMS	Trimethylsilane
TLC	Thin Layer Chromatography
Tol.	Toluene
TT	Triplet pair
UV	ultraviolet

Chapter 01

Introduction

1.1 Overview of functional molecular liquids in organic chemistry

Organic chemistry is the branch of chemistry that deals with the structure, properties, synthesis and reactions of carbon-containing compounds. Carbon is unique in its ability to form stable bonds with itself and other elements leading to an immense variety of organic molecules that serve as the foundation of life. Although many elements including metals and nonmetals can form element-element bonds in their elemental forms and allotropes, carbon is unique in its ability to form long, stable chains and rings leading to an immense variety of organic molecules that serve as the foundation of life. Centuries ago, chemists classified matter into organic and inorganic substances based on their origin. Organic compounds were believed to be formed by living organisms, either plants or animals. Inorganic compounds were associated with naturally occurring minerals or obtained through chemical processes. They believed that a mysterious vital force residing in living organisms converted inorganic substances into organic compounds. The long-standing distinction was overturned in 1828 when Friedrich Wohler synthesized urea from ammonium cyanate demonstrating that organic compounds could be artificially produced. This marked the beginning of modern organic chemistry.[1] Organic chemistry is the foundation of many other scientific disciplines including biochemistry, materials science, medicine and pharmaceuticals.

Organic chemistry encompasses a broad range of compounds that can be classified according to their origin, structure, functional groups and physical state. Organic compounds exist in various physical states including solids, liquids and gases. Traditionally, most of the research has focused on solid-state compounds, particularly crystalline materials and polymers, due to their structural stability and broad applications. Small volatile organic gases like methane, ethylene and formaldehyde play an important role in atmospheric chemistry and industrial applications but are less commonly studied while their significance is well established. In recent years there has been growing interest in the study of organic liquids, especially functional molecular liquids.

Functional molecular liquids (FML) are a class of soft materials composed of discrete functional molecules that retain fluidity near room temperature, even in solvent-free state. Most of these molecules are uncharged, hydrophobic, and non-ionic alkylated-π molecular units with low glass transition temperatures.[2]

1.1.1 The brief history of FMLs

The history of FMLs can be traced back to 1948, when Robert T. Hart et al. reported in a footnote that 2-*n*-decylnaphthalene **[01]** (Figure 1.1) exists as a liquid with a melting point of 13 °C.[3] This discovery highlighted the potential of low melting organic compounds to exist at or near room temperature. Thereafter, alkylated naphthalene attracted significant interest as synthetic fluids for lubricants, primarily due to their thermo-oxidative stability and favorable viscosity profiles compared to mineral base oils.[4] In the 1960s, a series of synthesized 4-alkyl and 4,4'-dialkylbiphenyl compounds

[04], characterized by melting points below room temperature, played a fundamental role in the development of the now highly developed field of liquid crystals.[5]

A study conducted by S. Gershuni et al. on the effects of substituents on the melting points of anthracenes **[05,06]** and *p*-terphenyls demonstrated that the introduction of alkyl and vinyl substitutions significantly reduced the melting points below room temperature. Furthermore, the researchers confirmed that the presence of two similar substituents was more effective in lowering melting points than a single substituent, while the incorporation of two different substituents proved even more impactful than two identical ones. These findings provide valuable insights that greatly contribute to ongoing research in this field.[6]

In 1989, research on liquid polymer materials led to the introduction of fluorene-based materials, specifically poly(9-alkylfluorene) **[02]** and poly(9,9-dialkylfluorene) **[03]** derivatives, into the field of FMLs. These polymers, characterized by their rigid conjugated backbones and tunable side chains, demonstrated liquid-like behavior under specific conditions. This advancement significantly expanded the structural diversity and functional scope of FMLs for future development.[7]

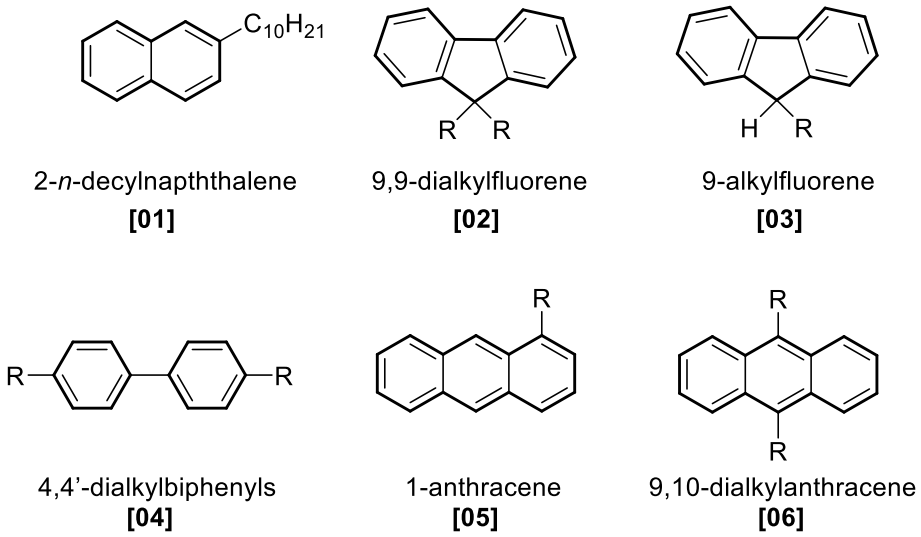

2-*n*-decylnapththalene **[01]** | 9,9-dialkylfluorene **[02]** | 9-alkylfluorene **[03]**

4,4'-dialkylbiphenyls **[04]** | 1-anthracene **[05]** | 9,10-dialkylanthracene **[06]**

Figure 1.1 – Functional molecular liquid derivatives in 19th century

Takashi Nakanishi is widely regarded as a pioneering figure in the development of FMLs particularly in the area of alkylated-π molecular liquids. Their groundbreaking discovery of 2,4,6-tris(alkyloxy)-phenyl-substituted C_{60}-fulleropyrrolidines **[07,** Figure 1.2**]** represents the first experimentally confirmed alkylated-π FML, as demonstrated by rheological studies on complex viscosity.[2]

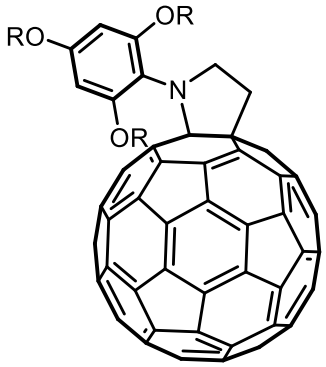

[07]

Figure 1.2 – First experimentally confirmed alkylated-π molecular liquids by Nakanishi

1.2 Strategies for liquefaction of organic molecules

Many large π-conjugated organic chromophores aggregate through π-π interactions, resulting in either crystalline or amorphous solid states at room temperature. Furthermore, non-covalent interactions such as van der Waals forces, dipole-dipole interactions, and hydrogen bonding can further strengthen the intermolecular interactions. Generally, the strategy to liquify organic chromophores involves introducing steric bulk to disfavor intermolecular π-stacking.

1.2.1 Incorporation of bulky groups

A widely employed strategy to induce a liquid state in organic chromophores involves the introduction of side chains to the conjugated system, which disrupts π-π stacking interactions and increases conformational entropy.[2] Bulky and flexible side alkyl groups enhance the thermal and photochemical stability of the π-core, preventing photooxidation and dimerization reactions. Additionally, these side chains effectively shield the π-core, preserving intrinsic single-molecular properties even in the bulk state.[2] The incorporation of bulky side chains into the π-conjugated core can be systematically classified according to the type, number of substituent groups, their position, and chirality.

The type of side chain plays a critical role in effective liquefaction, with common examples including alkyl, alkyl silyl, ester-functionalized alkyl, ether-functionalized alkyl, and ethylene glycol-based groups.[5] Studies by T. Takeda et al. on substituted tetraphenylethylene demonstrated that replacing tetradecylamide with 1-tetradecanoate as demonstrated in figure 1.3, side chains significantly reduced the melting temperature

T_m from 252 °C to 62 °C. Similarly, research by T. Machida et al. on tetraphenylethylene derivatives bearing ester- and ether-containing alkyl side chains has demonstrated that ester substituents result in higher melting temperatures, attributed to stronger intermolecular interactions arising from the polar carbonyl groups.[8] These findings highlight that even when chain lengths are identical, the nature of the functional group critically influences liquefaction behavior.[9]

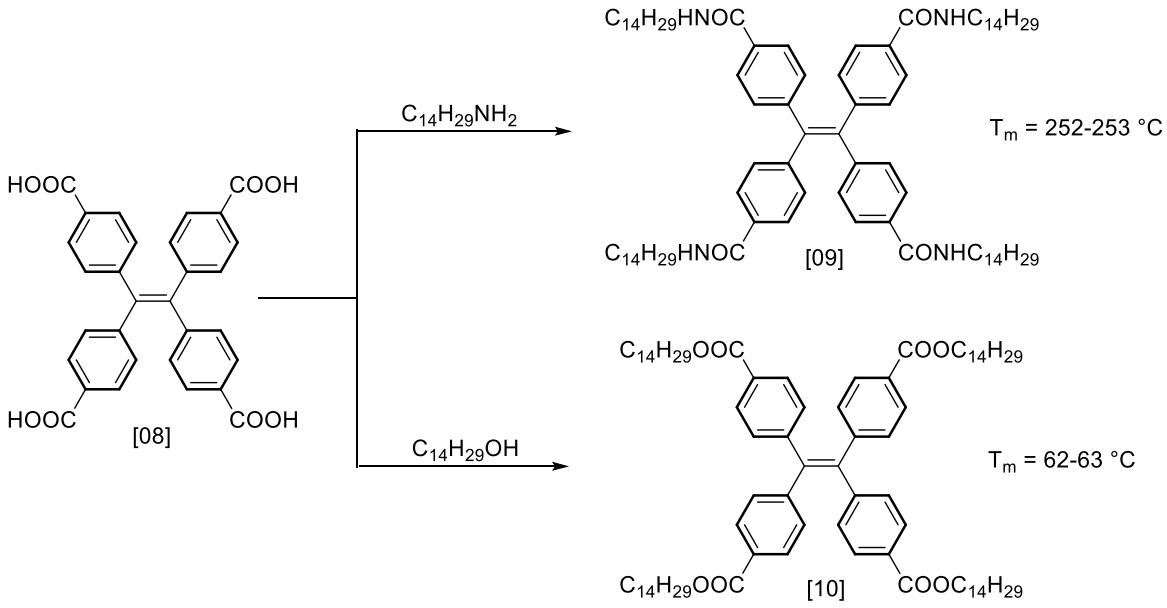

Figure 1.3 – Melting point difference between tetraamide and tetraester

A comparison of the T_m between the solid 9,10-dibutylanthracene **[11]** (T_m= 105 °C) and its isomer 9-butyl-10-(1-methylpropyl)anthracene **[12]** which is a liquid at room temperature reveals that the introduction of two distinct substituents has a greater impact on liquefaction than two identical ones,[6] primarily due to the disruption of molecular symmetry and the reduced packing efficiency between neighboring molecules.[5]

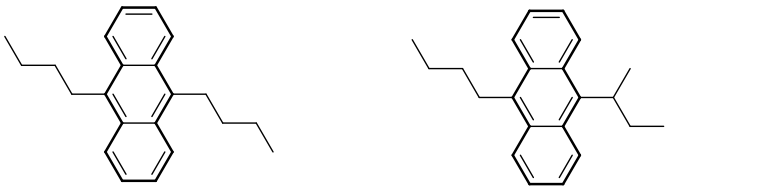

9,10-dibutylanthracene

[11]

9-butyl-10-(1-methylpropyl)anthracene)

[12]

Figure 1.4 –Anthracene isomers

Saturation of the side chains is another factor influencing the liquefaction behavior of alkylated-π FMLs. Studies by M. Taki et al. on trialkylsilyl-substituted pyrene derivatives have demonstrated that the introduction of silyl side chains as seen in figure 1.5 imparts a plasticizing effect, which significantly disrupts intermolecular π-π stacking interactions. This disruption leads to reduced crystallinity and a lower glass transition temperature (T_g). When comparing two pyrene cores substituted with either unsaturated or saturated alkylsilyl side chains of equivalent chain length, the unsaturated derivatives exhibit notably lower viscosities and T_g values.[10] When comparing the cis/trans isomerization effects on the liquefaction, cis unsaturation introduces a structural bend in the chain and disrupts the molecular packing thus reducing van der Waals interactions which induce a lower viscosity and T_g values compared to the trans isomer as the trans isomer maintains a more linear chain conformation enabling favourable molecular packing. This observation suggests that the presence of unsaturation in the side chains increases free volume and molecular mobility, contributing to enhanced fluidity.

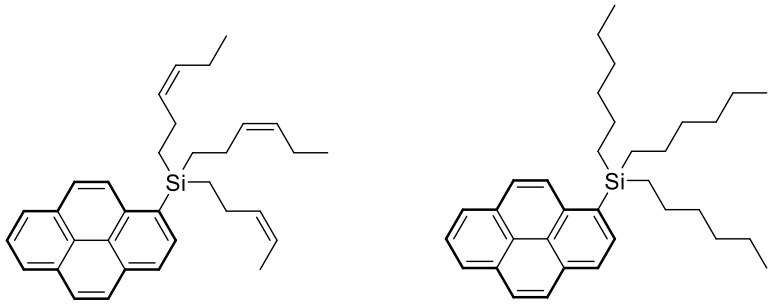

1-[Tri((Z)-3-hexen-1-yl)silyl]pyrene

T_g = -70.1 °C
Viscosity = 162 cP

[13]

1-(Trihexylsilyl)pyrene

T_g = -57.6 °C
Viscosity = 939 cP

[14]

Figure 1.5 – Effect of the degree of unsaturation on molecular fluidity

The position of the side chains plays a crucial role in determining the fluidic nature of conjugated chromophores. The orientation of these side chains, whether they extend inwards or outwards from the surface of the conjugated core, significantly influences molecular packing and fluidity. Side chains that extend inward are more effective at disrupting π-π stacking interactions due to their close proximity to the core and efficiently reduce the T_m and promote liquefaction. In contrast, the side chains that extend outwards have less impact on π-π interactions and often result in higher viscosities and elevated T_m values derived from interdigitation of alkyl groups and thus heightened van der Waals forces.[5]

Studies conducted by Fengniu Lu on substituted pyrene derivatives (Figure 1.6) have further elucidated this phenomenon. Pyrene derivatives with 3,5 substitution on phenyl rings, where both alkyl side chains extend outwards facilitate intermolecular interactions between alkyl chains, increasing friction and leading to higher viscosity of the liquid while derivatives with 2,5-disubstituted phenyl rings have a two-pronged effect directionally,

the 2,5-motif extends the alkyl groups above and below the plane of the chromophore, additionally the substituent in the 2-position biases the biaryl system towards large dihedral angles, further disfavoring intermolecular association.[11] Therefore, the orientation of the side chains, governed by the position of the side chains has a profound effect on the physical behavior of liquid chromophores.

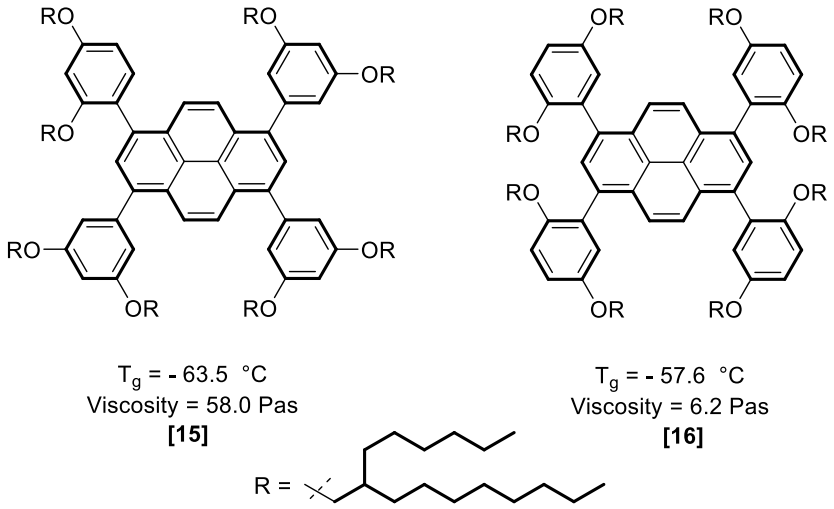

Figure 1.6 – Effect of the position of the side chains on molecular fluidity

The degree of chain branching significantly influences the liquefaction of the π-conjugated chromophores. Compared to long linear alkyl chains, branched side chains derived from Guerbet alcohols introduce greater steric bulk, which enhances molecular disorder and disrupts interchromophore interactions more effectively. However, excessive branching, especially hyperbranched chains, can lead to strong van der Waals interactions, which elevate the viscosity of the resulting fluid. Therefore, the degree of branching must be balanced to optimize fluidity.[5] Studies by S.S. Babu et al. on solvent-free luminescent organic liquids have demonstrated that π-conjugated organic cores substituted with branched alkyl chains exhibit significantly lower T_g, such as -44.2 °C,

while analogues bearing linear alkyl chains tend to crystallize, exhibiting T_m values around 64 °C. These findings confirm that the increase in the degree of branching enhances fluidity by suppressing crystallinity.

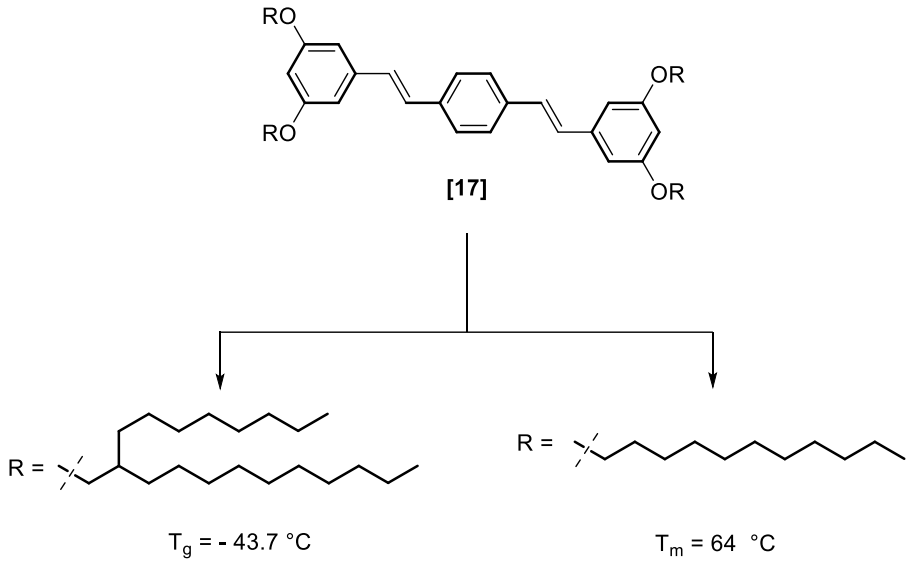

Figure 1.7 – Effect of Side Chain Branching on Molecular Fluidity

The chain length of alkyl substituents plays a vital role in governing the liquefaction behavior of π-conjugated alkylated molecules. For effective liquefaction, the alkyl chains must be sufficiently long to disrupt π-π interactions between the conjugated cores, thereby preventing aggregation. Conversely, the chains must be short enough to avoid excessive intermolecular van der Waals interactions which can increase the viscosity and hinder fluidity. Thus, achieving optimal liquefication requires a delicate balance in chain lengths.[5] In 1989, research on liquid polymer materials, specifically poly(9-alkylfluorene) **[03]**and poly(9,9-dialkylfluorene) **[02]**, revealed that the introduction of alkyl chain lengths ranging from C_3 to C_{12} led to a progressive decrease in the melting

point. However, beyond C_{12}, the melting point exhibited minimal variation, remaining nearly constant. These findings highlight the influence of alkyl chain length on FMLs.[7]

The number of side chains is another important structural parameter influencing liquefaction. In general, incorporating a greater number of side chains more effectively lowers the T_g, primarily due to the enhanced disruption of interchromophore interactions and promotion of greater molecular disorder.[5] The studies on non-volatile, room-temperature anthracene liquids prove that introducing a higher number of alkyl chains can reduce the T_g and viscosity while maintaining high fluorescent quantum yields and enhancing photostability.[12]

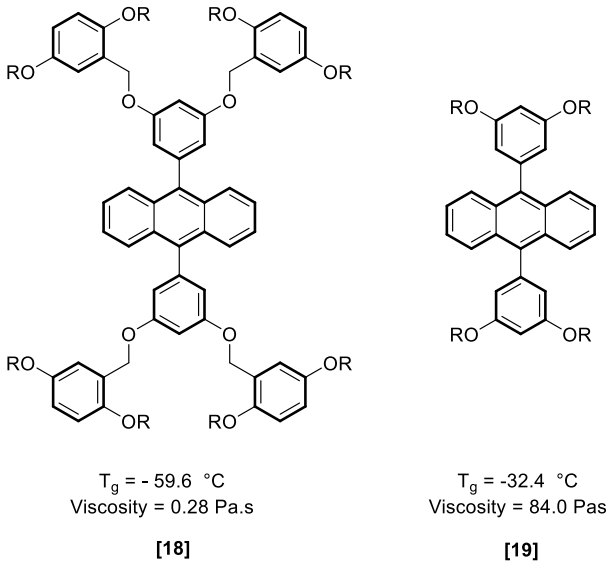

Figure 1.8 – Effect of number of side chains on molecular fluidity

Chirality of the side chains is another important factor that governs the liquefaction behavior of conjugated molecules**.** In many recent studies on liquid chromophores, chirality has been introduced through the substitution of the Guerbet

alcohols, which possess branched structures with stereogenic centers. These chiral side chains have the ability to disrupt the regular molecular packing and reduce crystallinity, thereby promoting the formation of stable molecular liquids.

The Guerbet reaction serves as a valuable synthetic route for synthesizing β-alkylated dimer alcohols through the self-condensation of primary alcohols.[13] The resultant alcohols were thus named Guerbet alcohols. Earlier this reaction was carried out using alkali metal hydroxides and hydrogenation catalysts, Raney Ni at higher temperature and pressure conditions. As indicated in scheme 1.1, in 2006 Matsu-Ura et al. reported that $(CpIrCl_2)_2$ was the best catalysts for this reaction yet discovered.

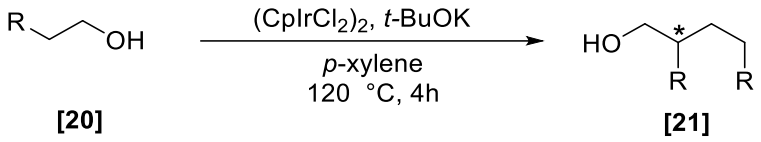

Scheme 1.1 – Guerbet reaction for synthesis of chiral branched alcohols

(* - Asymmetric center)

According to the studies by Walsh, the incorporation of eight Guerbet alcohol derived side chains into the pyrene core as indicated in figure 1.9 with 4 biaryl bonds gives rise to 8 stereocenters and 44 diastereomers. The diastereomers are significantly different in chromophore shapes, which disfavors stacking, induces low local symmetry and reduces the propensity towards crystallization yielding liquids at room temperature.[14] The greater number of diastereomers present decreases the T_m through simple melting point suppression.

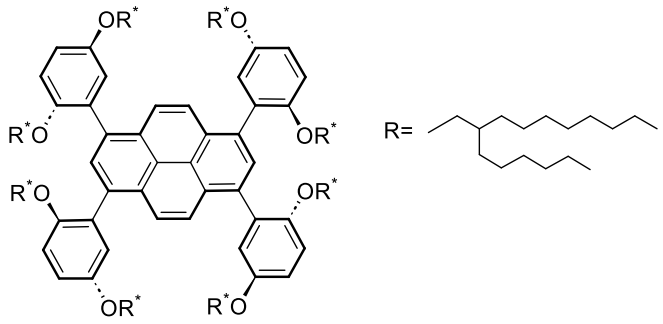

[22]

Figure 1.9 – Liquid pyrene derivatives containing stereogenic centers

Another approach to induce liquefaction in FMLs involves the generation of mixtures of diastereomers that are vastly different in shape and slowly interconvert on the timescale of molecular motion. This structural diversity disrupts π–π stacking and effectively suppresses crystallization. In contrast to the strategy employed by Nakanishi and coworkers, where biaryl atropisomerism and appended chiral side chains are used to introduce chirality and fluidity, this alternative method relies purely on the formation of conformationally distinct diastereomers without requiring branched or chiral substituents.

A clear demonstration of this concept appears in the study by Walsh on the synthesis of oligo(1,8-pyrenylenes) (Figure 1.10) as FMLs. There, biaryl 1,1′-bipyrenyl linkages combined with alkoxy chains generated rotational barriers that produced atropisomeric mixtures. These diastereomeric ensembles suppressed the material's ability to solidify and promoted fluidity within the fluorescent pyrene framework. [14] This strategy, which employs linear chains with greater conformational disparity between diastereomers, offers a more powerful and general route to liquefaction by exploiting slow interconversion and dramatic shape mismatch.[14]

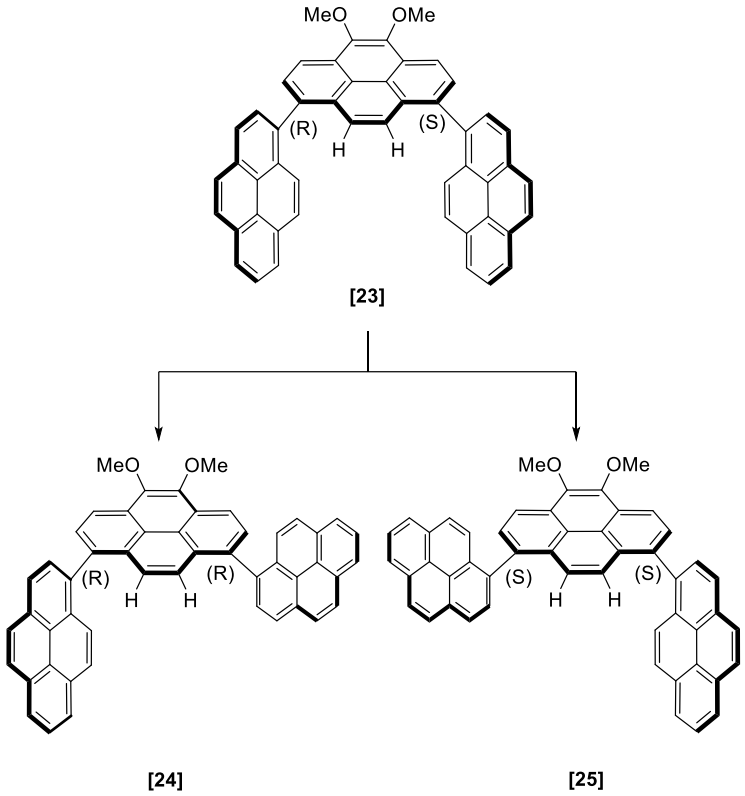

Figure 1.10 – The two diastereomers of 1,8-dipyren-1-ylpyrenes

1.2.2 Mixing of bulky groups

Another widely employed strategy for inducing liquefaction in π-conjugated chromophores involves the equimolar mixing of two structurally related compounds, leading to the formation of a molecularly mixed liquid. While the incorporation of long chain alkyl groups is commonly used to promote fluidity, such modifications unavoidably dilute the conjugated core, thereby reducing the material's optoelectronic activity. Therefore, it is important to minimize the addition of side chains and maximize the concentration of conjugated core to enhance orbital overlap and improve functional performance.

This can be achieved by mixing two low-melting derivatives containing short alkyl side chains, which increases configurational entropy and suppresses crystallization, yielding stable, low molecular weight liquids without excessive molecular dilution. Although this approach appears distinct from previous liquefaction strategies based on racemic mixtures and/or atropisomerism, all of these methods fundamentally operate by suppressing crystallization through the introduction of configurational or compositional disorder. What distinguishes this approach is its efficiency in achieving high chromophore density: by employing bulky but structurally similar groups to create disorder, it enables a liquid sate with minimal reliance on long side chains by preserving the optoelectronic properties of the conjugate core. high chromophore density with diminished reliance on long side chains. [15]

The study conducted by Kushwala et al. on high-entropy liquids, formed by the equimolar mixing of two low melting perylene derivatives, demonstrated the effectiveness of this strategy in achieving liquefaction while preserving high density of perylene based chromophores. The materials exhibit strong green fluorescence with an emission maximum around 530 nm, characteristic of excimer emission. Substitutions at the bay positions of perylene derivatives introduce steric hindrance, which induces a twisting occurs in the perylene core. This structural distortion reduces the effective π-surface area and thus π-π stacking interactions and limits molecular aggregation. Following this concept, in this study they modified perylene derivatives by introducing small alkyl groups at the 1st position of the perylene core to further lower the melting points. By mixing two of these modified derivatives in a 1:1 ratio, the researchers successfully obtained perylene compounds in the liquid state at room temperature.

According to their studies, when the two chromophores are substituted at the same position, they exhibit nearly identical photophysical properties.[15] This emphasizes the potential of chemical modification and compound mixing as an effective methodology for achieving liquefaction while preserving crucial chromophore characteristics.

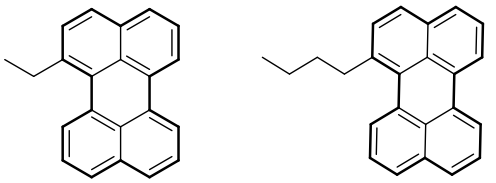

T_m = 70 °C
[26]

T_m = 82 °C
[27]

Figure 1.11 – Compounds undergo equimolar mixing

1.3 Advantages of liquid-phase materials over traditional solid-state materials

FMLs have emerged as a prominent class of materials due to their distinctive physical and functional properties. They have gained considerable attention due to advantages such as ease of handling, processability, high thermal stability and intrinsic flexibility which render them suitable for a broad spectrum of industrial applications.[2,11] Moreover, their compatibility with solvent-free processing contributes to environmentally sustainable material development. The non-volatile nature and tunable, versatile optoelectronic properties open new avenues for advancements in flexible electronics and photonic technologies.[2]

Compared to solid-state materials, the presence of bulky and flexible side chains provides shielding to the π core and enhances stability by suppressing oxidative and

photoinduced side reactions. Their fluidic nature enables facile refilling of devices, removal of degraded active layers, and extension of the lifespan of the electronic devices by capillary action. This potential refilling and replacement methodology could ultimately reduce the quantity of electronic waste. The high processability of FMLs allows them to fill into irregular geometries and even microscale spaces. Flexibility allows them to bend, twist or stretch without affecting their photophysical properties.

There are several draw backs of FMLs compared to solid state materials such as unpredictable phase behaviors of soft, fluidic nature and molecular interactions can complicate their applications in electric devices. Changes in the photophysical properties as luminescence with molecular packing and environment can negatively affect the reproducibility and reliability. Additionally, the application of liquids in electronic devices as LEDs tend to decrease the stability and lifetimes of the devices. The most common drawback is the complexity of the design and synthesis. Achieving the right balance between structure and functional properties of branched and long-chain alkyl chains are still being refined.[5]

1.4 Applications of FMLs in organic electronics, photonics, and materials science

Functional molecular liquids (FMLs) have emerged as versatile platforms for next-generation soft materials due to their unique combination of molecular precision and fluidic processability. Unlike their solid-state counterparts, FMLs offer distinct advantages such as intrinsic self-healing (ability to recover from bending and stretching and restore the structural integrity), absence of grain boundaries, reconfigurability, and

ease of processing without requiring solubilizing additives. These properties make them highly attractive for use in organic electronics, photonics, and materials science.

The fluid nature of FMLs enables homogeneous film formation on a variety of substrates, reduces interfacial defects, and allows for dynamic alignment under external fields (e.g., electric, magnetic, or shear). Additionally, their tunable viscosity and phase behavior can be leveraged for printing, coating, and flexible device integration, capabilities often limited or cumbersome with crystalline solids.

As a result, FMLs have recently been applied across a wide range of technologies, including organic light-emitting diodes (OLEDs), luminescent inks[16], charge-transport materials[17], data storage and memory devices[18], photon up-conversion systems[19], organic semiconductors, and liquid-state lasers[20]. In some cases, the use of FMLs has enabled device architectures that are otherwise inaccessible with rigid materials, particularly where mobility, stability, or interface conformity is critical. Furthermore, the potential to combine fluidity with high chromophore density opens pathways toward liquid-based solar thermal fuels and recyclable optoelectronic components.

1.4.1 Organic light emitting diodes (OLEDs)

Over the last two decades, the field of OLEDs have gained significant interest in both academic research and industrial applications, owing to their potential to enhance internal quantum efficiency and the continuous advancement of organic semiconducting materials. To date, more than 10,000 organic semiconducting materials have been reported contributing to improvements in electroluminescence, power conversion and quantum efficiency of OLEDs. The structural tunability of organic molecules provides a

versatile platform for novel molecular designs to enhance LED performance and broaden their applications.[16] While most of the prevailing OLEDs are based on solid state or liquid crystals, there remains considerable scope for the development of liquid-state OLEDs for emerging applications in flexible and wearable electronics.

In 2009, Xu and Adachi designed an OLED device incorporating a liquid semiconducting layer composed of 9-(2-ethylhexyl)carbazole (**28**), which remains in a liquid at room temperature and serves as the host material. Rubrene was introduced as the guest dopant to facilitate exciton formation within the emitting layer. However, the device exhibited a relatively low external quantum efficiency (EQE) of 0.03%.[16] To enhance device efficiency, the emitting layer was subsequently doped with an electrolyte (tetrabutylammonium hexafluorophosphate-TBAHFP) along with a new guest emitter (**32**).

Although this modification improved the EQE up to 0.30% it resulted in a reduced lifespan of the device caused by the application of liquid electrolyte material. To improve the operational lifetime of liquid OLEDs, Miho Tsuwaki et al. proposed a large area, flexible microfluidic OLED device where fresh light emitting organic liquid chromophore 1-Pyrenebutyric acid 2-ethylhexylester (**30**) can be continuously injected through flexible microchannels fabricated between flexible indium tin oxide (ITO) electrodes. Degraded emissive materials can be removed through an outlet, allowing device performance to be maintained over time.[17]

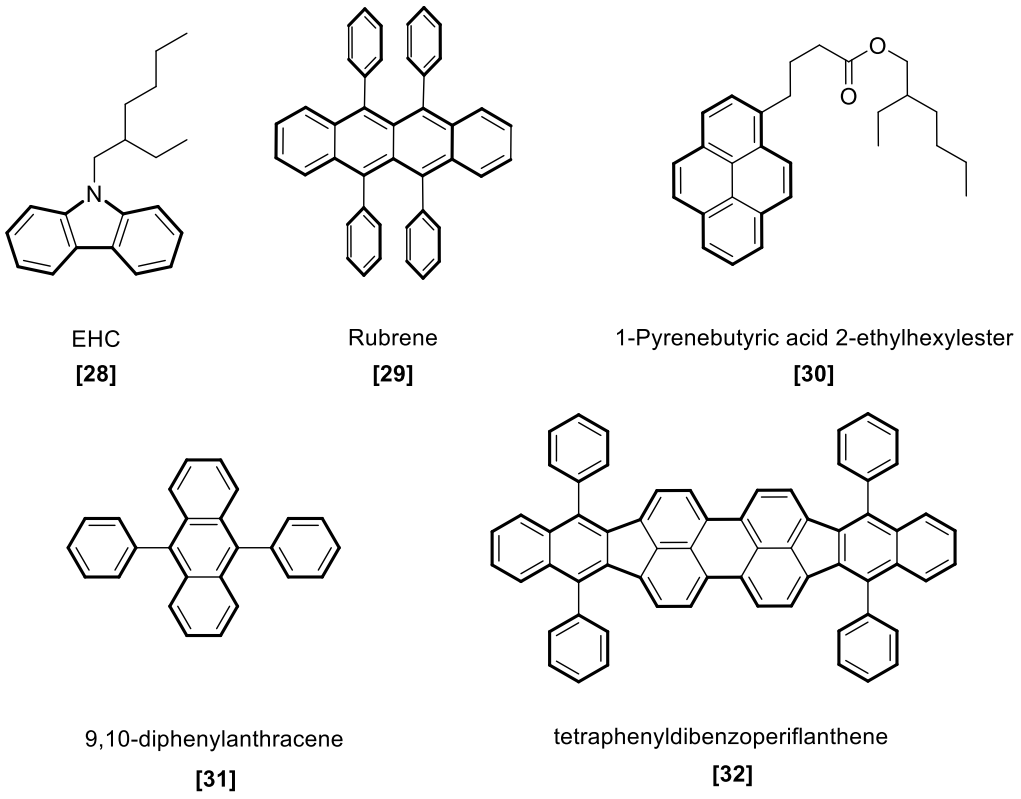

Figure 1.12 – Organic chromophores used in early OLEDs

Then in 2015 Kashara et al. introduced multicolor microfluidic electroluminescent OLEDs by doping emissive chromophores such as 9,10-diphenylanthracene **[31]**, rubrene **[29]**and tetraphenyldibenzoperiflanthene **[32]** doped rubrene into the host liquid matrix PLQ to obtain blue, yellow and red color emissions.[18] Thereafter flexible OLED ribbons were developed by integrating linear microchannels with flexible electrode surfaces to decrease the probability of device cracking and enhancing their potential for use in wearable electronic devices.[19] More recently, studies have been focused on the development of white light emitters[20] and deep blue emitting OLEDs[21]. Non-volatile, low viscous highly emissive room temperature liquid materials are promising candidates for cost effective energy saving light sources. Although they exhibit advantages such as

mechanical flexibility and high throughput fabrication, their performance remains limited in scope due to low brightness, stability and external quantum efficiency. Therefore, there is considerable scope for further development of these devices and for chemical modifications of the liquid chromophores.

1.4.2 Luminescent inks

White light emissive materials have gained significant research interest due to their applications in microscale displays and the increased demand for white lighting solutions. In 2012 S.S. Babu et al. demonstrated that liquid, blue emitting oligo(*p*-phenylene vinylene)s (OPV) can serve as both the blue-emitting counterpart and the solvent matrix for the preparation of white light emitting liquid inks.

Blending green-emitting tris(8-hydroxyquinolinato) aluminium and orange-emitting rubrene with a liquid OPV, followed by annealing for 2 minutes at 40 °C, results in a broad white emission spanning 400–700 nm. By precise modulation of the molar ratio between the matrix and dopants the emission can be tuned from blue-white, pure white to red-white. The viscosity of these white luminescent inks enables their use in rollerball pens and facilitates the coating of large areas.[22]

1.4.3 Charge Transport

Poly(*N*-vinylcarbazole) (PVK) polymer has been utilized in various optoelectronic applications due to its notable photoconductive properties. In their studies on carbazole derivatives to enhance the charge carrier properties, J.C. Ribierre et al. incorporated [**28**] liquids with low T_g into PVK polymer matrix. The faster molecular motion of the carbazole derivative facilitates efficient charge transport. Furthermore, the charge transport

properties and T_g values can be precisely tuned by varying the carbazole concentration within the polymer matrix.[23] Their studies in liquid fluorenes with siloxane side chains (figure 1.13) demonstrated that the charge carrier mobility can be enhanced by increasing the length of the π-conjugation, which in turn regulates the emission color.[24]

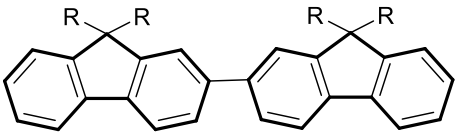

FLU - 01 - Blue emission

[34]

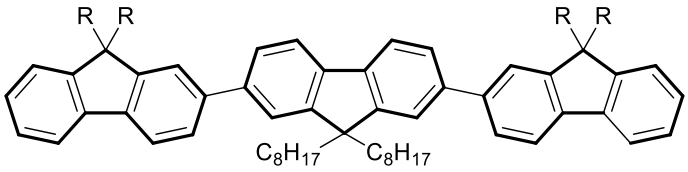

FLU - 02 - Green Blue emission

[35]

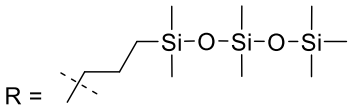

Figure 1.13 – Light emitting fluorene derivatives

1.4.4 Organic Laser Applications

Liquid organic lasers can be produced by doping conventional laser materials with FMLs. The incorporation of green emitting dye coumarin-153 and blue-emitting heptafluorene laser materials into liquid (**28**) enables the fabrication of flexible laser dyes. Fluidic organic dye lasers were then prepared under solvent free conditions by capillary action.[25] When the laser dye material blends are covered with flexible polyethylene terephthalate (PET) films, it is possible to obtain flexible organic devices. In

2016, the first monolithic liquid based organic laser modules were demonstrated using pure fluorene derivatives with higher photostability compared to solid-state materials.[24]

1.4.5 Photon upconversion

Photon upconversion is a promising strategy to improve the efficiency of functioning optical systems, converting low energy photons into a single high energy photon. This process enables the utilization of low energy photons that could be lost, by overcome the absorption threshold of many optoelectronic applications.[26] The major drawback of conventional photon upconversion devices is their high sensitivity to oxygen, which hampers the performances.[5] To address this issue, in 2013 Pengfei Duan et al. introduced an in-air functioning, oxygen tolerant, liquid upconversion system with Pt(II) porphyrin derivative donor and 9,10-diphenylanthracene **[31]** acceptors. The incorporation branched alkyl side chains ensured complete miscibility of the components resulting in a homogeneous, low viscous medium which facilitates the rapid molecular motion and donor acceptor collisions. It promotes energy transfer and triplet-triplet annihilation process faster than quenching with oxygen, achieving a high quantum efficiency of 28%.[27]

1.4.6 Thermometry

Thermoresposivness of FMLs can be applied in modern thermometric applications. Studies by Babu et al. have demonstrated that a mixture of europium complex **[38]**, substituted liquid chromophore 9,10-diphenylanthracene derivative **[36]** and 9,10-bis(phenylethynyl) anthracene **[37**] exhibited Thermoresposive ability. The compound mixture indicates red at 20 °C, yellow at 50 °C and green at 100 °C and returns to red upon

cooling. The Eu(III) complex is the primary emissive species while the anthracene derivatives act as energy transfer donors. The system can be described as a Thermoresponsive multi-chromophore solution containing FMLs. Therefore, liquid emissive FML materials can be used as indicators for thermometers.[12]

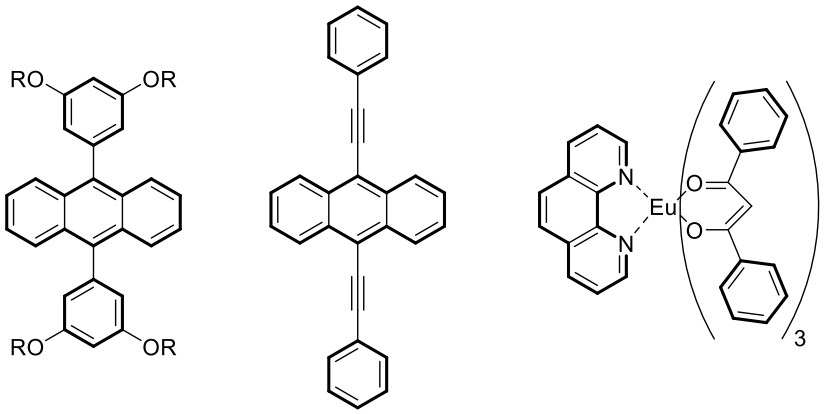

DPA [36] **BPA** [37] **EUC** [38]

Figure 1.14-Thermoresposive compound mixture

1.4.7 Memory devices

Organic bistable memory devices, characterized by high data density, considerable reading stability and long retention times, are potential candidates for future data storage applications. The incorporation of FMLs into these devices has gained significant research interest for the development of the next generation of flexible non-volatile memory devices. In 2011, the first step was undertaken by J.C. Ribierre et al who demonstrated a model of the first rewritable, non-volatile memory device utilizing liquid carbazole and silver nanoparticles. When the blend was sandwiched between ITO electrodes and a bias voltage was applied, they observed a bistable current with an on/off switching response

with the ability to read, write and erase data. Therefore, the hybrids of FMLs and inorganic nanoparticles can be used for the further development of rewritable memory devices.[18]

While this section highlighted some of the key applications of FMLs, ongoing research continues to expand their potential in acid sensors, luminescent nanoparticles, microemulsions, luminescent liquid conjugated polymers, and metal-free phosphorescent materials. The development of softened π-conjugated chromophores opened the door to an extraordinary number of applications in flexible photonic and electronic devices.

1.5 Motivation for research

Functional molecular liquids based on π-conjugated chromophores are promising candidates for next-generation technologies, unlocking extraordinary prospects in flexible and wearable devices. While FMLs have found use in a wide range of applications, this thesis highlights their potential in singlet fission and spin hydrodynamic generation. With the global transition to sustainable energy sources, solar energy has emerged as the most promising renewable energy solution for a greener future. The conversion of solar radiation into electricity using photovoltaics that exploit singlet fission is one of the most promising strategies for increasing power conversion efficiency. Rubrene derivatives have been identified as a promising candidate capable of undergoing efficient singlet fission in solid state. Studies involving high temperature molten chromophores in singlet fission have shown that rubrene in its molten state at 320 °C, exhibits enhanced singlet fission kinetics compared to crystalline state. This observation raises a compelling question: can

similar enhancements be achieved in a liquid rubrene derivatives at room temperature? Motivated by this, we attempted to explore the possibility of designing and synthesizing of novel liquid rubrene derivatives as a foundation step toward future investigation into their potential to support efficient singlet fission under ambient conditions.

Organic spintronics surpass conventional electronics due to their metal free nature and tunable photophysical properties of carbon-based materials. SHDG is the novel theoretical concept on spintronics which demonstrated using liquid metals. The main goal of this project is to integrate fundamental principles of synthetic organic chemistry, FMLs and spintronic functionality into a unified approach and synthesize stable organic liquid radical chromophore capable of undergoing SHDG at room temperature. This approach significantly impacts on the miniaturization of electronic devices as well as enhancing energy efficiency. Motivated by this, we focussed on the design and synthesis of stable organic liquid radical derivatives as a foundation for future studies on investigation their potential in SHDG.

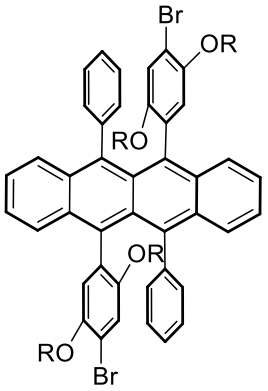

[39]

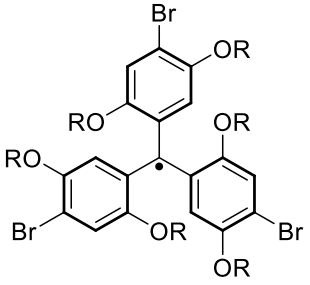

[40]

Figure 1.15 – Proposed liquid rubrene and radical derivatives

References

[1] H. J. Lucas, *Organic chemistry, American Book Co.* **1953**, 11.

[2] A. Ghosh, T. Nakanishi, *Chem. Commun.* **2017**, *53*, 10344-10357.

[3] B. T. Robert Hart, S. A. Robinson, *J. Am. Chem. Soc.* **1948**, *70*, 11,3731-3732

[4] M. J. Hourani, in *IJTC2006*, San Antonio, **2006**.

[5] F. Lu, T. Nakanishi, *Adv. Optical. Mater.* **2019**, *7*,201900176.

[6] R. B. Martin, J. L. Kropp, M. W. Windsor, Y. Haas, G. Stein, D. Horrocks, G. F. Schmidt, D. R. Sudnick, C. Kittrell, R. A. Bernheim, S. Gershuni, M. Rabinovitz, I. Agranat, I. B. Berlman, *J. Phys. Chem.* **1980**, *84*, 517-520.

[7] M. Fukuda, K. Sawada, K. Yoshino, *Jpn. J. Appl. Phys.* **1989**, *28*, 1433-1435.

[8] T. Machida, R. Taniguchi, T. Oura, K. Sada, K. Kokado, *Chem. Commun.* **2017**, *53*, 2378-2381.

[9] T. Takeda, S. Yamamoto, M. Mitsuishi, T. Akutagawa, *Org. Biomol. Chem.* **2016**, *14*, 8922-8926.

[10] M. Taki, S. Azeyanagi, K. Hayashi, S. Yamaguchi, *J. Mater. Chem. C Mater.* **2017**, *5*, 2142-2148.

[11] F. Lu, T. Takaya, K. Iwata, I. Kawamura, A. Saeki, M. Ishii, K. Nagura, T. Nakanishi, *Sci.Rep.* **2017,** *7*, 3416

[12] S. S. Babu, M. J. Hollamby, J. Aimi, H. Ozawa, A. Saeki, S. Seki, K. Kobayashi, K. Hagiwara, M. Yoshizawa, H. Möhwald, T. Nakanishi, *Nat. Commun.* **2013**, *4*, 1969

[13] T. matsu-ura, S. Sakaguchi, Y. Obora, Y. Ishii, *J. Org. Chem.* **2006**, *71*,21,8306-8308

[14] J. C. Walsh, D. T. Hogan, K. L. M. Williams, S. D. Brake, G. Venkataramana, T. A. Misener, B. J. Wallace, R. P. Johnson, D. W. Thompson, Y. Zhao, B. D. Wagner, G. J. Bodwell, *Chempluschem* **2019**, *84*, 754-765.

[15] K. Kushwaha, L. Yu, K. Stranius, S. K. Singh, S. Hultmark, M. N. Iqbal, L. Eriksson, E. Johnston, P. Erhart, C. Müller, K. Börjesson, *Adv. Sci.* **2019**, *6*, 1801650

[16] S. Santhosh Babu, J. Aimi, H. Ozawa, N. Shirahata, A. Saeki, S. Seki, A. Ajayaghosh, H. Möhwald, T. Nakanishi, *Angew. Chem. Int. Ed.* **2012**, *124*, 3447-3451.

[17] J. C. Ribierre, T. Aoyama, T. Muto, Y. Imase, T. Wada, *Org. Electron* **2008**, *9*, 396-400.

[18] J. C. Ribierre, T. Aoyama, T. Muto, P. André, *Org. Electron* **2011**, *12*, 1800-1805.

[19] P. Duan, N. Yanai, N. Kimizuka, *J. Am. Chem. Soc.* **2013**, *135*, 19056-19059.

[20] E. Y. Choi, L. Mager, T. T. Cham, K. D. Dorkenoo, A. Fort, J. W. Wu, A. Barsella, J.C. Ribierre, *Opt. Express* **2013**, *21*, 11368.

[21] D. Xu, C. Adachi, *Appl. Phys. Lett.* **2009**, *95,* 053304

[22] M. Tsuwaki, T. Kasahara, T. Edura, S. Matsunami, J. Oshima, S. Shoji, C. Adachi, J. Mizuno, *Sens. Actuators, A Phys.* **2014**, *216*, 231-236.

[23] T. Kasahara, S. Matsunami, T. Edura, R. Ishimatsu, J. Oshima, M. Tsuwaki, T. Imato, S. Shoji, C. Adachi, J. Mizuno, *Sens. Actuators, A Phys.* **2014**, *214*, 225-229.

[24] K. Sakamoto, H. Kuwae, N. Kobayashi, A. Nobori, S. Shoji, J. Mizuno, *Sci. Rep.* **2018**, *8*,2825.

[25] N. Kobayashi, T. Kasahara, T. Edura, J. Oshima, R. Ishimatsu, M. Tsuwaki, T. Imato, S. Shoji, J. Mizuno, *Sci. Rep.* **2015**, *5,* 14822.

[26] N. Kobayashi, H. Kuwae, J. Oshima, R. Ishimatsu, S. Tashiro, T. Imato, C. Adachi, S. Shoji, J. Mizuno, *J. Lumin.* **2018**, *200*, 19-23.

[27] J. C. Ribierre, L. Zhao, M. Inoue, P. O. Schwartz, J. H. Kim, K. Yoshida, A. S. D. Sandanayaka, H. Nakanotani, L. Mager, S. Méry, C. Adachi, *Chem. Commun.* **2016**, *52*, 3103-3106.

[28] J. C. Goldschmidt, S. Fischer, *Adv. Opt. Mater* **2015**, *3*, 510-535.

Chapter 2

Singlet Fission in Functional Molecular Liquids

2.1 Introduction to singlet fission and its significance in optoelectronics and photovoltaics

Upon photon absorption, an organic chromophore may transition from its ground state to a singlet excited state, after which it can undergo processes such as fluorescence, participate in photochemical reactions, or transfer its excitation energy to another molecule via singlet fission. Singlet fission (SF) is a spin-allowed photophysical process wherein a singlet excited chromophore transfers energy to a neighboring ground-state chromophore, resulting in the formation of two triplet excited states.[1] The two chromophores involved in SF can be either identical, in which case the process is termed *homofission*, or different, referred to as *heterofission*."[2]

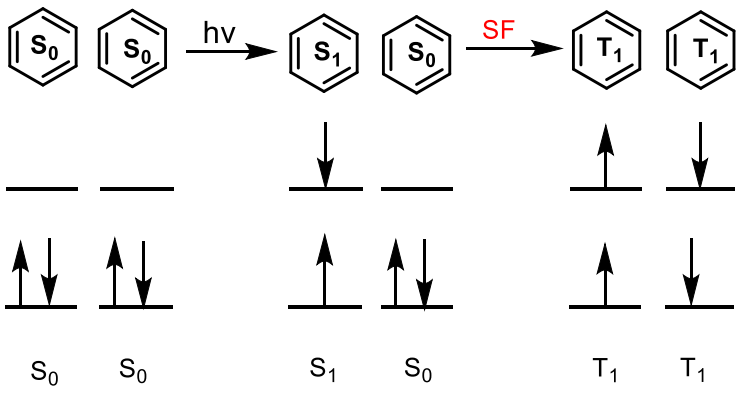

Figure 2.1 - Schematic diagram of singlet fission

The concept of singlet fission (SF) was first introduced in 1963, when Singh and Stoicheff invoked it to explain delayed fluorescence observed in anthracene crystals. Similar phenomena were subsequently reported in tetracene crystals.[3] SF was also detected in carotenoids[4] and conjugated polymers, but its efficiency was only measured in a few systems. Early measurements lacked precision due to limitations in instrumental techniques, leading to a decline in interest over time.[3] Research on SF regained significant attention in 2006 following the work of Hanna and Nozik, who proposed that multiple exciton generation via SF in organic materials could exceed the thermodynamic efficiency limit of single-junction solar cells. Their analysis demonstrated that SF has the potential to increase the efficiency of solar cells above the Shockley–Queisser theoretical efficiency limit of 33.7% to 44.4%.[5]

Michl and his colleagues have made significant contributions to advancing the modern understanding of singlet fission, substantially shaping subsequent research and providing a foundation for further theoretical studies in the field.[2,6] Today, theoretical modeling, computational simulations, and advanced spectroscopic techniques have significantly deepened the understanding of SF. Owing to its rich history and recent advancements, SF exhibits several unique and important features that underscore its value in contemporary research and applications. One such feature, as evaluated by Michl and colleagues, is the thermodynamic requirement that the energy of the singlet excited state (S_1) must be greater than or equal to twice the energy of the first triplet excited state (T_1) for a novel organic chromophore to undergo singlet fission.[3] The Jablonski diagram in Figure 2.2 illustrates this process.

$$E(S_1) > 2E(T_1) \; or \; E(S_1) \sim 2E(T_1)$$

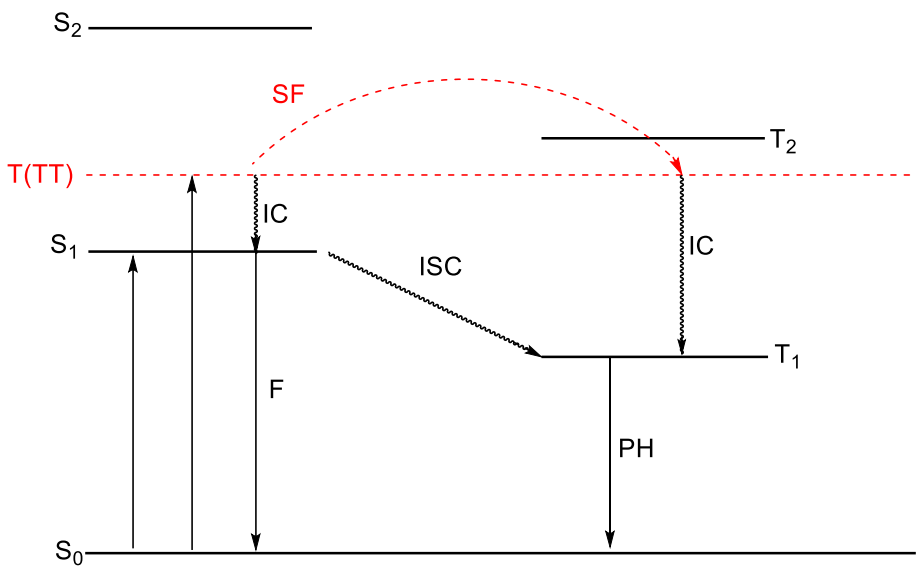

Figure 2.2 – Jablonski diagram with the singlet fission (SF)

(F- Fluorescence, IC-Internal Conversion, ISC-Inter System Crossing, PH-Phosphorescence, SF-Singlet Fission)

SF is a spin-allowed conversion, although it involves a change in the spins of individual chromophore, the coupled $2T_1$ exhibits an overall singlet state. [7] Therefore, SF is frequently associated with internal conversion (IC). As a non-radiative transition between two electronic states of the same spin multiplicity, it occurs on a picosecond or sub-picosecond timescale, faster than processes such as vibrational relaxation or fluorescence.[2] SF can achieve a high quantum yield potential as high as 200% as a single photon can generate two triplet excitons.[7]

Due to these remarkable properties, SF is increasingly being utilized in optoelectronics (OP) and photovoltaics (PV), where its ability to enhance energy

conversion efficiency is enabling breakthroughs in emerging technologies. Optoelectronic devices exploit the interaction between light and the electronic properties of materials to convert light energy into electrical signals or vice versa.[8] This includes photodetectors, solar cells, light-emitting diodes (LEDs), and related devices. Optoelectronic technologies play a crucial role in a wide range of industries, including energy, medicine, architecture, communication, transportation, security, and entertainment.[9] Photovoltaics is a sub class of optoelectronics. This chapter will focus more on photovoltaics.

Photovoltaic (PV) technologies which convert light into electric current present a valuable pathway toward sustainability, delivering a reliable and eco-friendly energy source with high efficiency.[10] In 1839, French physicist Edmond Becquerel discovered the photovoltaic effect and created the first photovoltaic cell using metal electrodes and an electrolyte solution, marking the beginning of solar cell development. The first solid-state solar cell, with an efficiency of approximately 1%, was later invented by Charles Fritts using Selenium in an attempt to compete with coal-fired power. In 1954, researchers Calvin Fuller, Gerald Pearson, and Daryl Chapin at Bell Laboratories demonstrated the first practical silicon-based solar cell. Since then, solar cell technology has advanced significantly, with commercial-grade silicon-based solar cells achieving efficiencies of around 27.6%, and research-grade multi-junction solar cells reaching efficiencies as high as 47.1%. [10]

The bulky, heavy, and rigid nature of silicon-based solar cells limits their suitability for modern applications such as wearable and portable devices, paving the way for alternative technologies like organic solar cells (OSCs). OSCs are constructed using small

organic chromophores or conductive organic polymers and can harvest high-energy ultraviolet (UV) or low-energy infrared radiation, depending on the band gap of the active layer material. They have attracted significant interest in a short period due to their simple fabrication processes, mechanical flexibility, lightweight nature, and potential for high-throughput, large-scale production enabled by the abundance of raw materials. [11]

A typical organic solar cell (OSC) comprises a substrate, electrodes, interlayers, and an active layer. The substrate serves as the foundational material upon which the device is built and is commonly made from polyester or glass. Charge-selective interlayers, positioned between the active layer and the electrodes, promote efficient charge transport. In the absence of a significant energy gradient across the active layer, these interlayers are essential for driving electrons and holes toward the respective electrodes.

The OSC incorporates two types of electrodes. The anode, a transparent electrode typically made of indium tin oxide (ITO) or conductive polymers, permits light to enter the active layer while conducting electricity. The cathode, usually composed of metals such as silver, gold, or aluminum, collects electrons and completes the circuit. For wearable electronics, both electrodes must be flexible and durable.

The active layer is the most critical component of the OSC. It consists of organic semiconductors, either conjugated polymers or small molecules, that absorb light and generate charge carriers. Most commonly, the active layer is designed as a bulk heterojunction, where donor and acceptor materials are blended to facilitate efficient exciton separation and charge transport. Materials that undergo efficient SF; tetracene, pentacene, Diphenylhexatriene can be used as acceptor materials while fullerene, PCBM

(phenyl-C_{61}-butyric acid methyl ester) and PDI (perylene diimide) materials act as the donor materials.

In OSC, a chromophore in the active layer absorbs incident photons and the energy of the absorbed photon is equal to or greater than the band gap of the material, an electron is excited from the highest occupied molecular orbital (HOMO) to the lowest unoccupied molecular orbital (LUMO), resulting in the generation of an electron–hole pair. A significant limitation of conventional silicon-based single-junction solar cells lies in their fixed band gap of approximately 1.1 eV. Photons with energy significantly higher than this threshold result in energy losses through thermalization, where the excess energy is dissipated as heat.[7] One promising strategy to mitigate this energy loss is the utilization of SF in organic chromophores.

This process enables the conversion of a high-energy singlet exciton into two lower-energy triplet excitons, effectively doubling the number of charge carriers generated per absorbed high-energy photon. Furthermore, organic chromophores offer the advantage of tunable band gaps through molecular engineering, allowing them to absorb high-energy photons and efficiently transfer the excess energy to neighboring molecules, enhancing overall device efficiency. To exploit the advantages of SF in OSC, the rational design and synthesis of suitable chromophores with appropriate electronic and structural properties is crucial.

2.2 Challenges in singlet fission materials: structural control, electronic coupling, and phase dependence

Singlet fission According to M.B. Smith et al., singlet fission (SF) materials face several challenges that must be addressed to realize their full potential. Firstly, SF cannot occur within a single small molecule; at least two chromophores are required to accommodate the two resulting triplet excitons, and the interaction between these chromophores must be finely tuned to facilitate efficient fission. Additionally, most organic chromophores do not naturally meet the optimal energetic conditions for SF, often requiring substantial thermal activation for the process to proceed from the first singlet excited state (S_1). Although rapid SF may occur from higher singlet states, it must effectively compete with internal conversion and vibrational relaxation. Furthermore, detecting SF is difficult when the triplet yield does not exceed 100%, and the occurrence of triplet–triplet annihilation, producing signals resembling ground-state absorption, poses an additional complication in characterizing SF behavior.[2]

One of the techniques employed for the SF detection is using transient absorption spectroscopy. It involves the monitoring the changes in transient absorption of a sample following excitation by a laser pulse. Upon excitation, molecules are promoted from the ground state (S_0) to the first excited singlet state (S_1^*), resulting in a characteristic ground state-bleach signal. Then these S_1^* interact with neighbouring S_0 molecules and form triplet pairs through SF. The monitoring of the temporal changes of the transient signals; the decay of the S_1^* and the rise of the triplet state (T_1) absorption, researchers can

determine the SF rate constant. Moreover, the comparison of amplitude changes in the transient absorption signals enables the quantification of triplet yields.[1]

Other than that, the time delayed fluorescence technique also had been used to investigate dynamics of SF particularly in rubrene. The process where a S_1^* is generated by the photoexcitation undergo SF into a lower energy triplet exciton which recombine and regenerate a singlet state, which then emit delayed fluorescence. The time and intensity of the delayed fluorescence provide the kinetics of the triplet pairs.[19]

For a molecule to undergo SF, it must possess specific properties that are critical for enabling the process. Key characteristics include an appropriate electronic structure, favorable chromophore packing, high absorption coefficients, long triplet lifetimes, sufficient triplet diffusion lengths, and the chemical and photostability of the organic chromophore.[7] First and foremost is the electronic structure. While various chromophores with different electronic configurations can participate in SF, not all are equally effective, as specific energetic criteria must be satisfied. For efficient SF to occur, the energy of the singlet exciton (S_1) should closely match—typically within 200–300 meV—twice the energy of the triplet exciton ($2\times T_1$). This precise energy alignment facilitates rapid conversion of the singlet state into a correlated triplet pair (TT), thereby minimizing competing decay pathways such as fluorescence or non-radiative relaxation.[7]

The absorption coefficient refers to a material's ability to absorb light or other electromagnetic radiation. A chromophore with a high absorption coefficient can absorb a significant amount of light over a short distance, enabling the use of thinner active layers

in photovoltaic or optoelectronic devices. This reduction in material thickness not only enhances device flexibility but also shortens the diffusion distance required for triplet excitons to reach interfaces or electrodes, thereby improving the efficiency of SF and boosting overall device performance.[7]

Another critical factor influencing the efficiency of SF is the appropriately balanced electronic coupling between chromophores. The coupling must be strong enough to facilitate efficient SF, yet sufficiently weak to allow the resulting triplet excitons to separate and diffuse independently. Achieving this balance relies heavily on the molecular arrangement, which can be controlled through precise chromophore packing.[6] Stronger coupling can be achieved through closer chromophore packing, and the relative orientation of the chromophores significantly influences the overlap of molecular orbitals, thereby enhancing SF efficiency.

Introducing molecular motions and fluidity through FMLs broaden the distribution of orientations and intermolecular distance but reduce coupling compared to the solid-state compounds. According to the studies of Lu et al. on pyrene-based molecular liquids, fluorescence spectra differ from liquid excimers with stronger π-π interactions to liquid monomers with weak coupling interactions based on the substituted alkyl chains. Although the electronic coupling is weaker than solids, FMLs can be used to optimize the rate of SF and exciton diffusion thorough the tunable π-π interactions.[21]

In addition, long triplet lifetimes and sufficient diffusion lengths are essential for effective SF. The generated triplet excitons must persist long enough and travel far enough

to reach a heterojunction or interlayer from the active layer, where they can be harvested and contribute to charge generation. [7]

The long-term stability of the organic chromophore is also a crucial factor for effective SF. Chromophores must retain their structural integrity and photophysical properties over time to ensure consistent performance. However, many acene-type organic chromophores, which are not inherently photostable, are susceptible to photodegradation in the presence of oxygen and light. This degradation often leads to the formation of endoperoxides, which quench excited states and significantly limit the practical application of these materials in singlet fission-based devices.[40] One of the best strategies to improve the stability of chromophores is the substituent groups. Steric bulk can protect the chromophore core from oxygen.

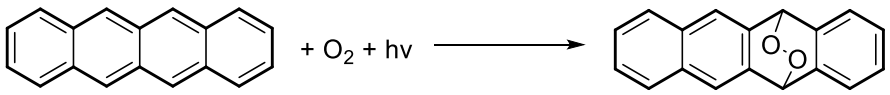

[41] [42]

Figure 2.3 – Endoperoxide formation of tetracene molecules

For several decades, the exploration and application of SF were confined to a narrow selection of organic chromophores known to exhibit the phenomenon.[30] With recent advancements in theoretical and experimental studies, the number of chromophores capable of undergoing SF has increased significantly, alongside the development of novel materials specifically designed to optimize this process. [7] It has

been shown that polyacenes (anthracene, Tetracene, pentacene), 1,3-diphenylisobenzofuran[13], rubrene[14], peropyrene[15] can undergo SF and those compounds are illustrated in figure 2.4.

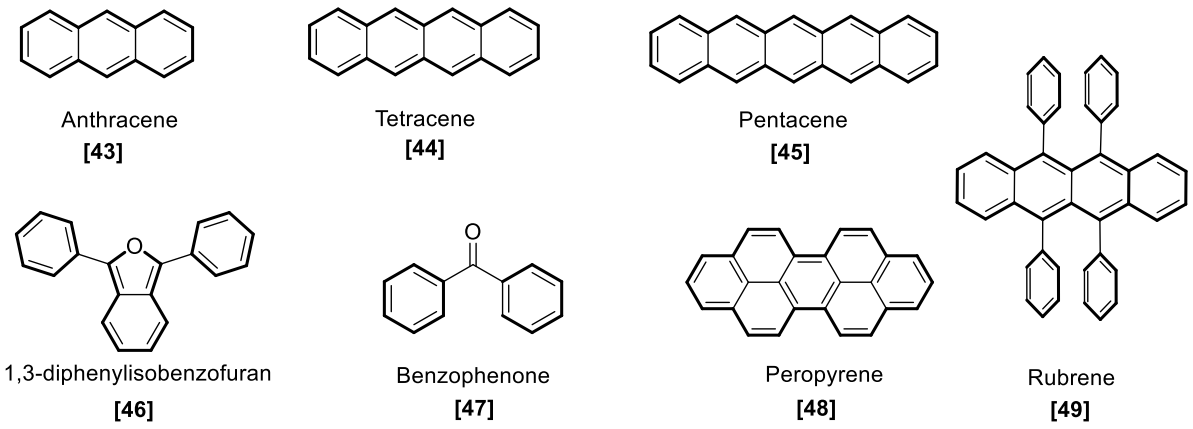

Figure 2.4 – Compounds that undergo Singlet Fission

2.3 The research question posed by Bardeen: Is molten rubrene a better singlet fission material due temperature effects or phase change?

5,6,11,12-Tetraphenyltetracene, colloquially known as rubrene **[49,** Figure 2.5**]** is a notable compound in the field of organic chemistry. This vibrant red polycyclic aromatic hydrocarbon is widely recognized for its exceptional optical and electronic properties, making it a valuable material in applications such as organic semiconductors, light-emitting devices, and SF research.

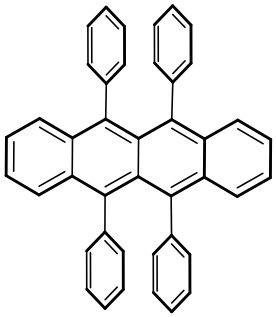

[49]

Figure 2.5 – Structure of Rubrene

Rubrene consists of four phenyl groups attached to a tetracene backbone at the 5, 6, 11, and 12 positions. The orthogonally predisposed phenyl moieties contribute to the photostability of the tetracene core by kinetically shielding the core. Notably, rubrene was among the first organic materials to exhibit high charge carrier mobility, establishing its significance in the development of organic electronic devices(10 $cm^2 V^{-1} s^{-1}$). [16] This high charge carrier mobility laid the foundation for rubrenes use as a semiconducting material, supporting hole transport and functioning as a p-type semiconductor. Owing to these properties, rubrene has been widely applied in modern organic optoelectronic devices such as organic light-emitting diodes (OLEDs) and organic field-effect transistors (OFETs). Additionally, rubrene exhibits a quantum yield of approximately 100%, making it an especially attractive candidate for applications in photovoltaic systems (PVs). [17].

According to studies conducted by Aleksandr Raczynski in 2011, rubrene in its orthorhombic crystalline form exhibits efficient singlet exciton fission. It also possesses long triplet lifetimes and significant exciton diffusion lengths, making it a promising candidate for singlet fission-based applications.[18]

In 2016, Christopher J. Bardeen and colleagues investigated time-resolved photoluminescence in high-melting-point compounds: tetracene, diphenylhexatriene, and rubrene, all of which are capable of undergoing SF. [19] Their studies indicated that tetracene's chemical decomposition hindered any in-depth analysis of SF, while the rapid non-radiative relaxation of diphenylhexatriene masked the fission process. Additionally, they demonstrated that rubrene in its molten state can undergo SF at a rate comparable to that in its crystalline form, but with a faster triplet pair dissociation. This accelerated dissociation may be attributed to either a shortened triplet lifetime or a decreased probability of triplet–triplet fusion.[19] This observation raises the question of whether the observed effect arises from high-temperature conditions or from the phase transition between solid and liquid states. *The primary objective of this project is to resolve this uncertainty.*

2.4 Investigating the role of molecular liquidity in exciton dynamics and energy transfer

An exciton is a quasiparticle formed through the Coulombic interaction between an electron–hole pair. It has the capacity to relax, transform, and transport energy over a certain distance before undergoing decay. These processes, along with the exciton's lifetime, are governed by the molecular structure of the exciton carrier and the surrounding environmental conditions.[20]

Functional molecular liquids (FML) composed of π conjugated molecules with long chain alkyl groups designed to remain in the liquid state at room temperature, offer a

platform to study the exciton dynamics. In solid state materials and polymers, the mobility of excitons is reduced by the energetic traps, static molecular arrangements and aggregation induced quenching.[20] The fluid nature of the FMLs provides enhanced molecular mobility and tunable intermolecular interactions, which affect exciton generation, diffusion and recombination. According to Nakanishi et al's studies on pyrene based FMLs excited state dynamics, the high viscosity of neat liquids restricts the rotational and translational motions which allows the excitons diffuse by the excitation energy transfer (EET) through the dipole coupling. Notably, EET occurs at a higher rate than the excited monomer decay in FMLs. [21]

The incorporation of flexible alkyl chains suppressed the π-π interactions between aromatic cores prevent the face-to-face stacking configuration[21] and minimize the rigidification into crystalline matter or aggregations which reduce the exciton quenching and improve energy transport efficiency.[20] Liquefaction by the changes in the length, branching and substitution patterns of the alkyl chains on π-conjugated molecules can be tunable to enable modulations on molecular packing, spatial separation, viscosity and interactions between chromophores to facilitate energy transferring process. The investigation on molecular liquidity in exciton dynamics and energy transferring is critical for the development of next generation optoelectronics and photovoltaics.

2.5 Design and synthesis of liquid-phase singlet fission materials

Recent studies by B.J. Walker et al. on SF in solutions utilizing bis(triisopropylsilylethynyl) (TIPS) pentacene [**50**, figure 2.6] have demonstrated that, at

high concentrations in solutions, TIPS pentacene molecules can be electronically decoupled and undergo SF efficiently. This electronic decoupling allowed individual molecules in solution to undergo SF more efficiently than the solid-state systems or covalent dimers due to the sufficient driving force to facilitate molecular interactions within the singlet lifetime. According to them the isotropic nature of TIPS pentacene in solution suggests that molecular diffusion and uniform distribution contributes to its efficient exciton behavior suggesting that this concept can be extended to for isotopic FMLs.[22]

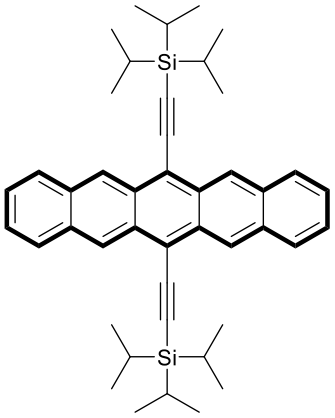

[50]

Figure 2.6 – Structure of TIPS pentacene

According to Bardeen's suggestions, it is possible that a liquid composed of rubrene chromophores could exhibit a unique combination of rapid SF along with long triplet lifetimes and diffusion lengths.[19] In this project, the primary objective is to synthesize liquid rubrene derivatives and evaluate their potential for SF applications. To achieve liquefaction, long-chain alkyl groups will be attached to the phenyl rings of rubrene. These chains are designed to be long enough to disrupt the π–π interactions between the

aromatic cores, yet short enough to minimize van der Waals interactions, thereby promoting a stable liquid state.[23] The alkyl chains may be either linear or branched, with the branched variants derived from Guerbet alcohols. As outlined in Section 1.3 of the introduction, branched alkyl chains exhibit a greater capacity to induce structural disorder and lower viscosity into the liquid phase.[24] Additionally, the incorporation of bromine enhances the kinetic stability and the viscosity of the liquid rubrene derivatives.[25]

2.6 Results and Discussion

Hydroquinone serves as the foundational scaffold in this research, functioning as the key starting material for both projects. Its reactivity, tunable electronic properties, and structural versatility enable the development of liquid organic chromophores discussed in this chapter and Chapter 03. First discovered by Wöhler in 1844, hydroquinone is a white crystalline solid at room temperature. Hydroquinone and its derivatives are widely utilized across various industries, including polymer and rubber manufacturing, photographic processing, antioxidant formulations, and agrochemical production. [26]

Benzene-1,4-diol, commonly known as hydroquinone, is an aromatic compound featuring two hydroxyl groups positioned para to each other on a benzene ring, classifying it as a type of phenol. Due to its phenol-like reactivity, hydroquinone readily forms a conjugate base in the presence of a base, enabling facile O-alkylation reactions. This allows one or both hydroxyl groups to be efficiently converted into ether functionalities.[26]

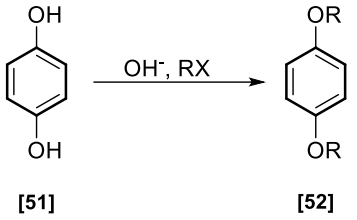

Scheme 2.1 – O-alkylation reaction of hydroquinone.

The synthesis of substituted rubrene from hydroquinone involves six key steps, as illustrated in Scheme 2.2. The synthetic pathway involves alkylation, bromination, Sonogashira coupling reaction, deprotection, nucleophilic addition, and finally, the dimerization of a highly substituted chloroallene to form rubrene. Each step requires careful control of reaction conditions—such as solvent systems, temperature, catalysts, reaction times, and atmospheric conditions—to optimize yields and ensure the success of the overall synthesis.

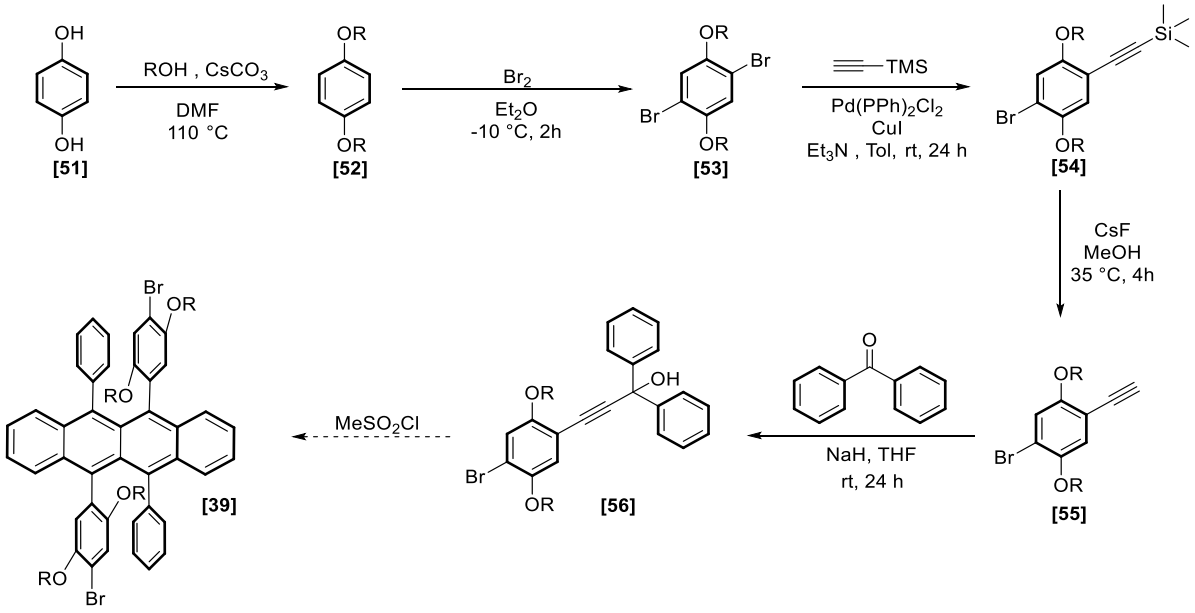

Scheme 2.2 – Synthesis Pathway – I

The first step is the alkylation of the hydroquinone. As the first rubrene derivative, methoxy groups were substituted to obtain the solid product. The incorporation of methoxy groups at the 2,5-positions significantly enhances the electron density of the aromatic core due to their strong electron donating nature. They introduce moderate polarity to the organic chromophores, which improves the solubility and facilitates the formation of homogeneous reaction mixtures in organic solvents. Additionally, the steric hindrance induced by substitution at 2,5-position effectively reduces the π-π stacking interactions which prevents undesired crystallization. The most important fact in this project is that those methoxy groups can be readily substituted with long-chain alkyl groups to further tune the molecular properties.

Methoxylation is the first reaction of the synthesis pathway-**I.** Several methods were explored to determine the optimal conditions for the reaction. Although these methods employed the same base, solvent, temperature, and alkyl halide, variations in procedure were tested to maximize efficiency. Sodium hydride (NaH), a highly reactive, non-nucleophilic, and strong base, was used to generate a nucleophilic alkoxide from hydroquinone. This alkoxide then undergoes an S_N2 substitution with the alkyl halide, resulting in successful O-alkylation. Dimethylformamide (DMF) was chosen as the reaction solvent due to its high polarity and dielectric constant, which allows for effective dissolution of the starting material and partial solubility of NaH, creating a uniform reaction environment. Additionally, DMF's excellent solvating ability stabilizes the alkoxide intermediate, minimizes side reactions, and promotes efficient S_N2 reactivity.[27]

Initially, following the reaction conditions detailed in scheme 2.3, hydroquinone was dissolved in DMF, followed by the addition of NaH to generate the conjugate base. Methyl iodide (MeI) was then added dropwise to initiate the nucleophilic substitution. After 24 hours of reaction time, the mixture was extracted into diethyl ether (Et_2O), and the crude product was isolated. Column chromatography yielded a white solid product with a 68% yield. Given that most alkylation reactions in the literature report higher yields, additional reaction conditions were explored to optimize the process. One possible reason for the relatively low yield is the partial water solubility of SF-01 **(Scheme 2.3)** (0.8 g/L), which may lead to product loss during aqueous workup. The most challenging aspect of the procedure was the removal of DMF due to its high boiling point and polarity. The rotary evaporator had to be used for extended periods to facilitate DMF removal. In a second attempt, rapid evaporation at elevated temperature was employed, which resulted in a thick black residue with a pleasant odor, likely due to thermal degradation or side reactions during the high-temperature evaporation process.

In the third attempt to improve the yield of the alkylation reaction, the extracted organic layer was washed with hydrochloric acid (HCl). This step neutralized any remaining base, enhanced phase separation, and facilitated the removal of DMF. In the fourth attempt, a 5% LiCl solution was employed to further assist in DMF removal and enhance product recovery, ultimately aiming to increase the overall yield of the desired product. LiCl alters the polarity of the extraction mixture and reduces the DMF's solubility in organic solvents and encourages phase separation and facilitates aqueous extraction of DMF. Finally, in conjunction with the LiCl workup, toluene was used as an azeotropic agent to facilitate the complete removal of DMF. This optimized procedure resulted in the

successful isolation of SF-01 with a 76% yield, making it suitable for the subsequent bromination step in the synthetic pathway.

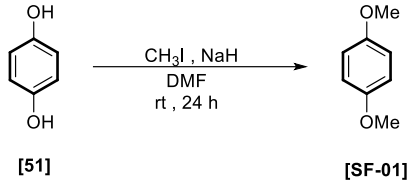

Scheme 2.3 – Methoxidation of hydroquinone

For the synthesis of SF-02, two distinct procedures were explored as indicated in Scheme 2.4. The initial approach involved bromination using molecular bromine. In the first attempt, the starting material was dissolved in Et_2O at -10 °C, followed by the dropwise addition of bromine to initiate electrophilic aromatic substitution. However, after workup and column chromatography, the reaction afforded a low yield of SF-02 (27%). This low yield was attributed to the incomplete dissolution of liquid bromine in Et_2O. To improve solubility, dichloromethane (CH_2Cl_2) was used as the solvent in a subsequent attempt. Despite this change, the reaction resulted in the formation of a black-colored solid, rather than the desired product, indicating potential dealkylation, oxidation and ultimately, the need for further optimization. In the next attempt, the starting material was again dissolved in CH_2Cl_2, and N-bromosuccinimide (NBS) was employed as a mild brominating agent. Acetic acid (AcOH) was added to enhance the electrophilicity of NBS in CH_2Cl_2. The reaction was conducted at room temperature for 16 hours yielding 18% of SF-02**.** Upon increasing the reaction temperature up to 45 °C, the yield significantly improved to 85%, leading to the successful synthesis of SF-02**.**

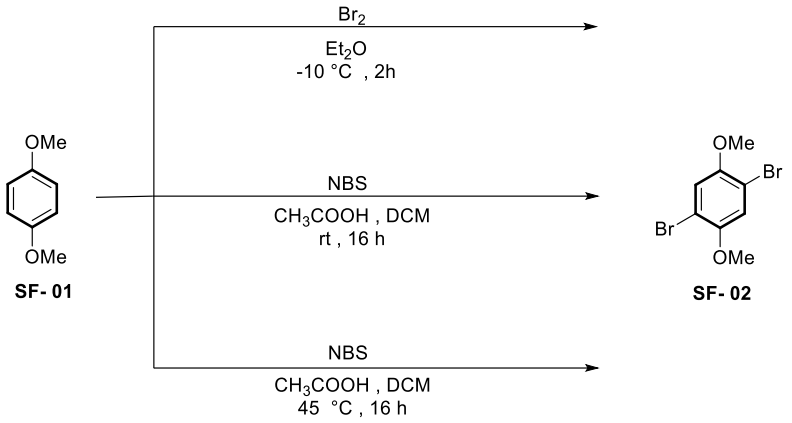

Scheme 2.4 – Bromination reaction of **SF-01**

The third step in the synthesis pathway is the Sonogashira reaction, which was carried out using $Pd(PPh_3)_2Cl_2$ and CuI as catalysts in a 1:1 mixture of toluene and triethylamine (NEt_3) as the solvent system. Due to the sensitivity of this reaction to moisture and oxygen, all procedures were conducted under an inert nitrogen (N_2) atmosphere to maintain optimal reaction conditions. In the first attempt, 2-methyl-3-butyn-2-ol was used as the alkyne coupling partner. The detailed mechanism of the Sonogashira reaction is illustrated in Scheme 2.5

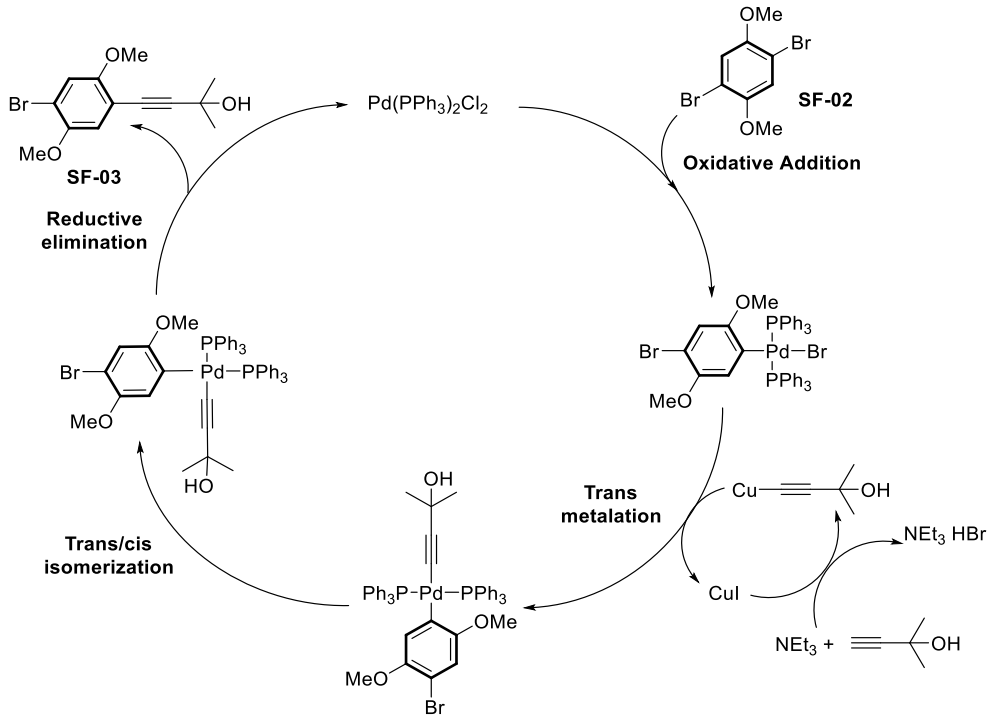

Scheme 2.5 – Sonogashira reaction mechanism

While the monosubstituted product (SF-03) was the expected outcome, the disubstituted product (SF-04) was also obtained as a byproduct as indicated in the scheme 2.6. Despite the alkyne being added in a 1:1 molar ratio with the starting material, both products were observed. This can be attributed to the presence of two bromine atoms with similar electronic environments and minimal steric hindrance, allowing for sequential substitutions rather than termination after the first. Moreover, the electron-donating nature of the dimethoxy groups enhances the nucleophilicity of the aromatic ring, increasing its susceptibility to Pd-catalyzed coupling and promoting further substitution. Additionally, the presence of CuI as a co-catalyst contributes to high conversion efficiency, further favoring the formation of the disubstituted product.

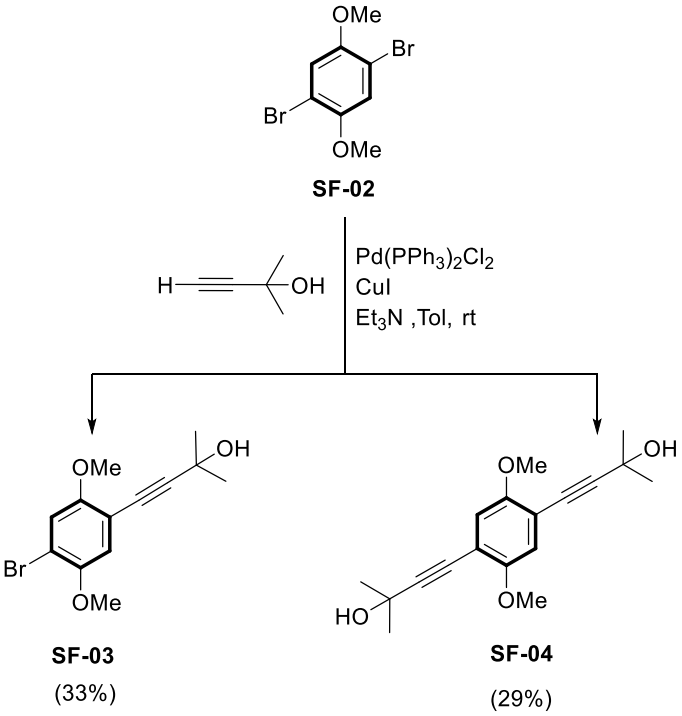

Scheme 2.6 – Sonogashira reaction of **SF-02**

The fourth step of the reaction pathway involved the deprotection process, carried out under the same conditions that Baroni et al. have applied in their deprotection of terminal alkyne[28]. To deprotect SF-03 basic conditions were necessary to deprotonate the tertiary alcohol group to facilitate acetone ejection. Additionally aqueous conditions were required to protonate terminal alkyne.

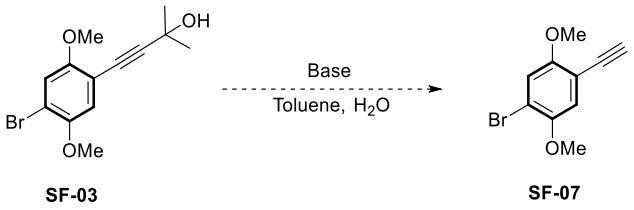

Scheme 2.7 – Attempt to synthesize terminal alkyne

To obtain the desired product, the conditions outlined in **Table 2.1** were applied. However, none of the reaction conditions proved effective as they yielded a bright yellow solid starting material which was sparingly soluble in $CDCl_3$.

Base	Solvent	Temperature	Reaction time
K_2CO_3	Toluene	110 °C	2 h
K_2CO_3	Toluene	110 °C	24 h
K_2CO_3	Toluene/H_2O	110 °C	2 h
NaOH (10%)	Toluene	110 °C	2 h
KOH (5M)	Toluene	110 °C	2 h

Table 2.1 – Attempted deprotection reaction conditions

After multiple unsuccessful attempts at the deprotection reaction which can be caused by the solubility issues of bases in the non-polar solvent or the stability of the protecting group requires acidic conditions for the deprotection reaction, attention shifted to an alternative Sonogashira reaction strategy employing trimethylsilylacetylene (TMS-acetylene), a commonly used alkynylating and protecting agent. The reaction was conducted under the same conditions as the previous attempt, with a 24-hour reaction time at room temperature as indicated in scheme 2.8. The product mixture contained unreacted starting material (SF-02), monosubstituted product (SF-05), and disubstituted product (SF-06), which proved inseparable despite repeated attempts using column chromatography. NMR analysis confirmed the presence of all three compounds.

To improve selectivity for SF-05, the reaction was modified: it was initiated at -10 °C with the addition of 1 equivalent of TMS-acetylene, followed by incremental additions (0.8 and 0.9 equivalents) at room temperature. However, each attempt consistently yielded a mixture of the three products, with a notably higher proportion of disubstituted product compared to the monosubstituted target. This outcome highlights a significant limitation of this approach in achieving selective mono-functionalization.

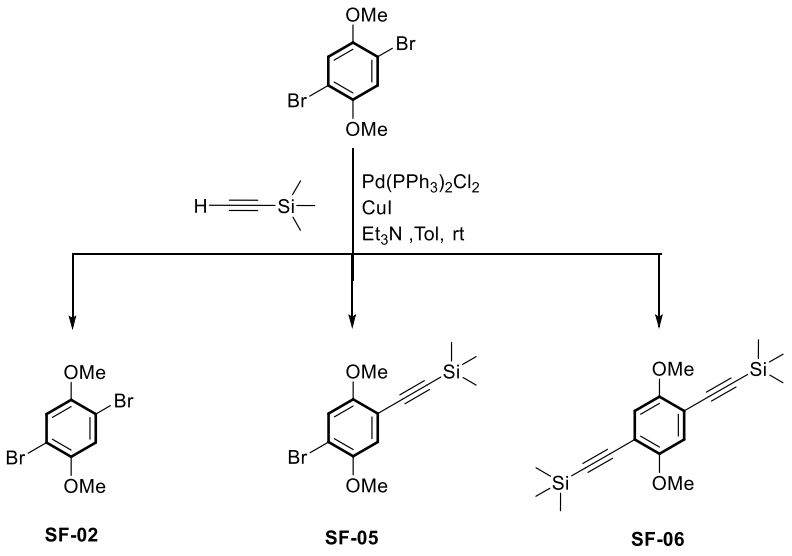

Scheme 2.8 – Sonogashira Reaction from TMS-Acetylene

The deprotection reaction was subsequently performed using cesium fluoride (CsF) in methanol at 35 °C via a nucleophilic substitution mechanism relying on the strength of the Si-F bond. In this process, the fluoride ion, acting as a strong nucleophile, attacked the silicon center of the trimethylsilyl (TMS) group, cleaving the C–Si bond and displacing the TMS group. The resulting acetylide anion was then protonated by methanol to yield the terminal alkyne. The TMS-F byproduct was efficiently removed through an aqueous

workup and rotary evaporation (b.p. 16 °C) . These mild reaction conditions proved to be both convenient and effective for achieving deprotection.

From the monosubstituted precursor SF-05, the expected terminal alkyne product SF-07 was successfully obtained, along with an inseparable side product SF-08, which originated from the disubstituted SF-06 as indicated in scheme 2.9. The presence of the terminal alkyne was confirmed by the disappearance of the TMS-acetylene signal and the appearance of a singlet at 3.56 ppm in the ^{1}H NMR spectrum. The resulting product mixture was then subjected to the propargyl alcohol synthesis reaction.

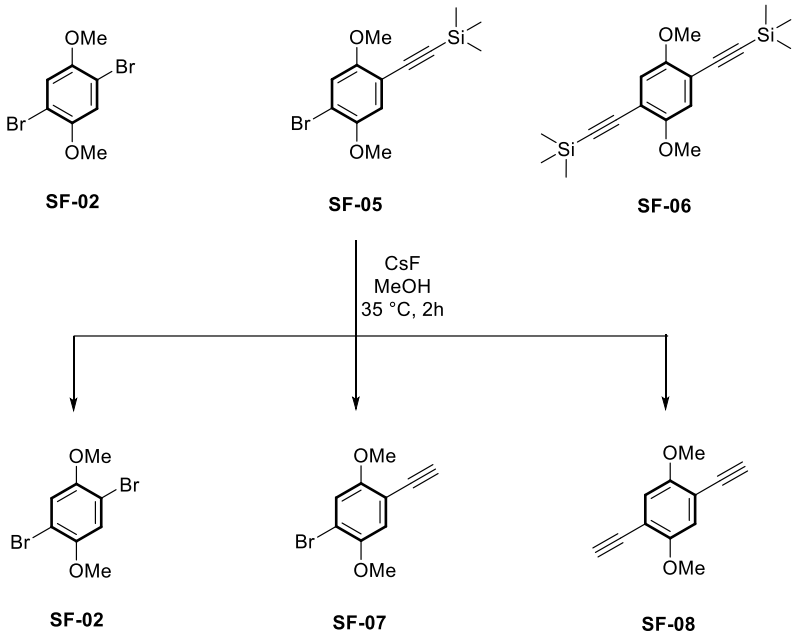

Scheme 2.9 – Deprotection reaction of TMS-Acetylene

The fifth step of the rubrene synthesis pathway-I involved a nucleophilic addition reaction. A product mixture containing SF-02, SF-07, and SF-08 was reacted with NaH and benzophenone to synthesize propargyl alcohols as indicated in scheme 2.10. NaH, a

strong base, abstracts the acidic proton from the terminal alkyne, generating the corresponding acetylide anion. This highly exothermic step must be conducted at 0 °C to prevent excessive heat generation and to maintain the stability of the acetylide ion. The nucleophilic acetylide ion then attacks the electrophilic carbonyl carbon of benzophenone, forming an alkoxide intermediate. A subsequent aqueous workup protonates the intermediate, yielding SF-09 and SF-10 from SF-07 and SF-08, respectively. Both products were successfully isolated, and SF-09 was carried forward to the next step in the synthesis pathway.

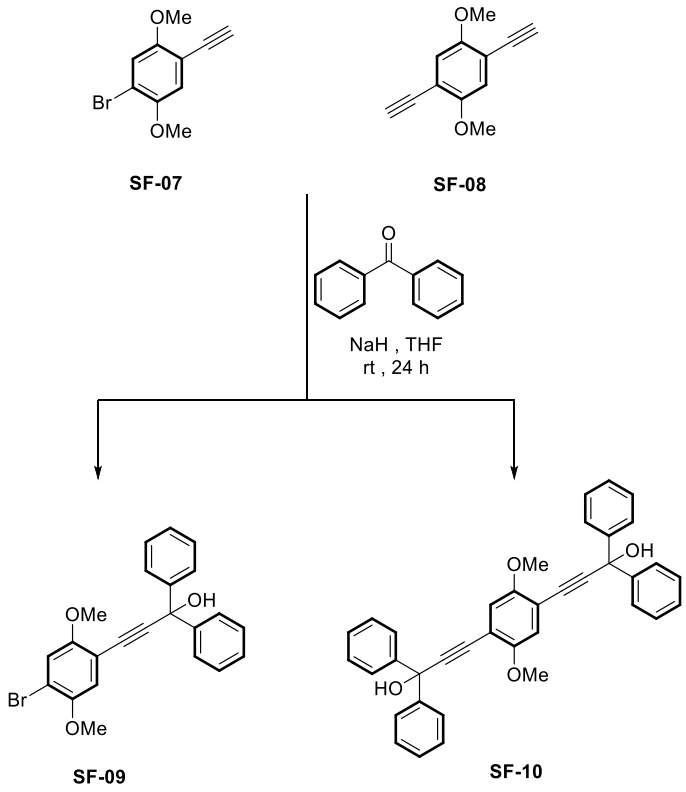

Scheme 2.10 – Synthesis of Propargyl alcohols

The final step in synthesis pathway-I involved the synthesis of rubrene. Commercially available rubrene is synthesized from 1,1,3-triphenylpropargyl alcohols, via dimerization of triarylchoroallenes obtain from the halogenation reaction of propargyl alcohols.[29] First, the alcohol is converted to a good leaving group via mesylation, followed by attack of chloride leads to elimination and finally formation of the chloroallene intermediate. One potential reaction mechanism is depicted in **Scheme 2.11**.

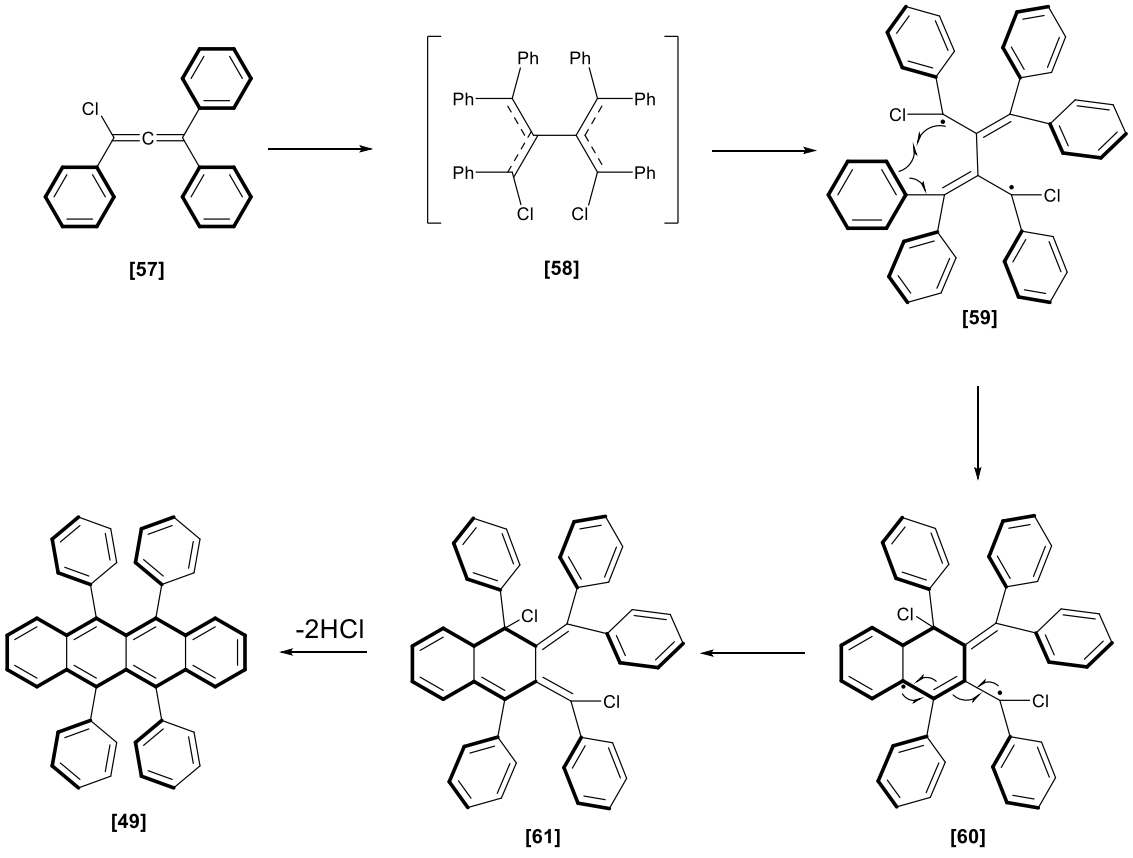

Scheme 2.11 – Rubrene synthesis mechanism

According to Yassar et al.[29], the synthesis of rubrene proceeds via a stepwise transformation. The process begins with a dimerization of two molecules of chlorotriphenylallene **[57]**, forming a bis(allenic) diradical intermediate **[59]**. This intermediate is stabilized through electron delocalization. It then undergoes sequential dehydrohalogenation, eliminating hydrogen chloride (HCl), which increases π-conjugation and extends the delocalized system. The resulting polycyclic intermediate **[61]** subsequently undergoes electrocyclic ring closure to yield rubrene. However, an alternative cyclization pathway can occur, leading to the formation of bis(alkylidene)cyclobutene as a byproduct. This undesired structure arises from an unfavorable ring closure that fails to achieve aromatic stabilization.

Multiple synthetic strategies were explored based on different literature procedures to obtain the desired rubrene product. The first attempt followed the one-pot synthesis methodology reported by Yassar et al., wherein the dimerization and cyclization steps were carried out in sequence in a single reaction setup.[29] In this approach, SF-09 was reacted with methanesulfonyl chloride ($MeSO_2Cl$), serving to first activate the hydroxyls leaving group potential and then the ejected chloride serves as a nucleophile generating the chloroallene. To achieve the elevated temperatures required for the subsequent dimerization, xylene was employed as a replacement solvent. However, after seven hours of reaction time, the expected product was not obtained, instead of black solid powder in which the NMR spectrum and ESI values did not correspond to the expected product.

A second attempt was based on the methodology outlined in a patent by Begley et al.[30] In this approach, $MeSO_2Cl$ and NEt_3 were refluxed in toluene at 110 °C for 8 hours.

(Scheme 2.12) The reaction yielded only the starting material. Assuming that longer reaction times might promote dimerization, the reaction duration was extended to 24 and then 48 hours. Despite these adjustments, no significant progress was observed, suggesting that even higher temperature conditions were necessary.

To address this, mesitylene was used as the solvent to allow the reaction to proceed at an elevated temperature of 170 °C. An excess of $MeSO_2Cl$ was also used to ensure sufficient chlorination. Nevertheless, the resulting ^1H NMR spectrum remained inconsistent with the expected rubrene structure. Some spectral features suggested that chloroallene may have formed during the reaction; however, attempts to isolate it via column chromatography were unsuccessful, and effective separation was not achieved.

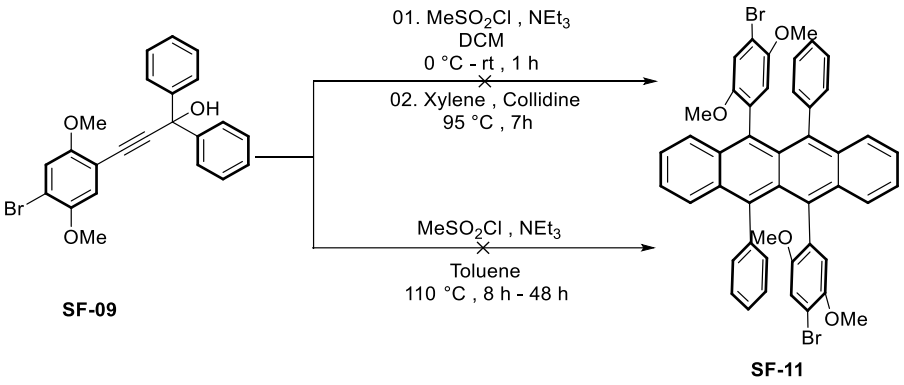

Scheme 2.12 – Synthesis of rubrene

One significant drawback of synthesis pathway-I was the high yield of the disubstituted product in the Sonogashira reaction, which necessitated multiple repetitions of the procedure to obtain adequate quantities of propargyl alcohols for the

final rubrene synthesis step. To address this limitation while also investigating the impact of two bromine atoms on singlet fission efficiency and the viscosity of liquid rubrene derivatives Synthesis Pathway-II was pursued. This alternative approach enabled the synthesis of rubrene from intermediate SF-12**.**

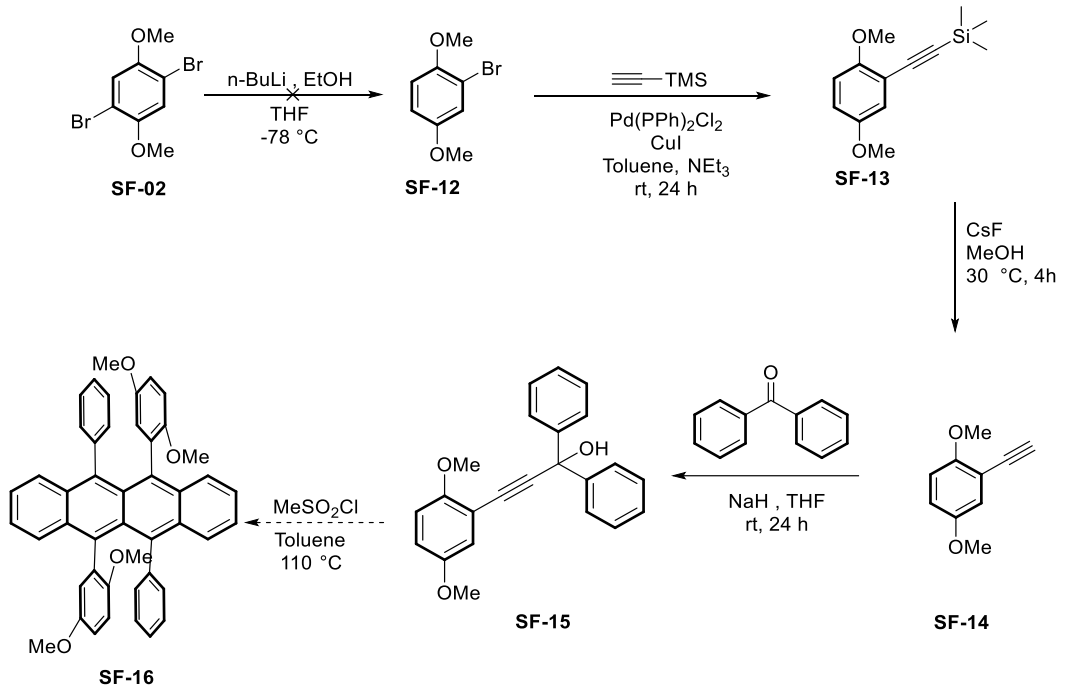

Scheme 2.13 – Rubrene synthesis pathway – II

The reaction conditions for Synthesis Pathway-II were largely optimized based on insights from the previous synthesis pathway. The initial step in this five-step process involved the synthesis of a mono-bromo-substituted dimethoxybenzene derivative. Due to the high yield and ease of separation, the first approach relied on a halogen–metal exchange reaction to obtain the mono-bromo-substituted product SF-12. In this method, SF-02 was treated with *n*-butyllithium (*n*-BuLi) to induce monolithiation, followed by

quenching with ethanol to facilitate protonation. However, this attempt was unsuccessful, resulting in the recovery of the starting material along with SF-01.

As an alternative, a milder bromination method was employed using NBS in the presence of DMF at room temperature. This reaction yielded a significant amount of SF-12, but a considerable quantity of DMF remained with the product even after purification via column chromatography, posing a challenge for downstream processing.

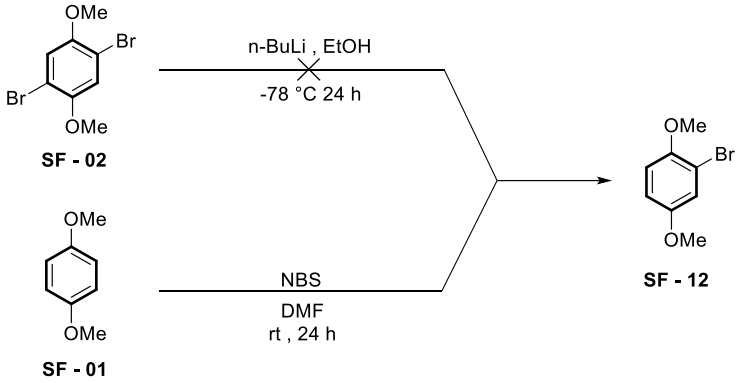

Scheme 2.14 – Mono bromination reaction

Then the Sonogashira reaction was carried out under the same conditions utilized in the previous synthesis pathway. Instead of the expected product a dialkyne was obtained in attempt 01. Due to the unexpected outcome, an alternative synthetic methodology was pursued which was successful and resulted in the expected Sonogashira reaction product SF-13. The revised conditions are outlined in **Table 2.2.**

	Attempt 01	Attempt 02
Starting material	1 equivalent	1 equivalent
CuI	5 mol%	1 mol%
$Pd(PPh)_3Cl_2$	5 mol%	2 mol%
TMS-Acetylene	2 equivalents	2 equivalents
Base	NEt_3	Piperidine
Solvent	Toluene	Piperidine
Temperature	Rt	110 °C
Result	1,3 - butadiene	SF-13

Table 2.2 – Sonogashira reaction conditions

The reaction was quenched with water, and solvent extraction was carried out using sodium bicarbonate ($NaHCO_3$) as the aqueous phase, with the product (SF-13) extracted into hexane. Following this, the Sonogashira reaction, deprotection, and nucleophilic addition steps were conducted as described in the previous pathway, successfully yielding intermediates SF-14 and SF-15, respectively. However, when the propargyl alcohol (SF-15) was subjected to the rubrene synthesis step, the expected product SF-16 was not obtained.

Due to the unsuccessful synthesis of substituted rubrene through both synthetic pathways, efforts shifted toward optimizing the reaction conditions. In an attempt to determine if the failure of the final step was a problem with the published methodology in our hands, the focus turned to the synthesis of non-substituted rubrene, using

phenylacetylene as the starting material. Phenylacetylene was subjected to a nucleophilic addition reaction in the presence of NaH and benzophenone, yielding propargyl alcohol SF-17. This intermediate was then used in the rubrene synthesis following the methodology outlined by Begley et al.[30]

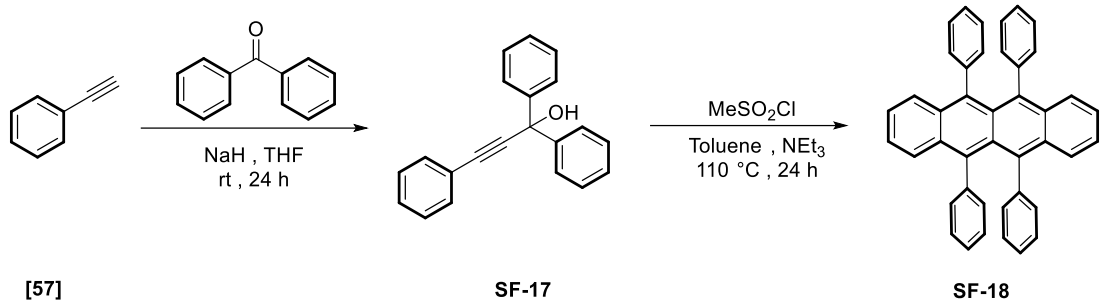

Scheme 2.15 – Rubrene synthesis pathway – III

After the 24 hours of reaction time, propargyl alcohol was converted into rubrene (SF-18)**,** which formed as a bright red solid. The presence of rubrene was confirmed through NMR spectroscopy and ESI-MS. Gratifyingly this result gave us confidence in our ability to perform the final step on an unsubstituted starting material. Initially, the prepared rubrene exhibited a bright red in $CHCl_3$,however after a few hours, the solution underwent a noticeable color change, shifting to light yellow likely from reaction with oxygen. Despite the transformation, it was confirmed from the NMR spectrum after few hours that the reaction had indeed occurred under the given conditions. It is possible that the substitution groups hindered the dimerization process.

In their studies, Yassar et al.[31] successfully isolated the chloroallene in a two step rubrene synthesis pathway instead of one pot synthesis. Therefore, another attempt was undertaken to synthesize chloroallene with the objective of isolating the compounds and

optimizing the conditions for its dimerization. The synthesis of chloroallene was carried out following the methodology described by G.V. Karunakar et al.'s study on the conversion of propargyl alcohols to chloroallene using $TiCl_4$.[31]

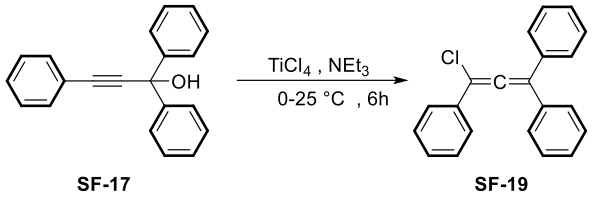

Scheme 2.16 – Synthesis of unsubstituted chloroallene

After 6 hours of reaction and workup, a complicated and inseparable reaction mixture was obtained. ESI confirmed the presence of the desired product, rubrene, although only as a trace. Therefore, the same reaction conditions were applied to the obtained the substituted chloroallene SF-20; but reaction did not proceed successfully.

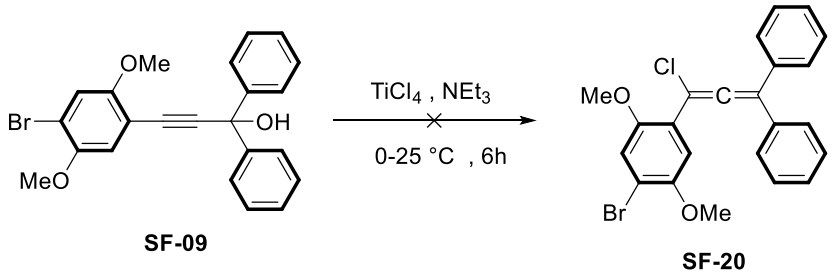

Scheme 2.17 – Attempted synthesis of substituted chloroallene

As the one pot synthesis of rubrene was unsuccessful, efforts continued with the dimerization of chloroallene for rubrene synthesis. Meanwhile an alternative approach was explored, yielding a distinct rubrene isomer compared to synthesis pathway-II. This method follows a similar strategy to that described by Allen and Gillman, starting with an established tetracene core containing 5,12-napthacenequinone.[32] The synthesis involves an initial double conjugate addition of two phenyl rings using phenyl magnesium bromide yielding diphenylnaphthacenequinone. Subsequently, the addition of dimethoxy substituted phenyllithium, followed by reductive aromatization, leads to the formation of rubrene derivatives, as depicted in Figure 2.18

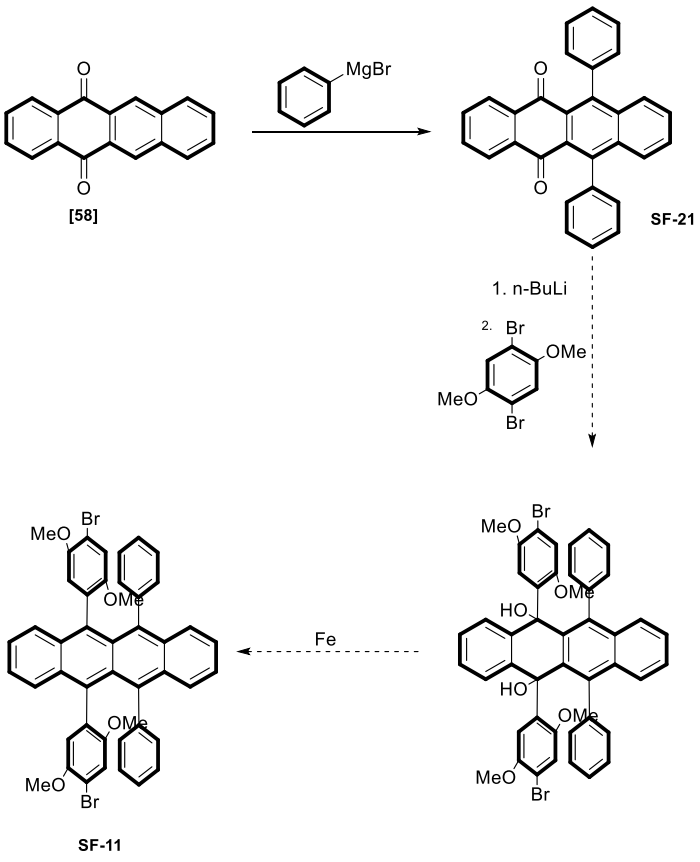

Scheme 2.18 – Synthesis of rubrene pathway – IV

The initial attempt on the Grignard reaction was conducted precisely following the methodology outlined by Allen and Gillman.[32] Instead of yielding the expected product, the reaction resulted only in the recovery of the starting material. Thereafter multiple attempts were made to synthesize diphenylnaphthacenequinone in accordance with the methodology by Peter Ribar et al.[34] In the first attempt, the 2:1 ratio of Grignard reagent to starting material was employed and the reaction was proceeded at room temperature for 14 hours, only the starting material was recovered indicating no significant product formation. A subsequent attempt increased the Grignard reagent to 20 equivalents with no observable reaction progress.

The third attempt was involving the *in-situ* synthesis of the Grignard reagent at the same number of equivalents, but the results remained unpromising. The fourth attempt was using fresh Grignard reagent at 10 equivalents showed some evidence of the product formation based on TLC and NMR spectra, but the product yield was not sufficient for the purification, a final attempt with higher temperature and extended reaction times still gave incompatible NMR spectra which failed to provide clear evidence of the desired product. As the fourth attempt showed some signs of success, future efforts will focus on optimizing the reaction conditions or modify the synthesis strategy to obtain the desired product. All the experiment conditions were shown in detail in **Table 2.3**.

Starting Material	Equivalence	Temperature	Reaction Time
$PhMgBr_{(old)}$	2	25 °C	2 h
$PhMgBr_{(old)}$	2	25 °C	14 h

PhMgBr (in situ)	20	25 °C	14 h
PhMgBr(new)	10	25 °C	24 h
PhMgBr(new)	20	35 °C	48 h

Table 2.3 – Reaction conditions for the synthesis of diphenylnaphthacenequinone.

During the synthesis of rubrene, some additional reactions were conducted utilizing byproducts generated during the reaction pathway-I. Notably, the Sonogashira reaction resulted in a significant yield of compound SF-04 and SF-10**,** which is no longer applicable to the objectives of the current project. Therefore, some attempts were undertaken out of scientific curiosity to investigate the potential synthesis of macrocycles from SF-10.

The initial attempt to synthesize SF-22 involved the use of a pyrene moiety and the Lewis acid $TiCl_4$. $TiCl_4$ facilitated the elimination of tertiary alcohol and leading to the formation of a highly reactive electrophilic propargyl cation. This intermediate subsequently reacted with the nucleophilic pyrene core, promoting ring formation via electrophilic substitution. The reaction failed to yield the expected product.

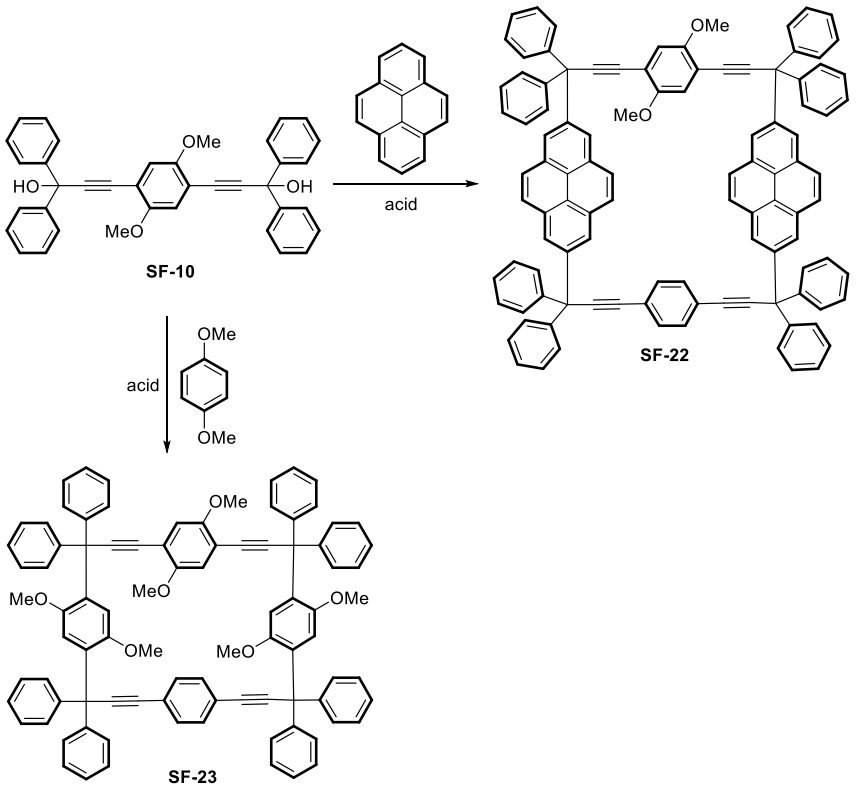

Scheme 2.19 - Attempted synthesis of macrocycles (SF-22 and SF-23)

Then, a milder Lewis acid $ZnCl_2$ was employed along with an extended reaction time to improve the outcome. Despite the modifications the experiment was unsuccessful. In the third attempt, instead of pyrene SF-01 was used as the nucleophile for the macrocyclization reaction with $TiCl_4$ to synthesize SF-23. The reaction again failed to synthesize the desired product. Assuming that the steric hindrance of the two phenyl groups attached to the tertiary carbon affects the reaction and the same procedure was followed using SF-04 and $TiCl_4$ but as indicated in scheme 2.20 the attempt was not successful. that attempt also not succeeded. Although the experimental conditions employed did not yield the desired results, further efforts will be made to the synthesis of macrocycles.

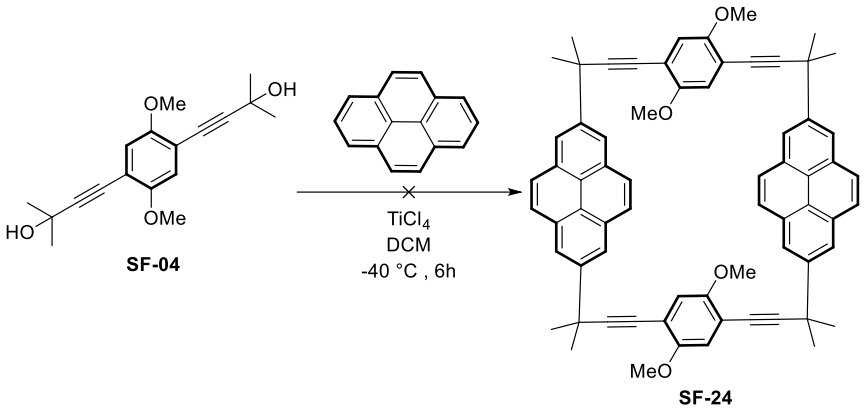

Scheme 2.20 – Attempted synthesis of macrocycle SF-24

According to J. Michl et al.[2] the substituted acene 5,12-diphenyltetracene (DPT) is a promising candidate for undergoing singlet fission. Several attempts were made to synthesize non substituted and substituted DPT. The experimental conditions established by Peter Ribar et al.[33] used were employed, utilizing n-BuLi for the addition reaction.

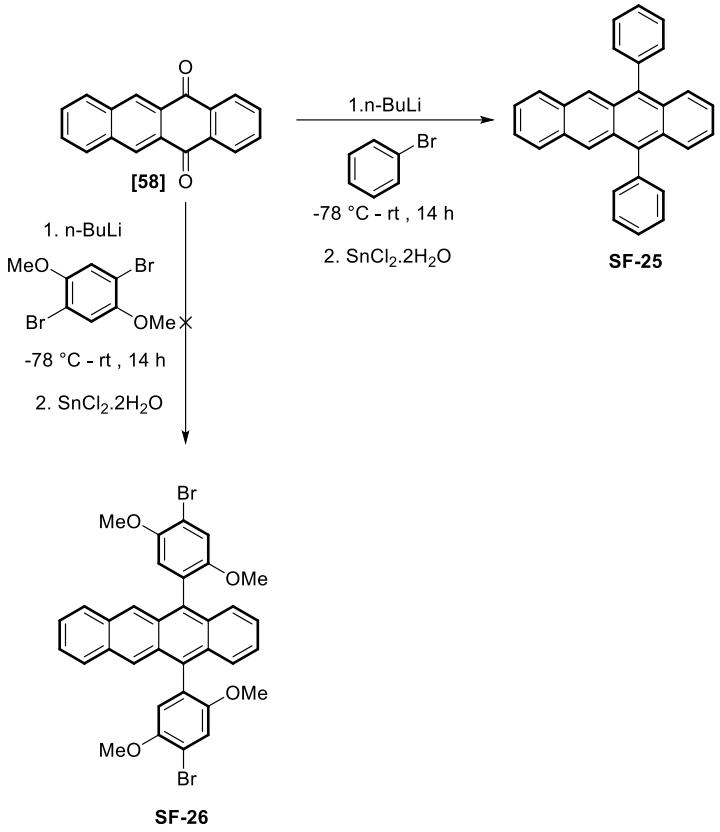

Scheme 2.21 – Attempted to synthesize substituted PDT

After 14 hours of reaction time, both experiments resulted in complex reaction mixtures, however, ESI analysis confirmed the successful synthesis of SF-25. Moving forward, further optimization of reaction conditions will be pursued to enhance yield and reproducibility in future studies.

SF-2, synthesized in this project, served as the starting material for project 02, as outlined in Chapter 03. Consequently, according to scheme 2.22 several attempts were made to synthesize SF-28 and SF-30 as starting materials for chapter 03 to evaluate the impact of long-chain alkyl groups substitution in chapter 03. Additionally, those materials can be utilized in the synthesis of rubrene derivatives.

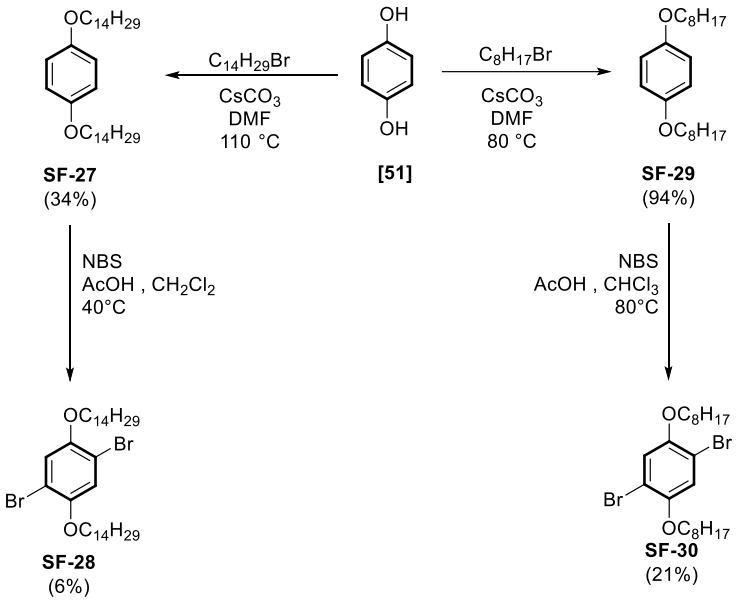

Scheme 2.22 – Synthesis of SF-27 to SF - 30

Due to the low yields observed, the reaction for the synthesis of SF-30 was temporarily halted. In contrast, the synthesis of rubrene was continued utilizing SF-30. For the alkylation reaction, Cs_2CO_3 was employed as the base. Initially, the reaction with 1-bromooctane was conducted at 110 °C, resulting in a moderate yield of 57%, therefore, to improve the yield of SF-29, the reaction temperature was reduced to 80 °C, which led to a significant increment in the product formation up to 94%.

In the first attempt at synthesizing SF-30, the same reaction conditions outlined in synthesis pathway-I were followed; but the yield was only 16% assuming that the long chain alkyl groups require higher temperature conditions for the bromination reaction, to enhance the product yield, the reaction was carried out at elevated temperatures using $CHCl_3$ as the solvent along with the AcOH. Then, the SF-30 underwent Sonogashira reaction, deprotection, and nucleophilic addition reactions following the same conditions as described in synthesis pathway-I.

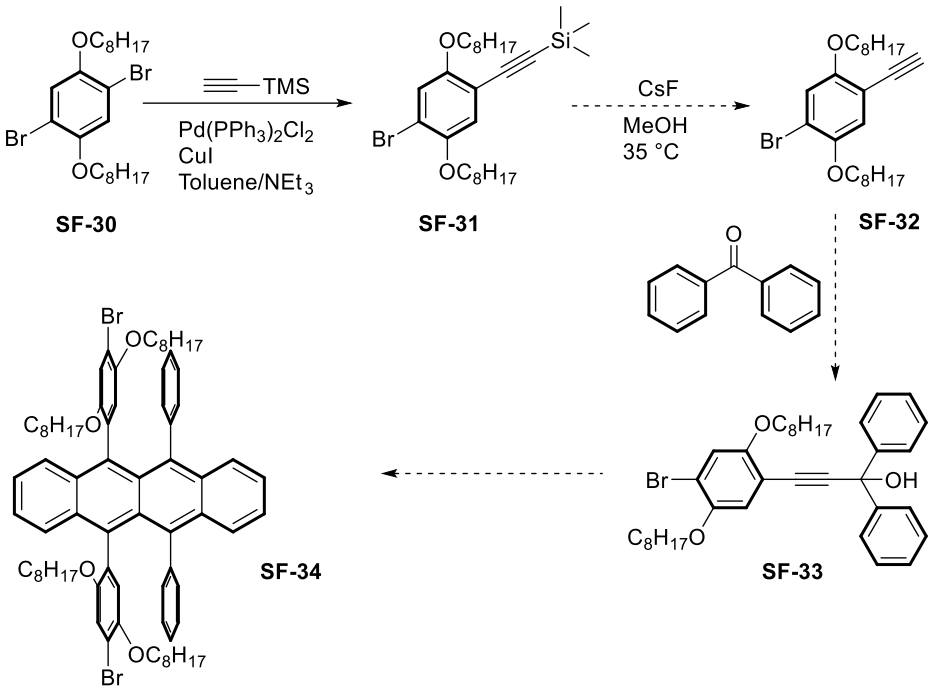

Scheme 2.23 – Rubrene synthesis pathway-V

The Sonogashira reaction successfully yielded the expected product SF-31. But the deprotection reaction did not produce the desired outcome due to the low solubility of SF-31 in methanol. THF was used to enhance solubility; yet the reaction did not yield an NMR spectrum consistent with the anticipated product. Moving forward, it will be necessary to optimize the reaction conditions to ensure successful deprotection and obtain the desired final product SF-34.

n-BuLi was employed at multiple steps across the reaction pathways in this study. Due to its high sensitivity to moisture and the volatility of the hexane solvent, the concentration of n-BuLi varies over time. Therefore, to ensure precise volume measurements, it was necessary to titrate the n-BuLi solution repeatedly. Initially n-BuLi

was titrated using diphenyl acetic acid as the standard, but the endpoint determination was challenging due to the intense of the yellow coloration. To address this issue, an alternative indicator, N-benzyl benzamide (SF-35) was synthesized from benzylamine and benzoyl chloride in the presence of NEt_3 as the base. Upon reaction with n-BuLi, N-benzyl benzamide gives a distinct color change from colorless to blue, which is an easily observable endpoint.

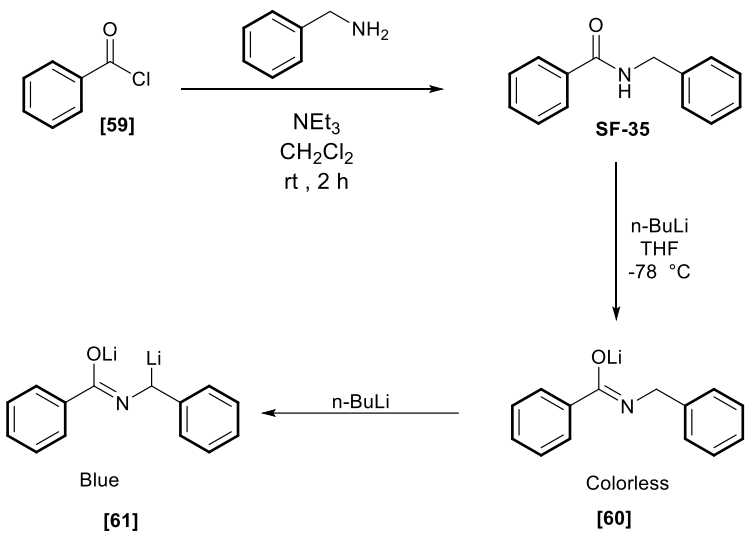

Scheme 2.24 – Synthesis and titration of N-Benzyl benzamide

2.7 Conclusion and Future Directions

One of the main goals of this project is to synthesis novel liquid rubrene derivatives. It is confirmed that the synthesis of solid rubrene (SF-18) was successful while synthesis of novel substituted liquid rubrene derivatives were successful up to the stage of propargyl alcohol.

The future direction of this project is focused on optimizing the reaction conditions for the synthesis of 5,11-bis(4-bromo-2,5-dimethoxyphenyl)-6,12-diphenyltetracene. The optimization will be done by modifying the substitution patterns on the aromatic rings, introduction of electron donating and electron withdrawing groups to evaluate their influence on reactivity and overall yield, explore alternative solvents, catalysts and temperature conditions to minimize by products. Furthermore, investigation of new synthetic routes to replace dimerization of propargyl alcohol to rubrene. Following successful synthesis, the 2,5-dimethoxy groups will be substituted with long chain and branched alkyl groups.

The resulting compounds will be evaluated for their photophysical properties, with particular attention to the effects of substitution patterns, alkyl chain branching and structural isomerization. Rheological characterizations will be performed using the rotational rheometer in the Walsh laboratory to analyse viscosity and flow properties, while photophysical analysis will be carried out in collaboration with Dr. Amy Stevens at the University of Saskatchewan, whose specialized instrumentation and expertise will support the investigation of these materials as potential singlet fission chromophores.

The final goal of this project is to develop liquid-phase novel rubrene derivatives that undergo singlet fission at room temperature and combine its high photophysical performance with favourable rheological properties, paving the pathway for next generation flexible and wearable photovoltaic and optoelectronic devices.

References

[1] J. Michl, *Mol. Front. J.* **2019**, *3*, 84-91.

[2] M. B. Smith, J. Michl, *Chem. Rev.* **2010**, *110*, 6891-6936.

[3] R. Casillas, I. Papadopoulos, T. Ullrich, D. Thiel, A. Kunzmann, D. M. Guldi, *Energy Environ. Sci.* **2020**, *13*, 2741-2804.

[4] H. Rademaker, A. J. Hoff, L. N. M. Duysens, *Biochim. BIophys. Acta,* **1980**, *592*, 240-257

[5] M. C. Hanna, A. J. Nozik, *J. Appl. Phys.* **2006**, *100*, 074510

[6] M. B. Smith, J. Michl, *Annu. Rev. Phys. Chem.* **2013**, *64*, 361-386.

[7] A. Rao, R. H. Friend, *Nat. Rev. Mater* **2017**, *2*, 17063.

[8] S. Mokkapati, D. Saxena, H. H. Tan, C. Jagadish, *Semiconductor Nanowires II: Properties and Applications* **2016**,*9,*1-15.

[9] A. Abate, *Front. Electron.* **2020**, *1*

[10] A. C. Lazaroiu, M. Gmal Osman, C. V. Strejoiu, G. Lazaroiu, *Sustainability* **2023,** *15*,1-24

[11] A. Jain, R. Kothari, V. V. Tyagi, R. Kumar Rajamony, M. Shakeel Ahmad, H. Mohan Singh, S. Raina, A. K. Pandey, *Sustain. Energy Technol.Assess.***2024**, *63*,103632

[12] A. N. Stuart, T. W. Kee, D. M. Huang, *J. Am. Chem. Soc.* **2024**, *146*, 2174-2186.

[13] J. L. Ryerson, J. N. Schrauben, A. J. Ferguson, S. C. Sahoo, P. Naumov, Z. Havlas, J. Michl, A. J. Nozik, J. C. Johnson, *J. Phys. Chem. C* **2014**, *118*, 12121–12132.

[14] G. B. Piland, J. J. Burdett, R. J. Dillon, C. J. Bardeen, *J. Phys. Chem. Phys. Lett.* **2014**, *5*, 2312-2319.

[15] V. M. Nichols, M. T. Rodriguez, G. B. Piland, F. Tham, V. N. Nesterov, W. J. Youngblood, C. J. Bardeen, *J. Phys.Chem. C* **2013**, *117*, 16802–16810.

[16] I. Biaggio, P. Irkhin, *Appl. Phys. Lett.* **2013**, *103*, 263301.

[17] S. Liu, H. Wu, X. Zhang, W. Hu, *Front. Phys.* **2021**,*16,*13304.

[18] A. Ryasnyanskiy, I. Biaggio, *Phys. Rev. B* **2011**, *84,* 193203.

[19] G. B. Piland, C. J. Bardeen, *Chem. Phys. Lett.* **2017**, *669*, 99-103.

[20] O. P. Dimitriev, *Chem. Rev.* **2022**, *122*, 8487-8593.

[21] F. Lu, T. Takaya, K. Iwata, I. Kawamura, A. Saeki, M. Ishii, K. Nagura, T. Nakanishi, *Sci. Rep.* **2017**, *7*,3416.

[22] B. J. Walker, A. J. Musser, D. Beljonne, R. H. Friend, *Nat. Chem.* **2013**,5,1019-1024.

[23] T. Michinobu, K. Okoshi, Y. Murakami, K. Shigehara, K. Ariga, T. Nakanishi, *Langmuir* **2013**, *29*, 5337-5344.

[24] A. Ghosh, T. Nakanishi, *Chem. Commun.* **2017**, *53*, 10344-10357.

[25] F. Lu, K. Jang, I. Osica, K. Hagiwara, M. Yoshizawa, M. Ishii, Y. Chino, K. Ohta, K. Ludwichowska, K. J. Kurzydłowski, S. Ishihara, T. Nakanishi, *Chem. Sci.* **2018**, *9*, 6774-6778.

[26] P. M. Hudnall, *Ullmann's Encyclopedia of Industrial Chemistry*, Wiley, **2000**.

[27] M. M. Heravi, M. Ghavidel, L. Mohammadkhani, *RSC Adv.* **2018**, *8*, 27832-27862.

[28] M. A. A. Aleixo, T. M. Garcia, D. B. Carvalho, L. H. Viana, M. S. Amaral, N. M. Kassab, M. C. Cunha, I. C. Pereira, P. G. Guerrero, R. T. Perdomo, M. F. C. Matos, A. C. M. Baroni, *J. Braz. Chem. Soc.* **2018**, *29*, 109-124.

[29] D. Braga, A. Jaafari, L. Miozzo, M. Moret, S. Rizzato, A. Papagni, A. Yassar, *Eur. J. Org. Chem.* **2011**, 4160-4169.

[30] W. J. Begley, M. Rajeswaran, N. Andrievsky, U.S. Patent 20060025642A1, **2006**

[31] G. V. Karunakar, M. Periasamy, *J. Org. Chem.* **2006**, *71*, 7463-7466.

[32] B. C. F H Allen, L. Gilman, *This J. Am. Chem. Soc.* **1936**, *58*, 937-940.

[33] P. Ribar, T. Šolomek, M. Juríček, *Org Lett* **2019**, *21*, 7124–7128.

Chapter 03

Organic Spintronics and Functional Molecular Liquids

3.1. Origins of radical chemistry: Gomberg's radical and the evolution of organic radical materials

Organic radicals are molecular entities that possess at least one unpaired electron.[1] Radicals, characterized by their open shell structure, typically exhibit high reactivity which allows them to undergo several chemical reactions such as hydrogen abstraction, dimerization, addition and rearrangement reaction. This means most radicals are short lived species.[2] Apart from the high reactivity exhibited by typical radicals, the presence of an unpaired electron gives rise to special magnetic, optical and redox properties, allowing multiple interesting applications such as spin probes, magnetic materials and optoelectronic materials.[3]

Radicals are categorized into two types based on their charge: neutral and charged. The charged species can be positive or negative. **Figure (3.1)** demonstrates the well studied and *relatively* stable neutral radical 2,2,6,6-tetramethyl-1-piperidinyloxy (TEMPO) **[62]**, 9-fluorenone radical anion **[63]** and dialkoxybenzene radical cation **[64]**.[4]

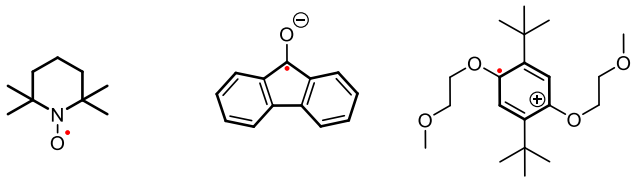

Figure 3.1 – Neutral, Positive and Negative charged Radicals

With respect to their reactivity, radicals can be categorized into three types as transient, persistent and stable radicals. Among them, the most important type of radical is the stable radical, which can be isolated, stored, and handled at ambient temperatures.[5] Stable radicals with unpaired electron(s) were recognized over a century ago due to their considerably long lifetimes to study through conventional spectroscopic methods as electron paramagnetic resonance (EPR) spectroscopy and their selective and controllable nature as opposed to reactive radicals as they can be used in chemistry for the development of novel technological applications using their magnetic and conductive properties.[6]

In the 19th century scientists hypothesized the existence of organic free radicals but after numerous unsuccessful attempts to isolate them, they concluded that carbon must form four bonds and be tetravalent. In 1900, Moses Gomberg discovered "triphenylmethyl," the first persistent trivalent organic free radical **[66]**. Other chemists of that time were doubtful of Gomberg's discovery with many firmly believing that carbon must be tetravalent.[7] While attempting to synthesize hexaphenylethane from triphenyl-methyl bromide Gomberg discovered the triphenylmethyl radical as a highly reactive species favors σ-dimer formation **[67]** as indicated in figure 3.2. The white solid he

obtained from evaporating benzene solvent, was found to be rapidly oxidized in the air and react with halogens, clear indications of the presence of an unpaired electron on the central carbon which was susceptible to dimerization. He observed that the radical could be stored for extended periods in solution and even in the crystalline state. This unexpected stability is caused by the steric hindrance from the surrounding three phenyl rings and their ability to delocalize the unpaired electron across the aromatic system. Although these observations strongly supported the existence of a radical, the concept was debatable at that period. After numerous experiments it was concluded that carbon centered radicals exist and there is an equilibrium between triphenylmethyl radical and its σ-dimer. This discovery paved the pathway for the development of organic radical materials.

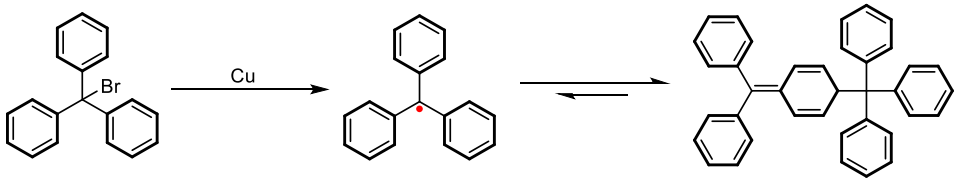

Figure 3.2 - Gomberg's discovery of the triphenylmethyl radical

The triphenylmethyl radical **[67]** is an excellent starting point for the exploration of stability and the persistence of radicals. When considering the stability of the radical the C-H bond dissociation energy (BDE) of triphenylmethyl (81 kcal mol^{-1}) is significantly lower than the BDE of methane (105 kcal mol^{-1}), still triphenylmethyl is relatively stable. Its apparent anomalous stability can be attributed to both kinetic and thermodynamic effects: the interaction between the unpaired electron of the central carbon atom and the π orbitals of the three phenyl rings which result in significant delocalization of the

unpaired electron and additionally, steric crowding of the adjacent phenyl groups results in deviation from planarity, shielding the central carbon atom. [8] The next section of this chapter will explain this in detail.

3.2 How molecular liquidity affects spin transport and radical stability

Due to the high reactivity of unpaired electrons, organic radicals are unstable moieties under most conditions. They can undergo electron transfer reactions and side reactions such as recombination and dimerization. [3] Stability of an organic radical can be induced by steric protection and delocalization of spin density. [3]

Steric protection is a common and highly effective strategy to stabilize organic radicals. This approach naturally prevents organic radicals from interacting with each other and reduces intermolecular side reactions. By employing steric protection through substitution of bulky moieties, the stability of an organic radical can be significantly increased. [3] As an example, the four methyl groups of the TEMPO radical (**Figure 3.1**) provide steric hindrance to prevent intermolecular H-atom abstraction. The propeller like conformation of triphenyl methyl radical by the three surrounding phenyl groups twisted approximately 30°, sterically hindered the spin center and provide the stability to the radical core. In perchlorinated radical where the hydrogens are replaced with heavier chlorine atoms further enhanced the steric protection. The twist angles are increased to ~53° from steric repulsion between each Cl atom and favours the steric shielding of the radical center even in harsh conditions.[9] The extraordinary stability mainly comes from

the six *ortho*-chlorine atoms shielding the central carbon.[6] The chemically inert nature requires extreme conditions to undergo reaction even with molecular oxygen.[6]

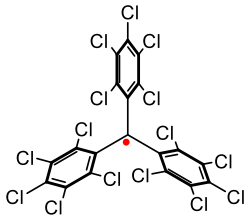

[68]

Figure 3.3 – Sterically hindered perchlorinated triphenylmethyl radical

Most organic radicals undergo dimerization or electron transfer reactions. The delocalization of spin density is one strategy to overcome this. It can be accomplished by three main approaches: extending π-conjugation, introducing polar substituents, and inserting heteroatoms. The extension of π-conjugation stabilizes radicals by delocalizing the unpaired electron over p-orbitals on a larger molecular core sharing spin density across multiple atoms thus reducing the reactivity of the radical.

Phenalenyl **[69, figure 3.4]** is an open shell, π-conjugated neutral and highly unstable radical with fused polycyclic planer molecular arrangement. The spin density of the unpaired electron delocalized in its α-positions, which significantly suppresses its dimer formation tendency.[3] The unpaired electron of the phenalenyl occupies a singly occupied molecular orbital (SOMO) which is delocalized over six carbon atoms located in the outer rings of the molecule **[70]**. Notably, the central carbon atom does not participate in this delocalization as there is no electron density (node) at that position in the SOMO. Phenalenyl consist with one Clar sextet (fully aromatic benzene ring) maintaining the aromatic stability of the molecule. Delocalization of the unpaired electron to the central

carbon atom **[71]** destroys the molecule's one Clar sextet and diminishes the aromatic stabilization. Furthermore, such delocalization would result in a 12π electron annulene which makes this resonance isomer suffer from antiaromatic destabilization energy according to Huckel's rule. Consequently, the phenalenyl avoids that unfavorable configuration and favors the delocalization at the α-position.[6]

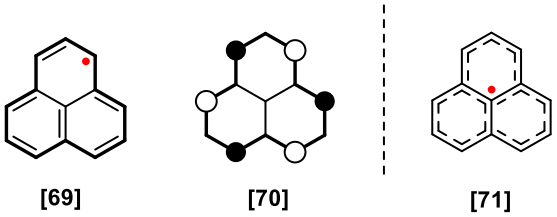

Figure 3.4 – The resonance structure of the Phenalenyl radical

The introduction of polar substituent groups such as electron withdrawing and electron donating groups can improve the stability of the radical by the distribution of unpaired electron through conjugation and inductive effects. As an example, electron withdrawing groups can reduce the affinity of electron transfer reactions between the radical and molecular oxygen. By incorporating both electron withdrawing and electron donating substituents or positive and negative charged substituents stability of a neutral radical can be increased. This process is called as synergistic captodative effect.[10] Incorporating hetero-atoms also stabilizes the radical center as they are efficient spin density carriers. Commonly, N, O and S centered radicals have higher stability as their tendency to form strong σ bonds is relatively low due to the repulsions between lone pairs. Their reactivity with oxygen is relatively lower than the carbon centered radicals as seen in TEMPO.[3]

Although the transition from solid to liquid is not inherently beneficial for the stability of the radical, there is a notable overlap between the strategies used to stabilize radicals and those that promote the liquefaction of polycyclic aromatic hydrocarbons as depicted in **Chapter 01**. This fortuitous overlap provides a unique advantage, enabling us to efficiently pursue the development of hybrid liquid radical species. According to the studies of Anthony J. Carrasquillo et al. the intermolecular (bimolecular) reaction between radical species containing long-chain alkyl groups are orders of magnitude slower than unimolecular reactions therefore the dimerization probability is relatively low which stabilizes the single electron center.[11]

According to the studies of Frank Mayo, the cage effect around the condensed phase radicals reduces the likelihood of encountering other reactive species which prolongs the lifetime by preventing side reactions.[12] The long-chain alkyl groups may have the ability to shield the C center by forming a sphere around the radical molecule. Radicals in the gas or solid state can undergo rapid recombination reactions due to their high mobility or close proximity. Liquefaction can reduce the radical diffusivity to slow down the bimolecular reactions.

The combination of open shell configuration and chemical stability is applied in radical mediated polymer synthesis, (co)catalysts in redox reactions, EPR imaging and have developed into promising candidates in the development of materials with magnetism and conductivity properties.[6] The major interest of this study is to apply stable organic liquid radicals in spintronics.

3.3. Historical context of spintronics, leading into organic spintronics

The electron is an elementary particle that carries inherent angular momentum known as electron spin. Advancements in nanotechnology have recently allowed the utilization of spin into a new concept called spintronics.[13] Spintronics or spin transport electronics, is a rapidly emerging field of science and technology. It is expected to have a notable impact on the future of electronics.[14] In spintronics, as opposed to traditional electronics, spin rather than charge is utilized. By utilizing the intrinsic spin of electrons, researchers aim to enhance the performance of electronic devices and introduce innovative functionalities to them. Therefore, it is a revolutionary approach for data processing and storage of data.[15]

The field of spintronics emerged from the groundbreaking discovery of giant magnetoresistance (GMR) in 1988 by the two scientists Albert Fert and Peter Grunberg. It laid the foundation for spin based electronic devices as before that the conventional electronics were based only on the charge of the electron.[15] In 2007, the Nobel prize in Physics was awarded to them for the discovery of GMR and set the foundation for spintronics. The theoretical proposal of Datta and Das on spin field effect transistors in 1990 marked another significant improvement in spintronics which opens the pathway for spin-based electronics with lower power consumption and higher efficiency.[16] In early 2000s organic spintronics emerged as an extension of the broader spintronics field.

3.4 Key developments in organic spintronics

Organic spintronics (OS) emerged as an alternative option to inorganic spintronics, utilizing the distinct characteristics of organic materials. It is an emerging interdisciplinary field that seeks to merge the advantages of organic chemistry with the degree of freedom resulting from electron spin in spintronics. The immense potential of synthetic chemistry to enable tunable electronic properties positions OS as a promising alternative to inorganic, metal-based spintronics.[17] From the first studies on organic spin valves in 2004 by Xiong et al. towards potential spintronics applications in magnetic random access memory, OS are further developed into spin valves with photo responsiveness, molecular spin photovoltaic devices, spin OLEDs and pure spin current type molecular spintronic devices.[18]

Organic molecules typically have long relaxation times and low spin-orbit coupling compared to metals. Spin-orbit coupling (SOC) is the interaction between the spin and the orbital angular momentum of a charged nucleus. Typically, the strength of the spin-orbital coupling is proportional to the fourth power of the atomic number. Most of the organic molecules are made from lightweight elements such as C, H, O and N which have low SOC which resulting long spin relaxation times. Those properties have been used in molecular spintronics recently. [19]

The development of OS has the potential to revolutionize the data processing and storage technologies by facilitating low power, potentially faster and non-volatile memory devices. The cheapness, chemically interactivity, flexibility and light weight of the organic chromophores allow the designing of novel electronics for various applications.[19]

3.5 Takahashi's recent work on spin hydrodynamic generation in metallic systems

Spin hydrodynamic generation (SHDG) involves generating an electric voltage via spin current from the coupling between the angular momentum of fluid flow and electron spin. It converts fluid kinetic energy into electricity without the requirement of an external magnetic field. SHDG is the bridge between spintronics and microfluidics. Since 2015, the phenomenon of spin hydrodynamic generation (SHDG) has gained significant attention, particularly following the studies by R. Takahashi et al. focused on SHDG in liquid mercury (Hg).[13]

The experiment used narrow quartz channels to flow liquid Hg under controlled flow conditions at room temperature. The chemically inert Pt electrodes are embedded in channel walls to measure the generated voltage difference between the channels. This setup allowed Takahashi et al. to observe SHDG from fluid motion. In their study they also observed that the generated voltage is solely based on a spin mediated process rather than being related to electrification or thermoelectric effects. They have proved that fluid dynamics can be converted into electricity without an external magnetic field.[13]

Their studies based on liquid Gallium (Ga), which has a weaker spin-orbital interaction compared to mercury (Hg) generated higher voltage than Hg which proves that the materials with lower spin orbital interactions are more suitable for SHDG. In 2020, research indicated that laminar flow has an energy conversion efficiency 10^5 times higher than turbulent flow. This discovery facilitates the miniaturization of fluid spintronics for applications such as micro- or nano-scale flow sensors, active cooling systems, and semiconductors.[20]

Takahashi's exceptional work on SHDG represents a significant step in spintronics because of its implementation in a new state of matter. The ability to generate spin current from fluid motion without an external magnetic field led to the development of more flexible and miniaturized spin-based devices and a positive environmental impact offering a cleaner and more sustainable energy solution.

3.6 Development of liquid state model compounds for organic spintronics

Molecular liquidity can significantly influence spin transport in several ways. The viscosity and the molecular diffusion in liquids govern the transport of spins. In low viscous liquids spins can diffuse freely, enhancing the ability to transport over long distances but in high viscous liquids have low spin transport speed but spin coherence times may increase due to the reduced molecular collisions.[21] Based on those factors, liquefaction positively affects the spin transport process. Therefore, liquid state molecular systems are good candidates for organic spintronics.

The observed overlap between strategies for liquefying polycyclic aromatic hydrocarbons (PAHs) and those used to stabilize organic radicals presents a valuable opportunity to address the longstanding challenge of realizing organic spin hydrodynamic generation (SHDG). Specifically, the incorporation of bulky alkyl groups can simultaneously promote radical stability and induce a liquid state—key prerequisites for SHDG candidate materials. To function effectively, such a material must (1) contain one or more unpaired electrons, (2) exhibit low intermolecular reactivity or a minimal tendency to dimerize, and (3) exist in the liquid state. While persistent radicals are

convenient, long-term stability is not strictly necessary if the system is isolated from reactive species like molecular oxygen. Ideally, the radical should be liquid at room temperature and remain so over a broad range to allow for flow testing across different thermal conditions, though simply being liquid at its melting point is sufficient for initial proof-of-concept demonstrations. A final, practical consideration is (4) the compound's synthetic accessibility and scalability, as sufficient material is required to generate measurable flows.

The confluence of these four demanding criteria: spin presence, reactivity control, fluid state, and synthetic practicality poses a significant design and synthesis challenge. However, certain well-characterized systems offer promising starting points. The triphenylmethyl radical, for instance, has been extensively studied and is known to be compatible with liquefaction strategies. When appropriately functionalized with sterically bulky groups, it also achieves a balance between radical persistence and manageable reactivity, making it a strong candidate for early-stage SHDG exploration.

3.7. Extension to long alkyl chain functionalization to introduce liquidity and enhance processability

Functionalizing organic molecules with long alkyl chains has become a widely utilized strategy in organic chemistry to improve liquidity to exist in a fluid state and apply processability to easily handle in manufacturing processes. The length of the alkyl chain, branching patterns and the position of the alkyl substitution are crucial factors to control the physical properties of the organic radicals.[22] The length of the alkyl chains

must be carefully maintained to ensure that they are long enough to reduce the π-π interactions while being short enough to minimize van der Waals interaction between neighbouring alkyl chains.[23] This concept can be used for the manufacturing of printable organic electronics.[22]

Functionalized the organic molecules with branched alkyl chains derived from the Guerbet alcohols also have the ability to inhibit the π-π interactions between the aromatic core and reduce the viscosity of the liquid molecules.[22] They also have the ability to disrupt regular packing of the molecules which may reduce the crystallinity[24] which is beneficial for the processability and this feature can be used in thin film applications.

3.8. Results and Discussion

Based on the previously mentioned concepts specially the studies of R. Takahashi et al. on the SHDG and T. Nakanishi et al. on liquid organic molecules, the goal of this project is to synthesize stable, organic liquid radical molecules capable of SHDG at room temperature conditions. In the radical synthesis pathway, various strategies have been employed to generate the final product in alignment with the previously outlined concepts.

According to Robin G. Hicks,[6] the tris(2,6-dimethoxyphenyl) methyl radical which is monomeric and relative stabile in air, has the propensity to from unusual peroxides by the reaction with oxygen in the solution form. In this study, the 2,5-substituion pattern of alkyl groups (methoxy groups) has reduced the peroxide formation.[6] The methoxy groups were substituted in the first step as the first radical precursor. Despite the small size of the methoxy groups chemically its electron donating ability, enhancement of

solubility of the compound, and it can serve as a convenient handle for alkylation reaction which allows the substitution with bulky alkyl groups.

According to the studies of Wilhelm P. Neumann et al. on triphenylmethyl radical dimerization, either donors or acceptors in the para position reduce the probability of dimer formation.[25] In this study, three bromine atoms were introduced onto the para position to achieve this effect. The incorporation of bromine atoms into the liquid radical increases the viscosity and improves the stability of the liquid chromophore.[26] The 2,5-substitution pattern, where one alkyl chain extended inwards and one outward reduces the intermolecular alkyl chain interactions and reduce the crystallization ability of the liquid chromophore.[27]

The first step of the radical synthesis pathway was the synthesis of tris(4-bromo-2,5-dimethoxyphenyl)methanol (**SF-36)** from the starting material 1,2-dibromo-2,5-dimethoxy benzene (**SF-02**). Synthesizing **SF-02** has described in chapter 02 with a detailed mechanism. As indicated in scheme 3.1 the same procedure that Peter Ribar et al. used in their first synthetic step for creating triangulene precursors[28] was followed to synthesize the tertiary alcohol.

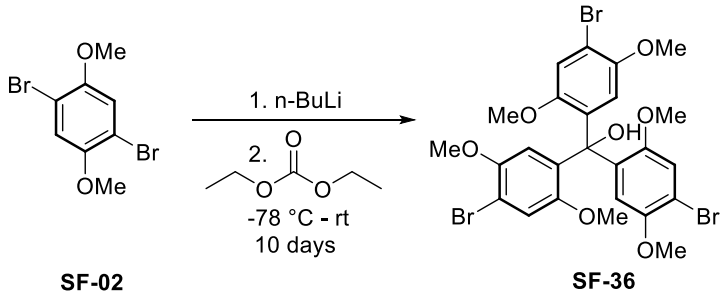

Scheme 3.1 – Synthesis of tris(4-bromo-2,5-dimethoxyphenyl)methanol (SF-36)

Three equivalents of SF-02 were dissolved in dry THF under a nitrogen atmosphere and reacted with three equivalents of *n*-BuLi for the halogen metal exchange reaction at -78 °C and a yellow solution was observed. Maintaining a temperature of -78 °C was critical to ensure controlled exchange, limit side reactions, stabilize intermediates, and prevent undesired products. Following two hours of stirring at -78 °C, diethyl carbonate was gradually added dropwise due to the reaction's exothermic nature. In this step, the nucleophilic organolithium attacked the electrophilic carbonyl carbon of the diethyl carbonate, yielding trityl alcohol after a triple nucleophilic addition. The reaction was conducted on a multigram scale to add low molecular weight diethyl carbonate accurately. The reaction mixture was stirred at room temperature for 10 days, then the dark brown reaction mixture was quenched with water. The resulting product, a white powder, was purified using column chromatography. Despite the prolonged stirring, the reaction had a relatively low yield of 4%, as a significant portion of the starting material remained unreacted.

The second step for the radical synthesis reaction involves the substitution of the alcohol group by a chlorine atom (scheme 3.2). The halogenation of the tertiary alcohol using hydrochloric acid proceeds through S_N1 type reaction mechanism. In this process, the hydroxyl group is protonated by the HCl, forming water as a good leaving group leading to the formation of a stable tertiary carbocation intermediate which is sterically hindered by the surrounding bulky groups. Then the chloride ion attacks the carbocation, resulting the formation of tertiary trityl chloride.

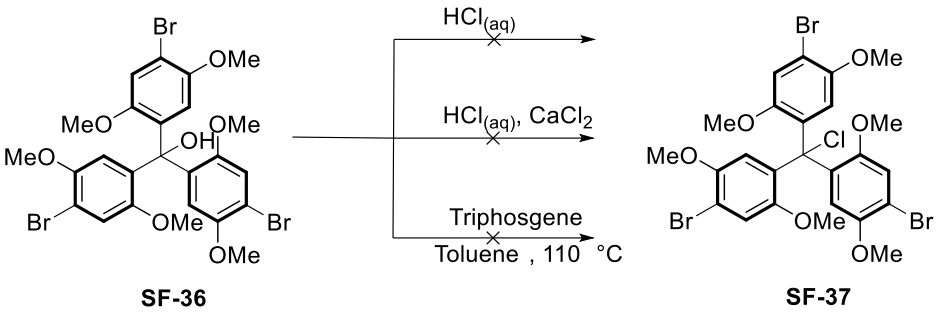

Scheme 3.2 – Attempt to synthesis of 5,5',5''-(chloromethanetriyl)tris(2-bromo-1,4-dimethoxy benzene) **(SF-37)**

Initially, to synthesize SF-37, an excess amount of HCl (10%) was added to SF-36**.** A green solution was observed, assumed to be the tertiary carbocation. After 2 hours of reaction time there was not any significant color change and another 2 hours of vigorous stirring and TLC monitoring did not give a positive result. Then method 02 was followed according to Lu Zhang et al.[29] Addition of excess of HCl (12%, 5 mL) and $CaCl_2$ (0.50 g) into the starting material dissolved in CH_2Cl_2 and the reaction mixture was stirred vigorously at 25 °C for 5 hours. As TLC gave negative results, stirring was continued for 24 hours. Despite the prolonged reaction time and the green coloration of the reaction mixture, starting material still remained and no success was observed based on the TLC monitoring.

Then the third methodology was followed according to the studies of Chen Jun et al.[30] using triphosgene as the halogenating agent. Staring material was dissolved in toluene and NEt_3 was added to the reaction and then triphosgene was added quickly to the reaction mixture. Initially, the reaction was stirred at room temperature, but still the starting material is remaining in the reaction therefore, an excess amount of triphosgene

was added and the reaction was refluxed for 24 hours to obtain the **SF-37**. As TLC analysis looked promising, column chromatography was done to separate the product. Unfortunately, when the compound was subjected to NMR spectroscopy the spectra indicated that the product had been converted back to the starting material although the TLC analysis indicated the presence of a new spot with less polarity. As none of the chlorination reactions succeeded, bromination of the hydroxyl group was attempted as an alternative pathway as bromine is more nucleophilic than chloride due to its size and the lower charge density. Bromination using HBr proceeds through the same mechanism mentioned above.

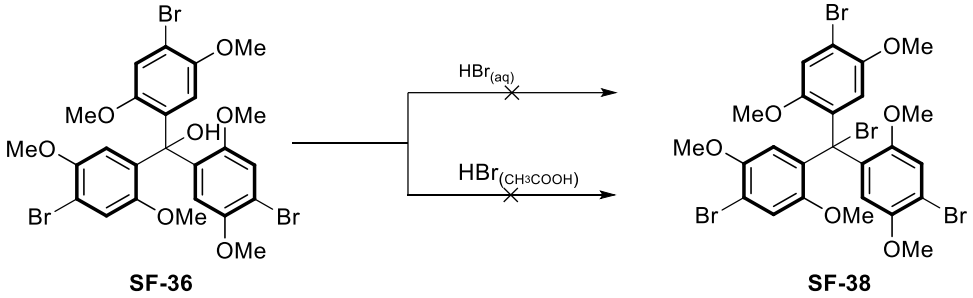

Scheme 3.3 – Attempt to synthesis of 5,5',5''-(bromomethanetriyl) tris(2-bromo-1,4-dimethoxy benzene) (SF-38)

The first attempted synthesis of 5,5',5''-(bromomethanetriyl) tris(2-bromo-1,4-dimethoxy benzene) used an excess of HBr in water with the starting material at room temperature under N_2 atmosphere for five hours but did not give a positive result. It can be caused by the high susceptibility of the carbocation intermediate to nucleophilic attack by water rather than by bromide. The 2,5-substitute dimethoxy groups induce steric

hindrance around the reaction center and prevent approach and attack by Br^-. As a result, smaller and more accessible water reacts with the carbocation, leading to apparent hydrolysis or reversal of the desired transformation.

Next, we sought to omit water from the reaction completely as it appeared product was formed from the appearance of a new spot in the TLC and then converted back to the starting material. Thus, we moved to non-aqueous sources of HBr, and the next reaction was performed using HBr (43% in CH_3COOH) and was subjected to longer reaction times. The resultant brown reaction mixture was first time quenched with water and run through the column and again starting material was obtained. In the next attempt the reaction mixture was directly transferred into the silica column without work up and the product was separated.

The absence of new tertiary carbon peaks in the ^{13}C NMR spectrum implied significant decomposition of the material into starting material [SF-36] under these conditions. Although acetic acid is less nucleophilic than water, it can still promote hydrolysis under acidic conditions. This issue can be hindered by using an anhydrous, aprotic system as HBr in diethyl ether. Further optimization of halogenation reaction could be achieved using ethereal HBr sources.

Since none of the halogenation reactions were successful according to the intended synthesis pathway an alternative route (scheme 3.4) was envisioned to obtain the radical moiety. The plan involved reduction of the tertiary alcohol through a protonation and hydride attack cascade, followed by generating the radical via either direct 1-electron oxidation or deprotonation followed by oxidation of the resulting anion.

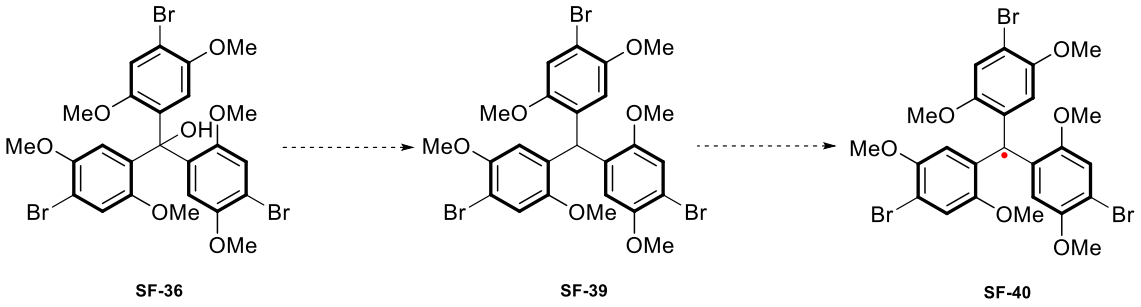

Scheme 3.4 Alternative pathway to synthesize **SF-40**

To synthesize tris(4-bromo-2,5-dimethoxyphenyl)methane **(SF-39),** As indicated in scheme 3.5, **SF-36** was reacted with excess trifluoroacetic acid which acts as the catalyst and the proton source. The observed green solution can be assumed to be the tertiary carbocation, which was reduced by the mild hydride source, triethylsilane. (scheme 3.5) The reduction occurs with high efficiency, resulting in 77% yield. The up-field signal shift of tertiary carbon in the ^{13}C NMR spectrum confirmed the product formation.

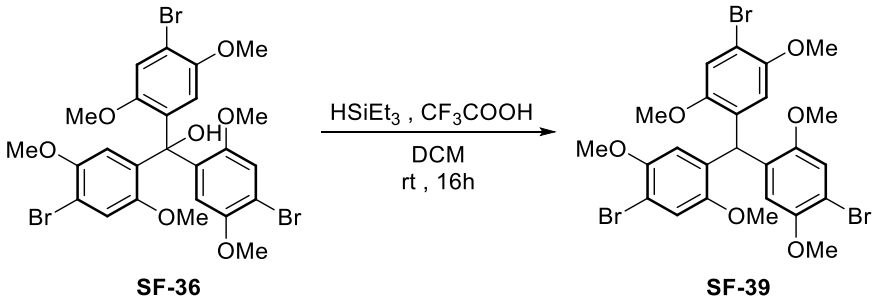

Scheme 3.5 – Synthesis of tris(4-bromo-2,5-dimethoxyphenyl)methane **(SF-39)**

The next attempt involved the hydrogen abstraction from the substituted trityl methane to obtain the stable radical precursor. As the first reaction lithium diisopropylamide (LDA), a strong non-nucleophilic base prepared *in situ* was reacted with **SF-39** for the formation of a carbanion intermediate which subsequently underwent a single electron transfer reaction (ETR) with 2,3-dichloro-5,6-dicyano-1,4-benzoquinone (DDQ) in chloroform-*d* resulting in a non-compatible NMR spectrum. Assuming that the oxidizing strength of DDQ was too strong for the radical synthesis, more selective, less aggressive oxidizing agent *p*-chloranil was used for the radical synthesis. The first attempt with anhydrous THF and *p*-chloranil did not give a positive result therefore anhydrous CH_2Cl_2 was used to increase the solubility of the *p*-chloranil but still the reaction conditions did not give a satisfying result. Then with *p*-chloranil strong bases as tetrabutylammonium hydroxide and potassium tert-butoxide were used but none of the reactions were successful.

Rather than relying on oxidation reactions, the focus shifted to follow radical synthesis pathways directly from the **SF-36.** As the first method Zn dust and HCl, then Cu metal with HCl was added to the **SF-36** and they did not give the intended product. Then, according to the studies of T. Nishiuchi et al.[31] **SF-36** was reacted with $SnCl_2 \cdot H_2O$ and HCl as indicated in scheme 3.6 and the reaction was monitored using NMR spectroscopy and the first evidence of radical formation was obtained by observing a black color change and the characteristic paramagnetic broadening of ^{1}H-NMR peaks which was indicated in the spectrum of **tris(4-bromo-2,5-dimethoxyphenyl)methyl radical (SF-40)** in the appendix.

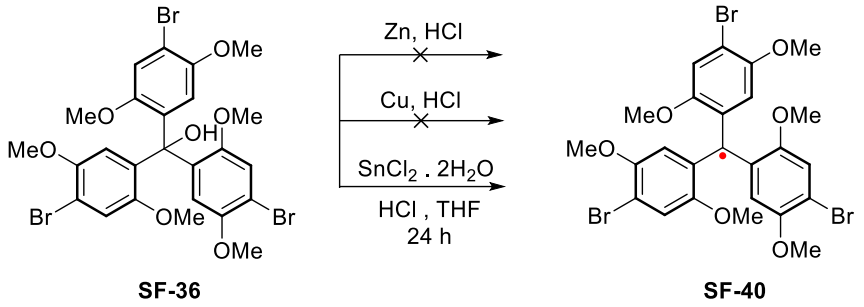

Scheme 3.6 – Synthesis of tris(4-bromo-2,5-dimethoxyphenyl)methyl radical **(SF-40)**

With a viable method to generate the radicals achieved, focus was shifted towards liquifying the system. The synthesis was started again from 1,4-dibromo-2,5-bis(octyloxy)benzene following the trityl alcohol synthesis according to the scheme 3.7 and the radical synthesis reaction. After 10 days of reaction time quenching and column chromatography as previously mentioned, a non compatible NMR spectra with the expected NMR spectrum and starting material were obtained. It is possible that the reaction required more reaction time or increased temperature conditions for the addition reaction due to the increased steric bulk of the aryl substituent.

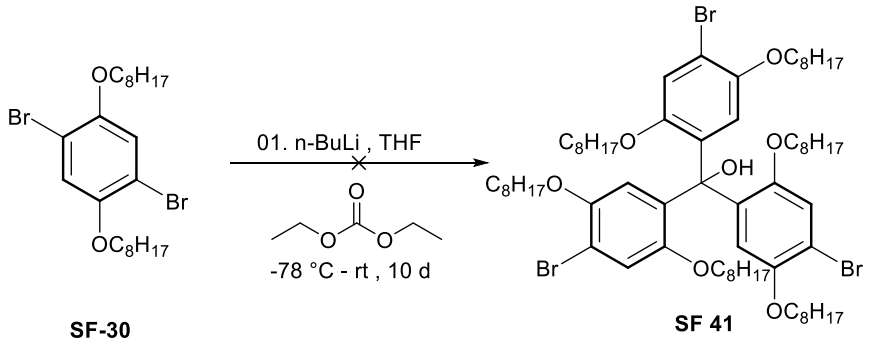

Scheme 3.7 – Synthesis of tris(4-bromo-2,5-bis(octyloxy)phenyl)methanol **(SF-41)**

3.9 Conclusion and Future Directions

One of the main objectives of this project is to synthesize the stable radical compound with 2,5-substituted methoxy groups. Evidence for the presence of the radical was obtained through NMR spectroscopy; but further characterization is required to conclusively confirm the formation and the stability of the radical species. One of the future objectives is to thoroughly investigate and confirm the presence of the radical and its properties. The next step of this project is to substitute methoxy groups with different alkyl groups; long chains and branched alkyl chains; with the aim of synthesizing the solvent-free, non-volatile, liquid radical derivatives that are stable at room temperature.

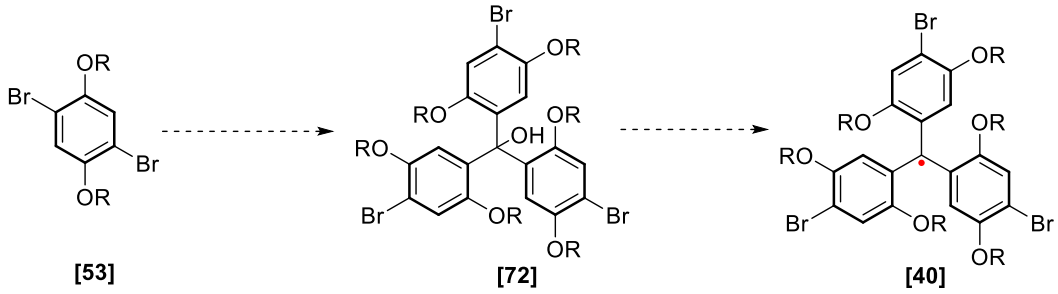

Scheme 3.8 – Synthesis of stable liquid radical derivatives

The next goal of this research is to explore the potential application of liquid radicals in spin hydrodynamic generation, in collaboration with Dr. Can-Ming Hu from the Department of Physics and Astronomy, an expert in the field of cavity spintronics.

Currently stable organic radical derivatives play an important role in advanced materials for energy, quantum applications and magnetism but predominantly focus on

solids and crystalline radicals. The development of solvent-free, room temperature liquid radical derivatives remain a challenge. Therefore, this study contributes to the design of a relatively underexplored chemical space involving non-volatile liquid radicals.

In summary, this thesis discusses the integration of liquidity into functional molecular systems, with the motivation of the development of liquid organic chromophores that undergo singlet fission and spin hydrodynamic generation. The intended FMLs were not entirely realized within the research period. However, both projects made significant progress in the successful synthesis of key intermediates for novel liquid rubrene derivatives and the development of foundational strategies for liquefaction and synthesis of stable radical derivatives. They are important milestones in this study. These results lay a strong foundation for further investigations, especially the achievement fully functionalized molecular liquids with tunable spintronics and optoelectronic properties. The two projects will be continued during my Ph. D. studies under the supervision of Dr. Joshua C. Walsh with collaborative efforts and advanced characterization will further enhance the understanding and applicability of FMLs in next generation of electronics.

References

[1] **2025**, DOI doi:10.1351/goldbook.R05066.

[2] A. Velloth, P. Kumar, S. Butt, S. Venkataramani, *Asian J. Org. Chem.* **2025,** *14*, e202400686.

[3] B. Tang, J. Zhao, J. F. Xu, X. Zhang, *Chem. Sci.* **2020**,*11*, 1192-1204.

[4] C. G. Armstrong, K. E. Toghill, *Electrochem. Commun.* **2018**, *91*, 19-24.

[5] M. Abe, *Chem. Rev.* **2013**, *113*, 7011-7088.

[6] R. G. Hicks, *Org. Biomol. Chem.* **2007**, *5*, 1321-1338.

[7] M. Gomberg, *The Discovery of Organic Free Radicals,* University of Michigan, Ann Arbor, MI, USA, **2000**.

[8] K. J. Romero, M. S. Galliher, D. A. Pratt, C. R. J. Stephenson, *Chem. Soc. Rev*. **2018**, *47*, 7851-7866.

[9] J. Veciana, J. Carilla, C. Miravitlles, E. Molinsb, J. Chem. Soc. **1987**,*109*,2657-2660.

[10] L. Wang, W. Niu, D. Tian, T. Jiao, L. Zhang, X. Hou, Y. Han, Y. Zou, J. Wu, G. Li, *Angew. Chem. Int. Ed.* **2025**, *64, e*202415746.

[11] A. J. Carrasquillo, K. E. Daumit, J. H. Kroll, *J. Phys. Chem. Lett.* **2015**, *6*, 2388-2392.

[12] F. R. Mayo, *J. Am. Chem. Soc.* **1967,** *89,* 2654-2661.

[13] R. Takahashi, M. Matsuo, M. Ono, K. Harii, H. Chudo, S. Okayasu, J. Ieda, S. Takahashi, S. Maekawa, E. Saitoh, *Nature Phys.* **2016**, *12*, 52–56.

[14] S. A. Wolf, A. Y. Chtchelkanova, D. M. Treger, IBM *J. Res. Dev.* **2006**, *50,* 101-110

[15] S. A. Wolf, D. D. Awschalom, R. A. Buhrman, J. M. Daughton, S. Von Molnar, M. L. Roukes, *Science* **2001**, *294*, 1488-1495

[16] S. Datta, B. Das, *Appl. Phys. Lett.* **1990**, *56*, 665-667.

[17] D. Sun, E. Ehrenfreund, Z. V. Vardeny, *Chem. Commun.* **2014**, *50*, 1781-1793.

[18] S. Ding, Y. Tian, W. Hu, *Nano Res.* **2021**, *14*, 3653-3668.

[19] W. J. M. Naber, S. Faez, W. G. Van Der Wiel, *J. Phys. D: Appl. Phys.* **2007**, *40*, R205

[20] R. Takahashi, H. Chudo, M. Matsuo, K. Harii, Y. Ohnuma, S. Maekawa, E. Saitoh, *Nat Commun.* **2020**, *11*, 3009

[21] B. Y. Mladenova, N. A. Chumakova, V. I. Pergushov, A. I. Kokorin, G. Grampp, D. R. Kattnig, *J. Phys. Chem. B* **2012**, *116*, 12295-12305.

[22] S. S. Babu, J. Aimi, H. Ozawa, N. Shirahata, A. Saeki, S. Seki, A. Ajayaghosh, H. Möhwald, T. Nakanishi, *Angew. Chem. Int. Ed. Engl.* **2012**, *124*, 3391-3395.

[23] T. Michinobu, K. Okoshi, Y. Murakami, K. Shigehara, K. Ariga, T. Nakanishi, *Langmuir* **2013**, *29*, 5337-5344.

[24] J. M. Brady, E. L. Thomas, *J. Polym. Sci.* Part B: *Polym. Phys.* **1988**, *26,* 2385-2398

[25] W. P. Neumann, A. Penenory, U. Stewen, M. Lehnig, *J. Am. Chem. Soc.* **1989**, *111,*5845-5851.

[26] F. Lu, K. Jang, I. Osica, K. Hagiwara, M. Yoshizawa, M. Ishii, Y. Chino, K. Ohta, K. Ludwichowska, K. J. Kurzydłowski, S. Ishihara, T. Nakanishi, *Chem. Sci.* **2018**, *9*, 6774-6778.

[27] F. Lu, T. Takaya, K. Iwata, I. Kawamura, A. Saeki, M. Ishii, K. Nagura, T. Nakanishi, *Sci. Rep.* **2017**, *7*, 3416.

[28] P. Ribar, T. Šolomek, M. Juríček, *Org. Lett.* **2019**, *21*, 7124-7128.

[29] L. Zhang, G. Tu, J. Xu, H. Jin, S. Wang, Q. Hu, S. Yang, H. Liu, **2022**, US 2022/0234970 A1

[30] C. Jun, C. Jin, W. Su, **2010**, CN 10171734 A

[31] T. Nishiuchi, K. Takahashi, Y. Makihara, T. Kubo, *Beilstein J. Org. Chem.* **2024**, 20, 2254-2260.

Appendix

Section 01 - Experimental Methods

General Information

All the chemicals were purchased from Sigma Aldrich Co. and Thermo Scientific Co. Ltd. All reactants were used without further purification unless otherwise stated. All manipulations were performed under a nitrogen atmosphere using standard Schlenk techniques. ^{1}H and ^{13}C NMR spectra were recorded on a Bruker 400 MHz spectrometer. Chemical shifts in ^{1}H and ^{13}C NMR spectra are reported in ppm relative to solvent peaks such as chloroform (δ 7.26 for ^{1}H NMR and δ 77.00 for $^{13}C\{^{1}H\}$ NMR). Column chromatography was carried out with 40N silica particle size and all solvents were used as purchased, without any further purification. ESI-MS analysis was performed using a Bruker Compact ESI QTOF Mass Spectrometer System.

01. Synthesis of 1,4-dimethoxybenzene (SF-01)

Method A - To a suspension of hydroquinone (1.00 g, 9.08 mmol) and NaH (1.09 g, 27.2 mmol) in DMF (20 mL), MeI (1.13 mL, 18.2 mmol) was added dropwise under N_2 atmosphere. The resultant dark brown solution was stirred for 24 hours at room temperature. The reaction mixture was quenched with water and dissolved in Et_2O (50 mL). The organic layers were washed with water (2 × 100 mL) to afford a light orange solution, which was dried over anhydrous Na_2SO_4 and concentrated under reduced pressure to obtain a light orange crude product. The crude was purified by silica gel chromatography using EtOAc/Pet. Ether (36-60 °C) (1:9 v/v) to afford a white solid. (0.85 g, 68%).

Method B – The same procedure as **Method A** was followed, and DMF was concentrated under reduced pressure at around 120 °C to afford a black solvent with a pleasant smell which could be the 4-methoxy benzaldehyde. ^{1}H NMR spectrum was not compatible with the expected structure.

Method C - To a suspension of hydroquinone (2.00 g, 18.2 mmol) and NaH (2.18 g, 54.5 mmol) in DMF (50 mL), MeI (2.26 mL, 54.5 mmol) was added dropwise under N_2 atmosphere. The resultant dark brown solution was stirred for 24 hours at room temperature. The reaction mixture was quenched with water and dissolved in EtOAc (50 mL). The organic layers were washed with HCl (1M, 3 x 50 mL) to afford a light brown solution which was dried over anhydrous Na_2SO_4 and concentrated under reduced pressure to obtain a crude product. The crude was purified by silica gel chromatography using EtOAc/Pet. Ether (36-60 °C) (1:9 v/v) and afford a white solid. (1.49 g, 59%)

Method D – To a suspension of hydroquinone (6.00 g, 54.4 mmol) and NaH (3.92 g, 163 mmol) in DMF (80 mL), MeI (6.78 mL, 108 mmol) was added dropwise under N_2 atmosphere. The resultant dark brown solution was stirred for 24 hours at room temperature. The reaction mixture was quenched with water and the DMF was evaporated under reduced pressure. The dark brown mixture was dissolved in EtOAc (50 mL), and the organic layers were washed with LiCl (5%, 3 x 50 mL) to afford a light brown solution which was dried over anhydrous Na_2SO_4 and concentrated under reduced pressure to obtain a crude product. The crude was purified by silica gel chromatography using EtOAc/Pet. Ether (36-60 °C), (1:9 v/v) and afford a white solid. (5.20 g, 69%)

Method E – To a suspension of hydroquinone (2.00 g, 18.2 mmol) and NaH (2.18 g, 54.5 mmol) in DMF (50 mL), MeI (2.26 mL, 54.5 mmol) was added dropwise under N_2 atmosphere. The resultant dark brown solution was stirred for 24 hours at room temperature. The reaction was quenched with water and EtOAc (50 mL) was added to the reaction mixture. The organic layer was washed with LiCl (5%, 3 x 50 mL) to afford a brown solution. The solvent was reduced, and toluene (3 x 20 mL) was added to the white solid with brown solution and the solvent was evaporated under reduced pressure to afford a yellow semi solid crude. The crude was purified by silica gel column chromatography using EtOAc/Pet. Ether (36-60 °C) (1:9 v/v) and afford a white solid.(1.92 g, 76%) ^{1}H NMR (400 MHz, Chloroform-*d*) δ 6.87 (s, 4H), 3.80 (s, 6H). ^{13}C NMR (101 MHz, Chloroform-*d*) δ 153.79, 114.67, 55.77. Calculated for $C_8H_{10}O_2$ $[M]^+$=138.0675, found= 138.0673

02. Synthesis of 1,4-dibromo-2,5-dimethoxybenzene (SF-02)

Method A - To a solution of 1, (**SF-01**, 0.85 g, 6.18 mmol) in Et_2O (20 mL) at -10 °C, Br_2 (0.16 mL, 3.09 mmol) was added dropwise using a dropping funnel. The resultant orange reaction mixture was stirred for 2 hours. Reaction mixture was quenched with water and Et_2O (20 mL) was added to the reaction mixture. The organic layer was washed with water (3 x 50 mL) and dried over anhydrous Na_2SO_4 and concentrated under reduced pressure to obtain a light-yellow crude product. The crude was purified by silica gel chromatography using EtOAc/Pet. Ether (36-60 °C) (1:3 v/v) and afford a white solid. (0.43 g, 24%)

Method B – Method A was followed using CH_2Cl_2 (20 mL) as the solvent. A black powder was obtained which was slightly dissolved in $CDCl_3$. ^1H NMR spectrum was not compatible with the expected structure.

Method C - To a solution of 1,4-dimethoxybenzene (**SF 01**, 0.50 g, 3.62 mmol) in CH_2Cl_2 (25 mL) and acetic acid (25 mL), *N*-bromosuccinimide (NBS, 1.63 g, 9.05 mmol) was added at 0 °C and stirred for 10 minutes. The white suspension was stirred at room temperature for 16 hours. After 16 hours, the reaction mixture has completely turned into a dark orange clear solution. The reaction was quenched by the addition of water and CH_2Cl_2 (50 mL) was added. The organic layer was washed with brine (3 x 50 mL), dried over anhydrous $MgSO_4$ and concentrated under reduced pressure and an orange crude product was obtained. The crude was purified by silica gel chromatography using CH_2Cl_2/Hexanes (2:5 v/v) and afford a white solid. (0.19 g, 18 %)

Method D - To improve the yield of the reaction a solution of 1,4-dimthoxybenzene (**SF 01**, 2.00 g, 14.5 mmol) in CH_2Cl_2 (25 mL) and acetic acid (25 mL), *N*-bromosuccinimide (7.82 g, 43.5 mmol) was added at 0 °C and stirred for 10 minutes. The white suspension was refluxed at 40 °C for 16 hours. After 16 hours, the reaction mixture has completely turned into a dark orange clear solution. After cooling to room temperature, the reaction was quenched by the addition of water and CH_2Cl_2 (50 mL) was added. The organic layer was washed with brine (3 x 50 mL), dried over anhydrous $MgSO_4$ and concentrated under reduced pressure and obtained an orange crude product. The crude was purified by silica gel chromatography using CH_2Cl_2/Hexanes (2:5 v/v) and afford a white solid. (3.64 g, 85

%) ^{1}H NMR (400 MHz, $CDCl_3$) δ 7.03 (s, 2H), 3.78 (s, 7H), ^{13}C NMR (101 MHz, $CDCl_3$) δ 150.55, 117.16, 110.51, 57.04. Calculated for $C_8H_8Br_2O_2$ $[M]^+$=293.8885, found 293.9995

03). Synthesis of 4-(4-bromo-2,5-dimethoxyphenyl)-2-methylbut-3-yn-2-ol(SF-03)

Method A - To a solution of 1,4-dibromo-2,5-dimethoxybenzene (0.100 g, 3.378 mmol), $Pd(PPh)_3Cl_2$ (0.012 g, 0.168 mmol, 5mol%) and CuI (0.003 g, 0.168 mmol, 5mol%) in a solution mixture of NEt_3 (5 mL) and toluene (5 mL), 2-methyl-3-butyn-2-ol (0.033 mL) was added and stirred under N_2 at room temperature for 24 hours. The resultant dark brown solution was quenched with water and EtOAc (50 mL) was added. The organic layer was washed with water (3 x 50 mL), dried over anhydrous Na_2SO_4 and concentrated under reduced pressure and obtained a brown crude product. The crude was purified by silica gel chromatography using EtOAc/Pet. Ether (36-60 °C) (1:3 v/v) and afford the light yellow mono substituted product, 4-(4-bromo-2,5-dimethoxyphenyl)-2-methylbut-3-yn-2-ol (**SF-03,** 0.034 g, 32%). ^{1}H NMR (400 MHz, Chloroform-*d*) δ 7.09 (s, 1H), 6.95 (s, 1H), 3.87 (s, 3H), 3.85 (s, 3H), 1.66 (s, 7H), 1.56 (s, 1H). ^{13}C NMR (101 MHz, Chloroform-*d*) δ 154.49, 149.80, 116.59, 116.56, 112.47, 111.57, 98.70, 77.80, 56.84, 56.64, 31.44, 31.05. Calculated for $C_{13}H_{14}BrO$ $[M]^+$=281.0171, found 281.0170. The column was flushed with EtOAc to afford the brown disubstituted product, 4-(4-bromo-2,5-dimethoxyphenyl)-2-methylbut-3-yn-2-ol. (**SF-04,** 0.259 g, 25 %)

04). Synthesis of ((4-bromo-2,5-dimethoxyphenyl)ethynyl) trimethylsilane (SF 05)

Method A - To a solution of 1,4-dibromo-2,5-dimethoxybenzene (0.500 g, 1.68 mmol), $Pd(PPh)_3Cl_2$ (0.059 g, 0.008 mmol, 5 mol%) and CuI (0.016 g, 0.008 mmol, 5 mol%) in a light yellow solution mixture of Net_3 (10 mL) and toluene (10 mL), trimethylsilyl

acetylene (1.68 mmol, 0.24 mL) was added dropwise and stirred under N_2 at room temperature for 24 hours. The resultant dark brown solution was quenched with water and EtOAc (50 mL) was added. The organic layer was washed with water (3 x 50 mL), dried over anhydrous Na_2SO_4 and concentrated under reduced pressure and obtained a brown crude product. The crude was purified by silica gel chromatography using EtOAc/Hexane (1:9 v/v) and non-separable product mixture of starting material (**SF-01**), mono substituted product ((4-bromo-2,5-dimethoxyphenyl) ethynyl)trimethylsilane (**SF-05**) Calculated for $C_{13}H_{17}BrO_2Si$ $[M+H]^+$= 313.0254, found 317.2410 and disubstituted product ((2,5-dimethoxy-1,4-phenylene) bis(ethyne-2,1-diyl))bis(trimethylsilane) (**SF-06**) were afforded. Calculated for $C_{18}H_{26}O_2Si_2$ $[M+H]^+$= 331.1544, found 331.2584

Method B – Method A was followed using trimethylsilyl acetylene (1.66 mmol, 0.23 mL). A product mixture of **SF-01, SF-05,** and **SF-06** was obtained.

Method C- Method A was followed using trimethylsilyl acetylene (1.64 mmol, 0.22 mL). A product mixture of **SF-01, SF-05,** and **SF-06** was obtained.

05. Attempted synthesis of 1-bromo-4-ethynyl-2,5-dimethoxybenzene (SF-07)

Method A - A mixture of 4-(4-bromo-2,5-dimethoxyphenyl)-2-methylbut-3-yn-2-ol (0.100 g, 0.033 mmol) and K_2CO_3 (0.230 g, 0. 165 mmol) in toluene (20 mL) was refluxed at 110 °C for two hours. The resulting dark yellow solution was quenched with water and EtOAc (30 mL) was added. The organic layer was washed with water (3 x 50 mL) and dried over anhydrous Na_2SO_4 and concentrated under reduced pressure and obtained a bright yellow solid. The solid is slightly dissolved in $CDCl_3$ and ^1H NMR spectrum was not compatible with the expected structure.

Method B – The same procedure was followed with 24 hours of refluxing to obtained a bright yellow solid. ^{1}H NMR spectrum was not compatible with the expected structure.

Method C – The same procedure was followed using K_2CO_3 (0.230 g, 0. 165 mmol) in a mixture of toluene (10 mL) and H_2O (10 mL). ^{1}H NMR spectrum was not compatible with the expected structure.

Method D - Method A was followed using NaOH (10%, 2.5 mL) in toluene (15 mL) and afforded a yellow solid. ^{1}H NMR spectrum was not compatible with the expected structure.

Method E - Method A was followed using KOH (5M, 2.5 mL) in toluene (15 mL) and afforded a yellow solid. ^{1}H NMR spectrum was not compatible with the expected structure.

06. Synthesis of 1-bromo-4-ethynyl-2,5-dimethoxybenzene (SF-07)

Method A – A product mixture of SF-02,SF-05 and SF-06 (0.20 g , 0.63 mmol) was dissolved in methanol (15 mL). CsF (0.96 g, 6.38 mmol) was added to the yellow reaction mixture and stirred at 35 °C for 4 hours in atmospheric conditions. The resultant brown reaction mixture was concentrated under reduced pressure to evaporate the methanol. Subsequently, EtOAc (30 mL) was added to dissolved the brown semi solid mixture, washed with water (3 x 50 mL)**,** dried over anhydrous $MgSO_4$ and concentrated under reduced pressure to obtained a light yellow solid which was an inseparable product mixture of starting material (**SF-02**), 1-bromo-4-ethynyl-2,5-dimethoxybenzene (**SF-07**) Calculated for $C_{10}H_9BrO_2$ $[M+H]^+$= 240.9859, found 240.2330 and 1,4-diethynyl-2,5-dimethoxybenzene (**SF-08**) calculated for $C_{12}H_{10}O_2$ $[M]^+$= 186.0675 , found 186.9843.

07. Synthesis of 3-(4-bromo-2,5-dimethoxyphenyl)-1,1-diphenylprop-2-yn-1-ol (SF-09)

Into an oven dried round bottom flask (50 mL), a product mixture of **SF-02, SF-07** and **SF-08** (0.15 g, 0.78 mmol) was added. Anhydrous THF (15 mL) was added under N_2 atmosphere, and the reaction mixture was cooled to 0 °C. NaH (0.11 g, 2.34 mmol) and benzophenone (0.29 g, 1.56 mmol) were added to the reaction mixture quickly and stirred for 10 minutes at 0 °C. The resultant bisque solution was stirred for 24 hours and quenched with water until the bubbling was finished. THF was concentrated under reduced pressure and EtOAc (50 mL) was added into the light solid and organic layer was washed with brine (3 x 50 mL), dried over anhydrous Na_2SO_4 and concentrated under reduced pressure and obtained a light brown crude. The crude was subjected to silica gel column chromatography using EtOAc: Hexane (1:9, v/v) to remove excess benzophenone and **SF-02**, EtOAc: Hexane (1:3, v/v) to afford 3-(4-bromo-2,5-dimethoxyphenyl)-1,1-diphenylprop-2-yn-1-ol (**SF-09**). ^{13}C NMR (101 MHz, Chloroform-*d*) δ 155.08, 149.83, 144.96, 128.30, 127.74, 126.17, 116.56, 116.29, 112.94, 111.40, 96.56, 83.04, 75.05, 56.90, 56.67, 29.72. Calculated for $C_{23}H_{19}BrO_3$ $[M+H-H2O]^+$= 405.0473, found 405.0470. The column was washed with EtOAc to afford 3,3'-(2,5-dimethoxy-1,4-phenylene)bis(1,1-diphenylprop-2-yn-1-ol) (**SF-10**) Calculated for $C_{38}H_{30}O_4[M+H-H_2O]^+$= 533.2111, found 533.2102

08). Attempted synthesis of 5,11-bis (4-bromo-2,5-dimethoxyphenyl)-6,12-diphenyltetracene (SF-11)

3-(4-bromo-2,5-dimethoxyphenyl)-1,1-diphenylprop-2-yn-1-ol (0.10 g, 0.24 mmol) was dissolved in anhydrous CH_2Cl_2 (2 mL) under N_2 atmosphere, and the reaction mixture was cooled to 0 °C. NEt_3 (0.07 mL, 0.36 mmol) and $MeSO_2Cl$ (0.05 mL, 0.36 mmol) was added dropwise. The resultant brown solution was stirred for 1 hour at 0 °C and warmed to room temperature. The reaction mixture was then concentrated under reduced pressure to evaporate CH_2Cl_2. Xylene (10 mL) was added to the brown solid and heated to 80 °C while stirring under N_2. Finally, collidine (0.05 mL, 0.36 mmol) was added dropwise and temperature was raised to 95 °C and stirred the reaction for 16 hours. Then the dark brown reaction was cooled to room temperature dissolve in EtOAc (30 mL) and washed with water(3 x 50mL), dried over anhydrous Na_2SO_4 and concentrated under reduced pressure and obtained a light brown condensed liquid crude. The crude was subjected to column chromatography using EtOAc: Hexane (1:6 v/v) to afford red condensed liquid and ^1H NMR spectrum was not compatible with the expected structure.

Method B - 3-(4-bromo-2,5-dimethoxyphenyl)-1,1-diphenylprop-2-yn-1-ol (0.10 g, 0.24 mmol) was dissolved in toluene (10 mL) with slight heating. The reaction was cooled and stirred to 0 °C under N_2 atmosphere. NEt_3 (0.05 mL , 0.36 mmol) and $MeSO_2Cl$ (0.04 mL, 0.36 mmol) was added dropwise and stirred the reaction mixture at 0 °C for 15 minutes and 15 minutes at room temperature. Then the brown reaction mixture was refluxed at 110 °C for 8 hours. The reaction was cooled to room temperature and diluted with EtOAc (20 mL) and washed with HCl (2M, 3 x 50 mL), dried over anhydrous $MgSO_4$ and

concentrated under reduced pressure and obtained a brown crude. The crude was subjected to silica gel column chromatography using EtOAc: Hexane (1:9, v/v) and a yellow condensed liquid was obtained and ^{1}H NMR spectrum was not compatible with the expected structure.

Method C- Same procedure was followed with extended reaction times of 24 hours to 48 hours. The resultant liquid ^{1}H NMR spectrum was not compatible with the expected structure.

Method D – 3-(4-bromo-2,5-dimethoxyphenyl)-1,1-diphenylprop-2-yn-1-ol (0.18 g, 0.42 mmol) was dissolved in mesitylene (10 mL). The reaction was cooled and stirred to 0 °C under N_2 atmosphere. NEt_3 (0.81 mL, 0.58 mmol) and $MeSO_2Cl$ (0.04 mL, 0.58 mmol) was added dropwise, and the reaction mixture was stirred at 0 °C for 15 minutes and 15 minutes at room temperature. Then the brown reaction mixture was refluxed at 110 °C for 16 hours. The reaction was cooled to room temperature and diluted with EtOAc (20 mL) and washed with HCl (2M, 3 x 50 mL), dried over anhydrous $MgSO_4$ and concentrated under reduced pressure and obtained a brown crude. The crude was subjected to silica gel column chromatography using EtOAc: Hexane (1:9, v/v) and a greenish yellow condensed liquid was obtained and ^{1}H NMR spectrum was not compatible with the expected structure.

09. Synthesis of 1-bromo-2,5-dimethoxy benzene (SF-12)

Method A – To an oven dried round bottom flask, 1,4-dibromo-2,5-dimethoxy benzene (SF-02, 2.00 g, 6.75 mmol) was obtained and dissolved in anhydrous THF (20 mL) at -78 °C under N_2 atmosphere and the reaction mixture was stirred for 2 hours. Then EtOH (2

mL) was added to the reaction, and it was allowed to stir for 10 minutes. The reaction was diluted with EtOAc (30 mL), washed with water (3 x 50 mL), dried over anhydrous $MgSO_4$ and concentrated under reduced pressure and obtained a light brown crude. TLC confirmed that the crude contained the SF-01 and SF-02.

Method B - 1,4-dimethoxybenzene (1.38 g, 0.01 mol) and NBS (1.78 g, 0.01 mol) were dissolved in DMF (12 mL) at room temperature under N_2 atmosphere. The colorless reaction mixture with white suspension of NBS was stirred for 16 hours. The color changed from colorless to yellow to orange after the reaction time. The reaction was diluted with EtOAc (30 mL), washed with LiCl (5%, 3 x 50 mL), dried over anhydrous $MgSO_4$ and concentrated under reduced pressure and obtained a reddish orange crude solution. The crude was subjected to column chromatography using EtOAc: Hexane (1:6 v/v) to afford orange condensed liquid. (0.61 g, 28%) ^{1}H NMR (400 MHz, Chloroform-*d*) δ 7.14 (d, *J* = 2.6 Hz, 1H), 6.83 (m, 2H), 3.85 (d, *J* = 1.4 Hz, 3H), 3.77 (d, *J* = 1.3 Hz, 3H). ^{13}C NMR (101 MHz, Chloroform-*d*) δ 154.04, 150.31, 119.02, 113.66, 112.93, 111.96, 56.85, 55.90. Calculated for C8H9BrO2 $[M]^+$= 215.9780, found = 215.9760.

10. Synthesis of ((2,5-dimethoxyphenyl)ethynyl)trimethylsilane (SF-13)

Method A - 1-bromo-2,5-dimethoxy benzene (SF-12, 0.15 mL, 1.00 mmol), CuI (0.01 g, 0.05 mmol) and $Pd(PPh)_3Cl_2$ (0.04 g, 0.05 mmol) was dissolved in a solution mixture of toluene (4 mL) and NEt_3(4 mL) at room temperature under N_2 atmosphere. Trimethylsilyl acetylene (2.00 mmol, 0.14 mL) was added dropwise into the yellow reaction mixture and stirred for 24 hours. The brown reaction was quenched with water, diluted with EtOAc, dried over anhydrous $MgSO_4$ and concentrated under reduced pressure and obtained the

crude product. The crude was subjected to column chromatography using EtOAc: Hexane (1:9, v/v) resulted the starting material along with the dialkyne.

Method B - 1-bromo-2,5-dimethoxy benzene (SF-12, 0.15 mL, 1.00 mmol), CuI (1.90 mg, 0.01 mmol) and $Pd(PPh)_3Cl_2$ (1.40 mg, 0.02 mmol) were dissolved in piperidine (5 mL) at room temperature under N_2 atmosphere. Trimethylsilyl acetylene (2.00 mmol, 0.27 mL) was added dropwise into the yellow reaction mixture and stirred for 24 hours at 110 °C. The dark brown reaction was concentrated under reduced pressure and diluted with $NaHCO_3$. The product was extracted into hexane (3 x 50 mL), washed with brine (3 x 50mL), dried over anhydrous $MgSO_4$ and concentrated under reduced pressure and obtained the dark brown crude product. The crude was subjected to column chromatography using EtOAc: Hexane (1:6, v/v) to obtain light brown ((2,5-dimethoxyphenyl)ethynyl)trimethylsilane. (0.09 g, 39%) ^{1}H NMR (400 MHz, Chloroform-*d*) δ 6.99 (d, *J* = 3.0 Hz, 1H), 6.86 (dd, *J* = 9.0, 3.0 Hz, 1H), 6.80 (d, *J* = 9.0 Hz, 1H), 3.86 (s, 3H), 3.78 (s, 3H), 0.29 (s, 9H). ^{13}C NMR (101 MHz, Chloroform-*d*) δ 154.91, 153.12, 118.49, 116.22, 112.79, 112.24, 101.14, 98.52, 56.51, 55.79, 0.07. Calculated for $C_{13}H_{18}O_2Si$ $[M]^+$= 234.1071, Found = 234.1680

11. Synthesis of 2-ethynyl-1,4-dimethoxybenzene (SF-14)

Method A - ((2,5-dimethoxyphenyl)ethynyl)trimethylsilane (0.09 g , 0.38 mmol) was dissolved in methanol (20 mL). CsF (0.29 g, 1.92 mmol) was added to the yellow reaction mixture and stirred at 35 °C for 4 hours in atmospheric conditions. The resultant brown reaction mixture was concentrated under reduced pressure to evaporate the methanol and diluted with EtOAc (30 mL), washed with water (3 x 50 mL), dried over anhydrous

$MgSO_4$ and concentrated under reduced pressure to obtain a brown solid crude. The crude was purified by silica gel chromatography using EtOAc/Hexane (1:6 v/v) and afford a dark yellow solid product 2-ethynyl-1,4-dimethoxybenzene. (0.03 g, 54%) ^{1}H NMR (400 MHz, Chloroform-*d*) δ 7.03 (d, *J* = 3.1 Hz, 1H), 6.90 (dd, *J* = 9.0, 3.1 Hz, 1H), 6.83 (d, *J* = 9.0 Hz, 1H), 3.88 (s, 3H), 3.78 (s, 3H), 3.33 (s, 1H). ^{13}C NMR (101 MHz, Chloroform-*d*) δ 155.10, 153.13, 118.77, 116.27, 111.94, 111.60, 81.10, 80.03, 56.40, 55.80. Calculated for $C_{10}H_{10}O_2$ $[M]^+$= 162.0675, found = 162.1156

12. Synthesis of 3-(2,5-dimethoxyphenyl)-1,1-diphenylprop-2-yn-1-ol (SF-15)

Method A - 2-ethynyl-1,4-dimethoxybenzene (SF-14, 0.16 g, 1.00 mmol), NaH (0.12 g, 3.00 mmol) and benzophenone (0.36 g, 2.00 mmol) were added into an oven dried round bottom flask (50 mL) and dissolved in anhydrous THF (15 mL) and added under N_2 atmosphere, and the reaction mixture was cooled to 0 °C. the reaction mixture was stirred for 10 minutes at 0 °C. The resultant light brown solution was stirred for 24 hours and quenched with water until the bubbling was finished while vigorously stirring to avoid overflow. THF was concentrated under reduced pressure and diluted with EtOAc (50 mL), washed with brine (3 x 50 mL), dried over anhydrous $MgSO_4$ and concentrated under reduced pressure to obtain a brown crude. The crude was subjected to silica gel column chromatography using EtOAc: Hexane(1:6, v/v) to afford yellow solid 3-(2,5-dimethoxyphenyl)-1,1-diphenylprop-2-yn-1-ol. (0.06 g, 15%)^{1}H NMR (400 MHz, Chloroform-*d*) δ 7.81 (m, 4H), 7.33 (m, 6H), 7.01 (d, *J* = 2.9 Hz, 1H), 6.89 (dd, *J* = 9.0, 3.0 Hz, 1H), 6.84 (d, *J* = 9.0 Hz, 1H), 3.82 (d, *J* = 39.3 Hz, 6H). ^{13}C NMR (101 MHz, Chloroform-*d*) δ 155.03, 153.20, 145.22, 130.10, 128.31, 128.24, 127.62, 126.21, 118.00, 116.07,

112.36, 112.24, 95.81, 83.67, 74.99, 56.52, 55.85. Calculated for $C_{23}H_{20}O_3$ $[M+H-H_2O]^+$= 327,1371, found = 327.1371

13.Attempted synthesis of 5,11-bis(2,5-dimethoxyphenyl)-6,12-diphenyl tetracene (SF-16)

Method A - 3-(2,5-dimethoxyphenyl)-1,1-diphenylprop-2-yn-1-ol (0.08 g, 0.24 mmol) was dissolved in toluene (10 mL) with slight heating. The reaction was cooled and stirred to 0 °C under N_2 atmosphere. NEt_3 (0.14 mL, 0.97 mmol) and $MeSO_2Cl$ (0.08 mL, 0.97 mmol) was added dropwise and stirred the reaction mixture at 0 °C for 15 minutes and 15 minutes at room temperature. Then the brown reaction mixture was refluxed at 110 °C for 8 hours. The reaction was cooled to room temperature and diluted with EtOAc (20 mL) and washed with HCl (2M, 3 x 50 mL), dried over anhydrous $MgSO_4$ and concentrated under reduced pressure and obtained a dark brown solid material. ^{1}H NMR spectrum was not compatible with the expected structure.

14. Synthesis of 1,1,3-triphenylprop-2-yn-1-ol (SF-17)

Phenylacetylene (0.10 mL, 0.91 mmol), NaH (0.06 g, 3.00 mmol) and benzophenone (0.33 g, 1.82 mmol) were added into an oven dried round bottom flask (50 mL) and dissolved in anhydrous THF (15 mL) was added under N_2 atmosphere, and the reaction mixture was cooled to 0 °C. The reaction mixture was stirred for 10 minutes at 0 °C. The resultant light brown solution was stirred for 24 hours and quenched with water until the bubbling was finished while vigorous stirring to avoid overflow. THF was concentrated under reduced pressure and diluted with EtOAc (50 mL), washed with brine (3 x 50 mL), dried over anhydrous $MgSO_4$ and concentrated under reduced pressure to obtain a dark brown

crude. The crude was subjected to silica gel column chromatography using EtOAc: Hexane(1:6, v/v) to afford light yellow 1,1,3-triphenylprop-2-yn-1-ol. (0.12 g, 40%) ^{1}H NMR (400 MHz, Chloroform-*d*) δ 7.73 (d, *J* = 7.6 Hz, 4H), 7.56 (m, 2H), 7.39 (m, 7H), 7.32 (t, *J* = 7.3 Hz, 2H), 2.92 (s, 1H). ^{13}C NMR (101 MHz, Chloroform-*d*) δ 145.04, 131.82, 128.73, 128.37, 128.35, 127.78, 126.10, 122.45, 91.73, 87.28, 74.88. Calculated for $C_{21}H_{16}O$ $[M+H-H_2O]^+$= 267.1162, found = 267.1162

15. Synthesis of 5,6,11,12-tetraphenyltetracene (SF-18)

1,1,3-triphenylprop-2-yn-1-ol (0.10 g, 0.35 mmol) was dissolved in toluene (10 mL) with slight heating. The reaction was cooled and stirred to 0 °C under N_2 atmosphere. NEt_3 (0.06 mL, 0.50 mmol) and $MeSO_2Cl$ (0.05 mL, 0.65 mmol) was added dropwise and stirred the reaction mixture at 0 °C for 15 minutes and 15 minutes at room temperature. Then the brown reaction mixture was refluxed at 110 °C for 24 hours. The bright red reaction was cooled to room temperature and diluted with EtOAc (20 mL) and washed with HCl (2M, 3 x 50 mL), dried over anhydrous $MgSO_4$ and concentrated under reduced pressure and obtained a bright orange crude. The crude was subjected to silica gel column chromatography using EtOAc: Hexane (1:9, v/v) and a bright red-orange condensed liquid was obtained, and methanol (5 mL) was added into the liquid and let it evaporate slowly to obtained bright red color 5,6,11,12-tetraphenyltetracene. (0.03 g, 14%)^{1}H NMR (400 MHz, Chloroform-*d*) δ 7.38 (m, 1H), 7.10 (m, 4H), 6.89 (m, 2H). ^{13}C NMR (101 MHz, Chloroform-*d*) δ 141.79, 137.05, 132.16, 130.27, 129.15, 127.22, 126.61, 125.76, 124.87. Calculated for C42H28 $[M+H]^+$= 533.2264, found= 533.2220.

16.Synthesis of (3-chloropropa-1,2-diene-1,1,3-triyl)tribenzene (SF-19)

1,1,3-triphenylprop-2-yn-1-ol (0.10 g, 0.35 mmol) was dissolved in CH_2Cl_2 (20 mL) and cooled to 0 °C under N_2 atmosphere. NEt_3 (0.10 mL, 0.70 mmol) and $TiCl_4$ (0.04 mL, 0.70 mmol) was added dropwise into the yellow reaction and stirred the reaction mixture at 0 °C for 30 minutes. The brown reaction mixture was stirred for 6 hours at room temperature. A saturated NH_4Cl (20 mL) was added to the reaction and stirred for 30 minutes. The organic layer was separated. The aqueous layer was extracted into CH_2Cl_2 (2 x 15 mL). Organic layers were combined, washed with brine (10 mL), dried over anhydrous Na_2SO_4 and concentrated under reduced pressure to obtain a brown solid crude with an inseparable product mixture. ^1H NMR spectrum was not compatible with the expected structure. ESI confirmed the presence of the expected product. Calculated for $C_{21}H_{15}Cl$ $[M]^+$ = 194.0935, found = 194.1768.

17. Attempted synthesis of (3-(4-bromo-2,5-dimethoxyphenyl)-3-chloropropa-1,2-diene-1,1-diyl)dinezene (SF-20)

3-(4-bromo-2,5-dimethoxyphenyl)-1,1-diphenylprop-2-yn-1-ol (0.10 g, 0.24 mmol) was dissolved in CH_2Cl_2 (20 mL) and cooled to 0 °C under N_2 atmosphere. NEt_3 (0.07 mL , 0.48 mmol) and $TiCl_4$ (0.03 mL, 0.24 mmol) was added dropwise into the yellow reaction and stirred the reaction mixture at 0 °C for 30 minutes. The brown reaction mixture was stirred for 6 hours at room temperature. A saturated NH_4Cl (20 mL) was added to the reaction and stirred for 30 minutes. The organic layer was separated. Aqueous layer was extracted into CH_2Cl_2 (2 x 15 mL). Organic layers were combined, washed with brine (10 mL), dried over anhydrous $MgSO_4$ and concentrated under reduced pressure to obtain a

solid brown crude. The crude was subjected to silica gel plug column chromatography using Hexane to afford brown solid. ^{1}H NMR spectrum was not compatible with the expected structure.

18.Attempted synthesis of 6,11-diphenyltetracene-5,12-dione (SF-21)

Method A - 5,12-naphthacenequinone (0.05 g, 0.20 mmol) was dissolved in Et_2O (10 mL) under N_2 atmosphere and cooled to -78 °C. Phenylmagnesium bromide (0.22 mL, 1.2 mmol) was added into the reaction mixture dropwise. The reaction mixture was allowed to warm to room temperature and refluxed for 2 hours at 35 °C. After two hours the yellow reaction was transfer into ice and mixed with a diluted solution of NH_4Cl. Organic layer was separated and diluted with Et_2O, concentrated under reduced pressure to obtain the yellow starting material.

Method B - 5,12-naphthacenequinone (0.05 g, 0.20 mmol) was dissolved in THF (10 mL) under N_2 atmosphere and cooled to -78 °C. Phenylmagnesium bromide (0.07 mL, 0.20 mmol) was added dropwise to the yellow solution. The reaction mixture was stirred at -78 °C for 2 hours and it was allowed to warm to room temperature and stirred for 14 hours. Then, iodine (15.0 mg, 0.12 mmol) was added, and the reaction mixture was heated under air at 65 °C for 2 hours. NaOH (10 mL, 2 M) was added to the orange reaction mixture and product was extracted into CH_2Cl_2 (3 x 10 mL). The combined organic layers were washed with water (2 x 50 mL), brine, dried over anhydrous Na_2SO_4, concentrated under reduced pressure to afford a yellow crude. The crude was purified by silica gel column chromatography over using hexane/EtOAc (9:1) to afford the starting material.

Method C – Method B was followed with 14 hours longer reaction time to afford the starting material.

Method D – Mg (0.96 g, 4.00 mmol) and Et_2O (20 mL) was added into an oven dried round bottom flask (25 mL) under N_2 atmosphere and cooled to -78 °C. Then, phenyl bromide (0.42 mL, 4.00 mmol) was added dropwise, and the reaction mixture was stirred at 30 °C until the colorless solution converts to a brown solution. Then the solvent part of the reaction mixture was transferred into the 5,12-naphthacenequinone (0.05 g, 0.20 mmol) reaction flask and the same procedure was followed as Method B to afford the starting material.

Method E – Grignard reagent was synthesized according to method D using THF as the solvent and the same procedure as method B was followed to afford the starting material.

Method F – Method B was followed using commercially available phenylmagnesium bromide in 10 equivalent ratio. ^1H NMR spectrum was not compatible with the expected structure.

Method G - Method B was followed using commercially available phenylmagnesium bromide in a 20 equivalent ratio. ^1H NMR spectrum was not compatible with the expected structure.

19.Synthesis of (SF-22)

Method A - 3-(4-bromo-2,5-dimethoxyphenyl)-1,1-diphenylprop-2-yn-1-ol (55.0 mg, 0.10 mmol) and pyrene (20.2 mg, 0.10 mmol) was dissolved in CH_2Cl_2 (5 mL) and cooled to 0 °C under N_2 atmosphere. Then, $TiCl_4$ (0.01 mL, 0.10 mmol) was added dropwise to

the reaction mixture. The reaction mixture was stirred for 5 minutes at 0 °C warmed up to room temperature and stirred for 24 hours and quenched with water, diluted with EtOAc, washed with water (3 x 50 mL), dried over $MgSO_4$, concentrated under reduced pressure to afford a brown crude. The crude was subjected to silica gel column chromatography using EtOAc: Hexane(1:6, v/v). ^1H NMR spectrum was not compatible with the expected structure.

Method B - 3-(4-bromo-2,5-dimethoxyphenyl)-1,1-diphenylprop-2-yn-1-ol (55.10 mg, 0.100 mmol) and pyrene (20.22 mg, 0.100 mmol) was dissolved in CH_2Cl_2 (5 mL) and cooled to 0 °C under N_2 atmosphere. Then, anhydrous $ZnCl_2$ (0.007 mg, 0.050 mmol) was added to the reaction mixture. The reaction mixture was stirred for 5 minutes at 0 °C warmed up to room temperature and stirred for 1 hour. The reaction was resultant only the starting material, anhydrous $ZnCl_2$ (0.007 mg, 0.050 mmol) was added to the reaction mixture again and stirred the reaction mixture for 16 hours. Water (5 mL) was added to the dark blue reaction mixture and stirred for 5 minutes. The brown colour organic layer was separated, washed with brine, dried over $MgSO_4$, concentrated under reduced pressure to afford a brown crude. The crude was subjected to silica gel column chromatography using EtOAc: Hexane(1:6, v/v). ^1H NMR spectrum was not compatible with the expected structure.

20. Synthesis of (SF-23)

3-(4-bromo-2,5-dimethoxyphenyl)-1,1-diphenylprop-2-yn-1-ol (0.55 g, 1.00 mmol) and dimethoxybenzene (0.276 g, 1.00 mmol) was dissolved in CH_2Cl_2 (15 mL). Then, $TiCl_4$ (0.10 mL, 1.00 mmol) was added dropwise to the reaction mixture and cooled the

reaction to -40 °C for 6 hours under N_2 atmosphere. The reaction mixture was warmed up to room temperature and saturated K_2CO_3 (20 mL) was added to the brown reaction. Aqueous layer was extracted into CH_2Cl_2 (2 x 15 mL). Organic layers were combined, washed with brine (10 mL), dried over anhydrous $MgSO_4$, concentrated under reduced pressure to afford a brown crude. The crude was subjected to silica gel column chromatography using EtOAc: Hexane(1:99, v/v). ^{1}H NMR spectrum was not compatible with the expected structure.

21. Synthesis of (SF-24)

Method A - 4-(4-bromo-2,5-dimethoxyphenyl)-2-methylbut-3-yn-2-ol (0.10 g, 0.33 mmol) and pyrene (66.9 mg, 0.33 mmol) was dissolved in CH_2Cl_2 (5 mL) and cooled to 0 °C under N_2 atmosphere. Then, $TiCl_4$ (0.02 mL, 18.1 mmol) was added dropwise to the reaction mixture. The reaction mixture was stirred for 5 minutes at 0 °C warmed up to room temperature and stirred for 24 hours and quenched with water, diluted with EtOAc, washed with water (3 x 10 mL), dried over $MgSO_4$, concentrated under reduced pressure to afford a brown crude. The crude was subjected to silica gel column chromatography using EtOAc: Hexane(1:6, v/v). ^{1}H NMR spectrum was not compatible with the expected structure.

22. Synthesis of 5,12-diphenyltetracene (SF-25)

In an oven dried round bottom flask bromobenzene (0.21 mL, 2.00 mmol) and THF (3.00 mL) was added and stirred under N_2 atmosphere and cooled to -78 °C. n-BuLi (0.60 mL, 2.00 mmol) was added dropwise into the reaction and stirred the reaction for 20 minutes at -78 °C. 5,12-naphthacenequinone (0.05 g, 0.20 mmol) was dissolved in THF (12 mL)

under N_2 atmosphere in and cooled to -78 °C another oven dried round bottom flask. Then, phenyllithium solutions transferred into the starting material solution dropwise. The yellow reaction was turned to green. The reaction was stirred for 48 hours at room temperature and the colour was changed from green to light brown to bright orange color. The reaction was transferred into a separatory funnel contained saturated NH_4Cl (50 mL) with the help of diethyl ether. Aqueous layer was extracted into Et_2O (3 x 30 mL). Organic layers were combined, dried over Na_2SO_4 and concentrated under reduced pressure to obtain a brown crude. The crude and $SnCl_2$ was dissolved in toluene (20 mL) and stirred for 48 hours at room temperature under N_2 atmosphere. Reaction was quenched with water, diluted with EtOAc (50 mL), washed with water (50 mL), dried over Na_2SO_4 and concentrated under reduced pressure to obtain a brown crude product. The crude was purified by silica gel chromatography using EtOAc/Hexanes (1:9 v/v) and afford a white solid. ^1H NMR spectrum was not compatible with the expected structure. ESI was indicated the presence of the compound. Calculated for $C_{30}H_{20}$ $[M+H]^+$ = 381.1638, found = 381.2130.

23. Attempted synthesis of 5,12-bis(4-bromo-2,5-dimethoxyphenyl)tetracene (SF-26)

Method A - In an oven-dried round bottom flask, 1,4-dibromo-2,5-dimethoxybenzene (0.05 g, 0.20 mmol) and THF (3.00 mL) was added and stirred under N_2 atmosphere and cooled to -78 °C. n-BuLi (0.60 mL, 2.00 mmol) was added dropwise into the reaction and the reaction was stirred for 20 minutes at -78 °C. 5,12-naphthacenequinone (0.05 g, 0.20 mmol) was dissolved in THF (12 mL) under N_2 atmosphere in and cooled to -78 °C

another oven dried round bottom flask. Then, light brown phenyllithium solutions transferred into the starting material solution dropwise. The yellow reaction was turned to dark brown. The reaction was stirred for 48 hours at room temperature. The reaction was transferred into a separatory funnel containing saturated NH_4Cl (50 mL) with the help of diethyl ether. Aqueous layer was extracted into Et_2O (3 x 30 mL). Organic layers were combined, dried over Na_2SO_4 and concentrated under reduced pressure to obtain a brown crude. The crude and $SnCl_2$ (0.15 g, 0.80 mmol) was dissolved in toluene (20 mL) and stirred for 48 hours at room temperature under N_2 atmosphere. Reaction was quenched with water, diluted with EtOAc (50 mL), washed with water (50 mL), dried over Na_2SO_4 and concentrated under reduced pressure to obtain a dark brown crude product. The crude was purified by silica gel chromatography using EtOAc/Hexanes (1:9 v/v) and afford a brown solid. ^1H NMR spectrum was not compatible with the expected structure.

24. Synthesis of 1,4-bis(tetradecyloxy)benzene (SF-27)

Method A – To a solution of hydroquinone (1.10 g, 10.0 mmol) and Cs_2CO_3 (9.77 g, 30.0 mmol) in DMF (30 mL), 1-bromotetradecane (8.92 mL, 30.0 mmol) was added dropwise to the dark yellow suspension while stirring at room temperature under N_2 atmosphere. The resultant orange reaction mixture was transferred into a hot oil bath and a brown reaction mixture was observed. The reaction mixture was refluxed at 110 °C for 16 hours. Reaction mixture was cooled to room temperature and quenched with water. The white undissolved solid was filtered out using CH_2Cl_2. Most of the DMF solvent was evaporated under reduced pressure and the remaining crude was dissolved in CH_2Cl_2 (50 mL). The organic layer was washed with water (2 x 50 mL), brine (50 mL) and dried over Na_2SO_4

and concentrated under reduced pressure to obtain a dark brown crude product. The crude was purified by silica gel chromatography using EtOAc/Hexanes (1:9 v/v) and afford a white colour solid. (1.74 g, 34%) ^{1}H NMR (400 MHz, Chloroform-*d*) δ 6.84 (s, 4H), 3.92 (t, *J* = 6.6 Hz, 4H), 1.76 (m, 4H), 1.45 (m, 4H), 1.29 (s, 40H), 0.90 (m, 6H). ^{13}C NMR (101 MHz, Chloroform-*d*) δ 153.21, 115.40, 68.69, 31.94, 29.71, 29.69, 29.67, 29.62, 29.60, 29.44, 29.42, 29.38, 26.08, 22.71, 14.14. Calculated for $C_{34}H_{62}O_2$ $[M]^+$= 502.4744, found = 504.5115

25. Synthesis of 1,4-dibromo-2,5-bis(tetradecyloxy)benzene (SF-28)

Method A - 1,4-bis(tetradecyloxy)benzene (0.50 g, 1.00 mmol) was dissolved in a mixture of $CHCl_3$ (20 mL) and acetic acid (20 mL) and cooled to 0 °C. *N*-bromosuccinimide (0.53 g, 3.00 mmol) was added at 0 °C and stirred for 10 minutes. The white suspension was refluxed at 60 °C for 16 hours. After 16 hours, as some amount of starting material left in the reaction mixture but the reaction mixture has completely turned into an orange clear solution. After cooling to room temperature, the reaction was quenched by the addition of water and CH_2Cl_2 (50 mL) was added. The organic layer was washed with brine (3 x 50 mL), dried over anhydrous $MgSO_4$ and concentrated under reduced pressure and obtained an orange liquid which solidify as soon as it was taken out from the hot water bath. The orange solid was purified by silica gel chromatography using CH_2Cl_2/Hexanes (2:5 v/v) and afford a light orange solid. (0.03 g, 6%)^{1}H NMR (400 MHz, Chloroform-*d*) δ 6.84 (s, 2H), 3.92 (t, *J* = 6.6 Hz, 2H), 1.77 (dt, *J* = 14.7, 6.7 Hz, 2H), 1.45 (m, 2H), 1.32 (m, 8H), 1.29 (s, 14H), 0.90 (m, 3H). ^{13}C NMR (101 MHz, Chloroform-*d*) δ 150.11, 118.50, 111.16, 70.34, 31.94, 31.60, 30.06, 29.71, 29.70, 29.67, 29.59, 29.56, 29.38, 29.31, 29.13,

25.94, 22.71, 22.67, 14.21, 14.13, 1.04. Calculated for $C_{34}H_{60}Br_2O_2$ $[M]^-$= 658.2955, found = 659.2620

26. Synthesis of 1,4-bis(octyloxy)benzene (SF-29)

Method A – To a suspension of hydroquinone (0.55 g, 5.00 mmol) and Cs_2CO_3 (6.48 g, 20.0 mmol) in DMF (30 mL) under N_2 atmosphere 1-bromooctane (3.44 mL, 20.0 mmol) was added dropwise to the dark yellow suspension while stirring at room temperature. The dark brown reaction mixture was refluxed at 110 °C for 16 hours. Most of the DMF solvent was evaporated under reduced pressure and the remaining crude was dissolved in CH_2Cl_2 (50 mL). The organic layer was washed with water (2 x 50 mL), brine (50 mL) and dried over Na_2SO_4 and concentrated under reduced pressure to obtain a dark brown crude product. The crude was purified by silica gel chromatography using EtOAc/Hexanes (1:9 v/v) and afford a white solid. (0.96 g, 57%)

Method B – To a suspension of hydroquinone (1.10 g, 10.00 mmol) and Cs_2CO_3 (12.95 g, 40.0 mmol) in DMF (40 mL) under N_2 atmosphere 1-bromooctane (6.87 mL, 40.0 mmol) was added dropwise to the dark yellow suspension while stirring at room temperature. The dark brown reaction mixture was refluxed at 80 °C for 16 hours. The reaction mixture was cooled to room temperature and EtOAc (50 mL) was added to the resultant mixture and washed with HCl (10%, 3 x 50 mL). Organic layer was dried over $MgSO_4$ and concentrated under reduced pressure to obtain a dark brown crude product. Toluene (2 x 20mL) was added to the crude and solvent was evaporated under reduced pressure. The crude was purified by silica gel chromatography using EtOAc/Hexanes (1:9 v/v) and afford a white solid. (3.14 g, 94%) ^{1}H NMR (400 MHz, Chloroform-*d*) δ 6.84 (s, 1H), 3.92

(t, *J* = 6.6 Hz, 1H), 1.77 (m, 1H), 1.47 (m, 1H), 1.36 (m, 1H), 1.33 (m, 3H), 0.91 (m, 1H). Calculated for $C_{22}H_{38}O_2$ $[M]^+$= 334.2862, found = 334.2860

Method C – Hydroquinone (0.58 g, 5.30 mmol) was dissolved in dry ethanol (50 mL) under N_2 atmosphere. Potassium hydroxide (0.59 g, 10.6 mmol) was added, and the reaction mixture was stirred for 30 minutes under reflux. 1-bromooctane (1.82 mL, 10.6 mmol) was added and stirred the dark brown reaction mixture for another 2 hours under reflux. Reaction mixture was cooled to room temperature and ethanol was evaporated under reduced pressure. The reaction mixture was dissolved CH_2Cl_2 (30 mL) and wash with water (2 x 50mL) and once more with saturated $NaHCO_3$. Filter the organic layer and dried over anhydrous $MgSO_4$ and concentrated under reduced pressure to obtain a brown crude product. The crude was purified by silica gel chromatography using EtOAc/Hexane (1:9 v/v) and afford a white solid. (1.22 g, 69%)

27. Synthesis of 1,4-dibromo-2,5-bis(octyloxy)benzene (SF-30)

Method A - 1,4-bis(octyloxy)benzene (3.77 g, 11.2 mmol) was dissolved in CH_2Cl_2 (30 mL) and acetic acid (30 mL) and cooled to 0 °C. *N*-bromosuccinimide (7.97 g, 44.8 mmol) was added at 0 °C and stirred for 10 minutes. The white suspension was refluxed at 40°C for 16 hours. After cooling to room temperature, the reaction was quenched by the addition of water and CH_2Cl_2 (50 mL) was added. The organic layer was washed with brine (3 x 50 mL), dried over anhydrous $MgSO_4$ and concentrated under reduced pressure and obtained an orange liquid which solidify as soon as it was taken out from the hot water bath. The orange solid was purified by silica gel chromatography using CH_2Cl_2/Hexanes (2:5 v/v) and afford a light orange solid. (0.93 g, 16%)

Method B - 1,4-bis(octyloxy)benzene (3.15 g, 9.40 mmol) was dissolved in $CHCl_3$ (30 mL) and acetic acid (30 mL) and cooled to 0 °C. *N*-bromosuccinimide (6.69 g, 37.6 mmol) was added at 0 °C and stirred for 10 minutes. The white suspension was refluxed at 40 °C for 16 hours. After cooling to room temperature, the reaction was quenched by the addition of water and CH_2Cl_2 (50 mL) was added. The organic layer was washed with brine (3 x 50 mL), dried over anhydrous $MgSO_4$ and concentrated under reduced pressure and obtained an orange liquid which solidified as soon as it was taken out from the hot water bath. The orange solid was purified by silica gel chromatography using CH_2Cl_2/Hexanes (2:5 v/v) and afford a light orange solid. (1.84 g, 39%) ^{1}H NMR (400 MHz, Chloroform-*d*) δ 7.11 (s, 2H), 3.97 (t, *J* = 6.5 Hz, 4H), 1.82 (dq, *J* = 8.5, 6.7 Hz, 4H), 1.50 (ddd, *J* = 14.9, 9.0, 6.9 Hz, 4H), 1.33 (m, 22H), 0.91 (m, 7H). ^{13}C NMR (101 MHz, Chloroform-*d*) δ 150.11, 118.50, 111.16, 70.34, 31.81, 31.77, 29.28, 29.23, 29.14, 25.95, 22.68, 22.64, 14.12, 14.09. Calculated for $C_{22}H_{36}Br_2O_2$ $[M]^+$= 490.1077, found = 490.1845.

28. Synthesis of ((4-bromo-2,5-bis(octyloxy)phenyl)ethynyl)trimethylsilane (SF-31)

Method A – To a solution of 1,4-dibromo-2,5-bis(octyloxy)benzene (0.200 g, 0.407 mmol) $Pd(PPh)_3Cl_2$ (0.014 g, 0.02 mmol, 5 mol%) and CuI (0.003 g, 0.02 mmol, 5 mol%) in a light yellow solution mixture of NEt_3 (10 mL) and toluene (10 mL), Trimethylsilyl acetylene (0.400 mmol, 0.056 mL) was added dropwise and stirred under N_2 at room temperature for 24 hours. The resultant dark brown solution was quenched with water and EtOAc (50 mL) was added. The organic layer was washed with water (3 x 50 mL), dried over anhydrous Na_2SO_4 and concentrated under reduced pressure and obtained a

brown crude product. The crude was purified by silica gel chromatography using EtOAc/Hexane (1:9 v/v) and non separable product mixture of starting material, mono substituted product **SF-31** ((4-bromo-2,5-bis(octyloxy)phenyl) ethynyl)trimethylsilane, and disubstituted product ((2,5-bis(octyloxy)-1,4-phenylene)bis(ethyne-2,1-diyl))bis(trimethylsilane) were afforded.

29. Attempted synthesis of 1-bromo-4-ethynyl-2,5-bis(octyloxy)benzene (SF-32)

Method A – A product mixture of 1,4-dibromo-2,5-bis(octyloxy)benzene, ((4-bromo-2,5-bis(octyloxy)phenyl)ethynyl)trimethylsilane and ((2,5-bis(octyloxy)-1,4-phenylene) bis (ethyne-2,1-diyl))bis(trimethylsilane) (0.09 g, 0.38 mmol) was dissolved in methanol (20 mL). CsF (0.29 g, 1.92 mmol) was added to the yellow reaction mixture and stirred at 35 °C for 4 hours in atmospheric conditions. The resultant yellow reaction mixture was concentrated under reduced pressure to evaporate the methanol. subsequently, EtOAc (30 mL) was added to dissolve the brown semi solid mixture, washed with water (3 x 50 mL)**,** dried over anhydrous $MgSO_4$ and concentrated under reduced pressure to obtain a light-yellow solid which was the starting materials.

30. Synthesis of N-Benzyl benzamide (SF-35)

Method A - Benzylamine (5.20 mL, 47.6 mmol) was added to a solution of benzoyl chloride (5.53 mL, 47.6 mmol) and triethylamine (10mL) and CH_2Cl_2 (50 mL). The yellow colour reaction mixture was stirred for 2 hours, washed with HCl (1M, 2x50mL) and brine (1x50 mL), concentrated under reduced pressure to obtained yellow solid crude.(18.878 g) The crude was recrystallized with hexane/EtOH to afford a white solid product. Calculated for $C_{14}H_{13}NO$ $[M+H]^+$ = 212.1069, found = 212.1069

31. Synthesis of tris(4-bromo-2,5-dimethoxyphenyl)methanol (SF-36)

Method A - To an oven-dried round bottom flask (250 mL), 1,4-dibromo-2,5-dimethoxybenzene (6.00g, 20.3 mmol) was added and dissolved in dry THF (130 mL) under N_2 atmosphere at -78 °C. A cooled solution (-78 °C) of n-butyllithium (8.10 mL, 20.3 mmol, 2.5 M solution in hexane) was added dropwise to the light yellow reaction mixture through the walls via a long needle and the reaction mixture was stirred at -78 °C for 2 hours. Diethyl carbonate (0.79 mL, 20.3 mmol) was added dropwise to the center of the dark yellow reaction mixture, and it was stirred for 10 minutes. Then, the orange reaction mixture was stirred for ten days at room temperature. After 10 days the dark brown suspension was quenched with water (100 mL) and extracted into CH_2Cl_2 (3 x 50 mL). The combined organic layers were dried over anhydrous $MgSO_4$ and concentrated under reduced pressure and a light brown solution was obtained. Hexane was added to the solution and it was left to cool at -10 °C for 24 hours to obtain a yellow precipitate. The precipitate was purified by silica gel chromatography using EtOAc/Hexanes (1:3 v/v) and afford a white solid. (0.61 g, 4%) ^{1}H NMR (400 MHz, Chloroform-*d*) δ 7.01 (s, 3H), 6.79 (s, 3H), 3.71 (d, *J* = 2.6 Hz, 18H). ^{13}C NMR (101 MHz, Chloroform-*d*) δ 151.04, 150.18, 130.72, 116.09, 112.14, 110.59, 66.98, 56.96, 56.25. Calculated for $[C_{17}H_{18}Br_2O_4]^+$= 444.9468, found = 444.9460

32. Attempted synthesis of 5,5',5''-(chloromethanetriyl)tris(2-bromo-1,4-dimethoxy benzene) (SF-37)

Method A - tris(4-bromo-2,5-dimethoxyphenyl)methanol (0.05 g, 0.07 mmol) was dissolved in toluene (10 mL) at room temperature under N_2 atmosphere. HCl (10%, 0.17

mL, 0.70 mmol) was added to the reaction. The reaction color was changed from yellow to green. After 4 hours reaction time of vigorous stirring the reaction was quenched with water and diluted EtOAc (15 mL) and washed with water and concentrated under reduces pressure to afford yellow starting material.

Method B - tris(4-bromo-2,5-dimethoxyphenyl)methanol (0.05 g, 0.07 mmol) was dissolved in CH_2Cl_2 (10 mL) at room temperature under N_2 atmosphere. HCl (10%, 0.17 mL, 0.70 mmol) was added to the reaction. The reaction color was changed from yellow to green. After 14 hours reaction time of vigorous stirring the reaction was quenched with water and diluted EtOAc (15 mL) and washed with water and concentrated under reduces pressure to afford yellow starting material.

Method C - tris(4-bromo-2,5-dimethoxyphenyl)methanol (0.05 g, 0.07 mmol) was dissolved in CH_2Cl_2 (10 mL) at room temperature under N_2 atmosphere. HCl (12% , 0.14 mL, 0.70 mmol) and anhydrous $CaCl_2$ (0.05 g, 0.45 mmol) was added to the reaction. The reaction color was changed from yellow to green. After 24 hours of reaction time the reaction was quenched with water and diluted with EtOAc (15 mL) and washed with water and concentrated under reduces pressure to afford yellow starting material.

Method D - tris(4-bromo-2,5-dimethoxyphenyl)methanol (0.05 g, 0.07 mmol) was dissolved in toluene (10 mL) at -78 °C under N_2 atmosphere. NEt_3 (0.10 mL, 0.70 mmol), Triphosgene (0.04 g, 0.14 mmol) was added quickly to the reaction and stirred for 24 hours. The reaction color was changed from yellow to green. After 24 hours of reaction time the reaction was quenched with water and diluted EtOAc (15 mL) and washed with water and concentrated under reduces pressure to afford yellow colour starting material.

33. Attempted synthesis of 5,5',5''-(bromomethanetriyl)tris(2-bromo-1,4-dimethoxy benzene) (SF-38)

Method A - tris(4-bromo-2,5-dimethoxyphenyl)methanol (0.05 g, 0.07 mmol) was dissolved in toluene (10 mL) at room temperature under N_2 atmosphere. HBr $_{(aq)}$ (0.08 mL, 0.70 mmol) was added dropwise to the reaction and stirred for 14 hours. The reaction color was changed from yellow to brown. After 14 hours of reaction time the reaction was quenched with water and diluted with EtOAc (15 mL) and washed with water and concentrated under reduced pressure to afford brown crude. The crude was purified by silica gel chromatography using EtOAc/Hexanes (1:3 v/v) and afford the yellow starting material.

Method B - tris(4-bromo-2,5-dimethoxyphenyl)methanol (0.05 g, 0.07 mmol) was dissolved in toluene (10 mL) at room temperature under N_2 atmosphere. HBr (CH_3CO_2H) (43%, 0.08 mL, 0.70 mmol) was added dropwise to the reaction and stirred for 14 hours. The reaction color was changed from yellow to brown. After 14 hours of reaction time the reaction was quenched with water and diluted EtOAc (15 mL) and washed with water (3 x 30 mL) and concentrated under reduced pressure to afford brown crude. The crude was purified by silica gel chromatography using EtOAc/Hexanes (1:3 v/v) and afford the yellow starting material.

Method C - tris(4-bromo-2,5-dimethoxyphenyl)methanol (0.05 g, 0.07 mmol) was dissolved in toluene (10 mL) at room temperature under N_2 atmosphere. HBr $_{(CH3COOH)}$ (43%, 0.08 mL, 0.70 mmol) was added dropwise to the reaction and stirred for 14 hours. The reaction color was changed from yellow to brown. After 14 hours of reaction the

brown reaction mixture was purified by silica gel chromatography using EtOAc/Hexanes (1:3 v/v) and afford the yellow starting material.

34. Synthesis of tris(4-bromo-2,5-dimethoxyphenyl)methane (SF-39)

Method A - To a yellow solution of **SF 36** (0.068 g, 0.100 mmol) in CH_2Cl_2 (10 mL) under N_2 atmosphere, trifluoroacetic acid (0.60 mL) was added dropwise and to obtain a green solution. To the mixture triethyl silane (0.60 mL, 3.75 mmol) was added dropwise and stirred the brown reaction mixture for 24 hours at room temperature under N_2 atmosphere. The reaction was quenched with water, dissolved in CH_2Cl_2 (50 mL), washed with water (3 x 50 mL), dried over anhydrous $MgSO_4$ and concentrated under reduced pressure and a light brown crude product was obtained. The crude was purified by silica gel chromatography using EtOAc/Hexanes (1:4 v/v) and afford a white colour solid. (0.05, g, 77%) ^{1}H NMR (400 MHz, Chloroform-*d*) δ 7.07 (s, 1H), 6.71 (s, 1H), 3.88 (s, 1H), 3.81 (s, 3H), 3.79 (s, 3H). ^{13}C NMR (101 MHz, Chloroform-*d*) δ 151.96, 149.95, 128.78, 115.80, 114.93, 109.01, 56.95, 56.17, 30.15, 6.83, 6.44. Calculated for $C_{17}H_{18}Br_2O_4$ $[M]^+$= 443.9566, found = 443.9284

35. Synthesis of tris(4-bromo-2,5-dimethoxyphenyl)methyl radical (SF-40)

Method A – Diisopropylamine (0.10 mL, 0.08 mmol) was dissolved in anhydrous THF (5 mL) and cooled up to -78 °C under N_2 atmosphere. Then n-BuLi (0.02 mL, 0.08 mmol) was added into the reaction dropwise and stirred the reaction mixture for 30 minutes. In

an oven-dried round bottom flask tris(4-bromo-2,5-dimethoxyphenyl)methane (50.0 mg, 0.08 mmol) was dissolved in THF (10 mL) and LDA (0.50 mL) was added to the reaction mixture. The reaction mixture was stirred until green coloration was observed. Then 2,3-Dichloro-5,6-dicyano-1,4-benzoquinone (DDQ, 0.17 g, 0.07 mmol) was added to the reaction and stirred the reaction for 2 hours. Then, THF was evaporated under reduced pressure and chloroform-*d* (1 mL) was added to the reaction. A non compatible NMR spectra was observed.

Method B - tris(4-bromo-2,5-dimethoxyphenyl)methane (34.0 mg, 0.05 mmol) and *p*-chloranil were dissolved in THF (5 mL) at room temperature under N_2 atmosphere and stirred for 1 hour at room temperature under N_2 atmosphere to afford the starting material.

Method C - tris(4-bromo-2,5-dimethoxyphenyl)methane (34.0 mg, 0.05 mmol) and *p*-chloranil were dissolved in CH_2Cl_2 (5 mL) at room temperature under N_2 atmosphere and stirred for 1 hour at room temperature under N_2 atmosphere to afford the starting material. The reaction time was increased up to 24 hours also resultant the starting material.

Method D - tris(4-bromo-2,5-dimethoxyphenyl)methane (5.00 mg, 7.00 μmol) and potassium tert-butoxide (2.00 mg, 14 μmol) was dissolved in THF (2 mL) and stirred at room temperature for 3 hours under N_2 atmosphere. Then *p*-chloranil (2.5 mg, 10.5 μmol) was added into the reaction mixture and stirred for 30 minutes to afford the starting material.

Method E - tris(4-bromo-2,5-dimethoxyphenyl)methane (5.00 mg, 7.00 μmol) and tetrabutylammonium hydroxide (3.63 mg, 14 μmol) were dissolved in THF (2 mL) and stirred at room temperature for 3 hours under N_2 atmosphere. Then, *p*-chloranil (2.5 mg, 10.5 μmol) was added into the reaction mixture and stirred for 30 minutes to afford the starting material.

Method G - To a solution of tris(4-bromo-2,5-dimethoxyphenyl)methanol (34.0 mg, 0.05 mmol) and stannous chloride dihydrate (17.0 mg, 0.08 mmol) in THF (3 mL) at room temperature under N_2 atmosphere, HCl (12M, 0.40 mL) was added to the reaction mixture and stirred for 24 hours at room temperature. Then the black reaction mixture was concentrated under reduced pressure and chloroform-*d* (0.5 mL) was added to the crude. A compatible NMR spectrum was observed, and further characterization was required for the confirmation.

36. Attempted synthesis of tris(4-bromo-2,5-bis(octyloxy)phenyl)methanol (SF-41)

Method A - To an oven-dried round bottom flask (100 mL), 1,4-dibromo-2,5-bis(octyloxy)benzene (2.00 g, 4.00 mmol) was added and dissolved in dry THF (50 mL) under N_2 atmosphere at -78 °C. A cooled solution (-78 °C) of n-butyllithium (3.19 mL, 7.98 mmol, 2.5 M solution in hexane) was added dropwise to the light yellow reaction mixture through the walls via a long needle and the reaction mixture was stirred at -78 °C for 2 hours. Diethyl carbonate (0.15 mL, 1.27 mmol) was added dropwise to the center of the dark yellow reaction mixture, and it was stirred for 10 minutes. Then the orange reaction mixture was stirred for ten days at room temperature. After 10 days the light orange

suspension was quenched with water (100 mL) and extracted into CH_2Cl_2 (3 x 50 mL). The combined organic layers were dried over anhydrous $MgSO_4$ and concentrated under reduced pressure to afford a greenish yellow solid crude. The crude was purified by silica gel chromatography using EtOAc/Hexanes (1:3 v/v) and afford a yellow solid. A non compatible NMR spectra was observed.

Section 02 – Spectral Data

1,4-dimethoxybenzene (SF-01)

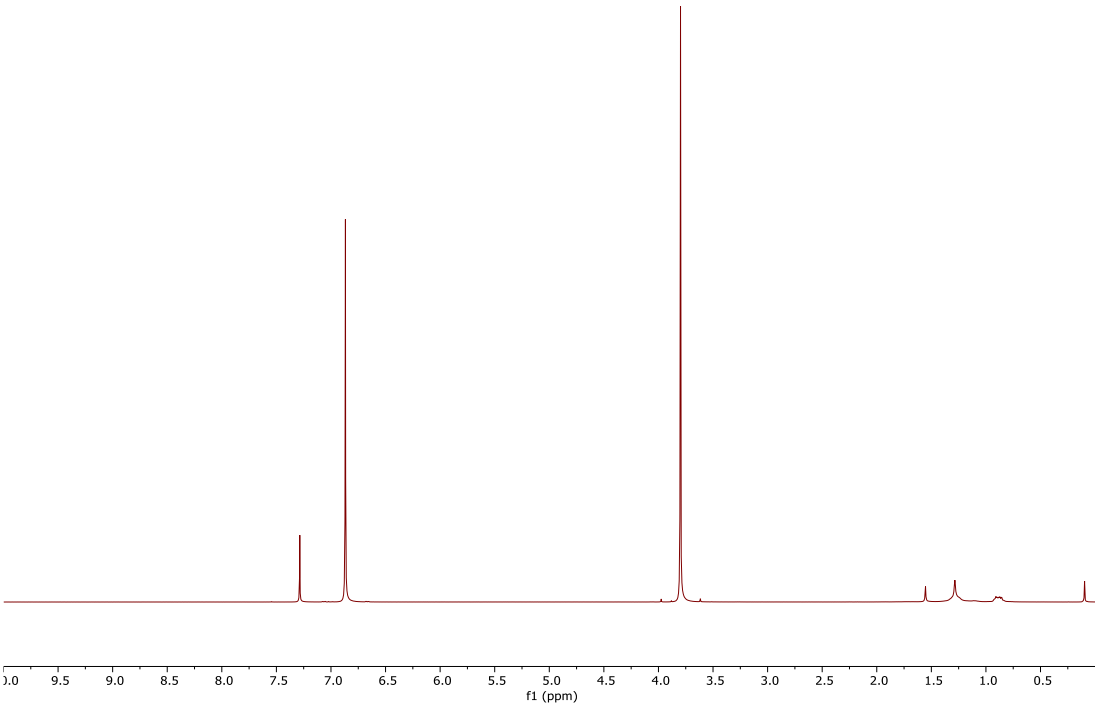

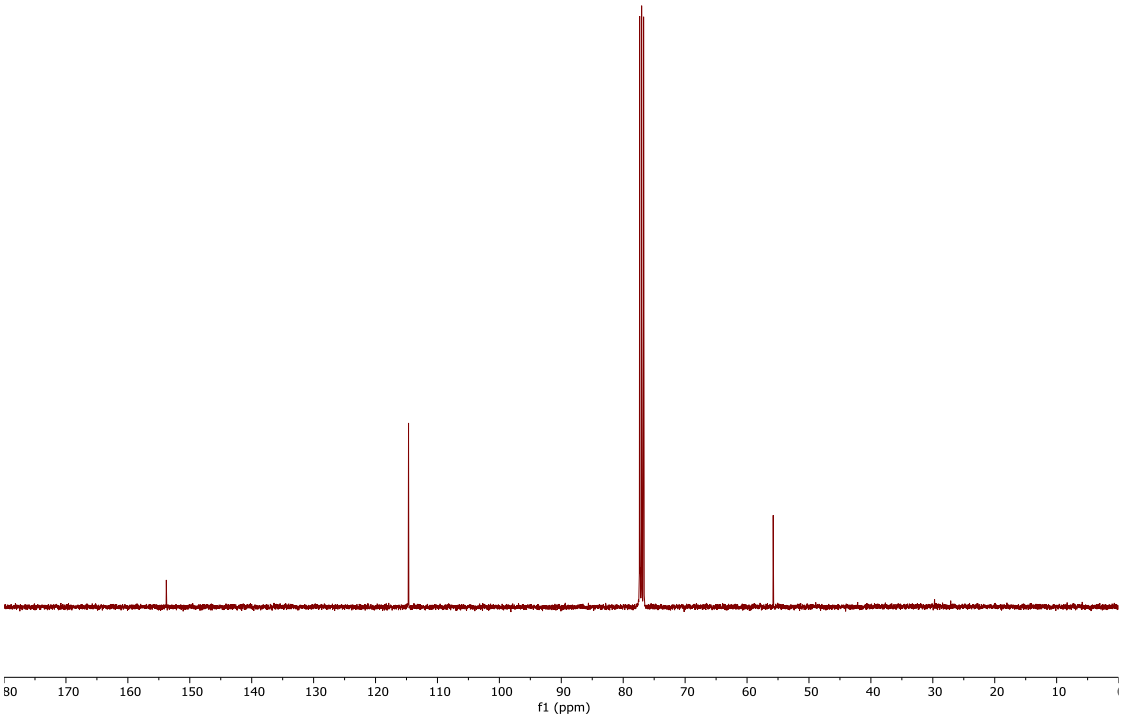

1,4-dibromo-2,5-dimethoxybenzene (SF-02)

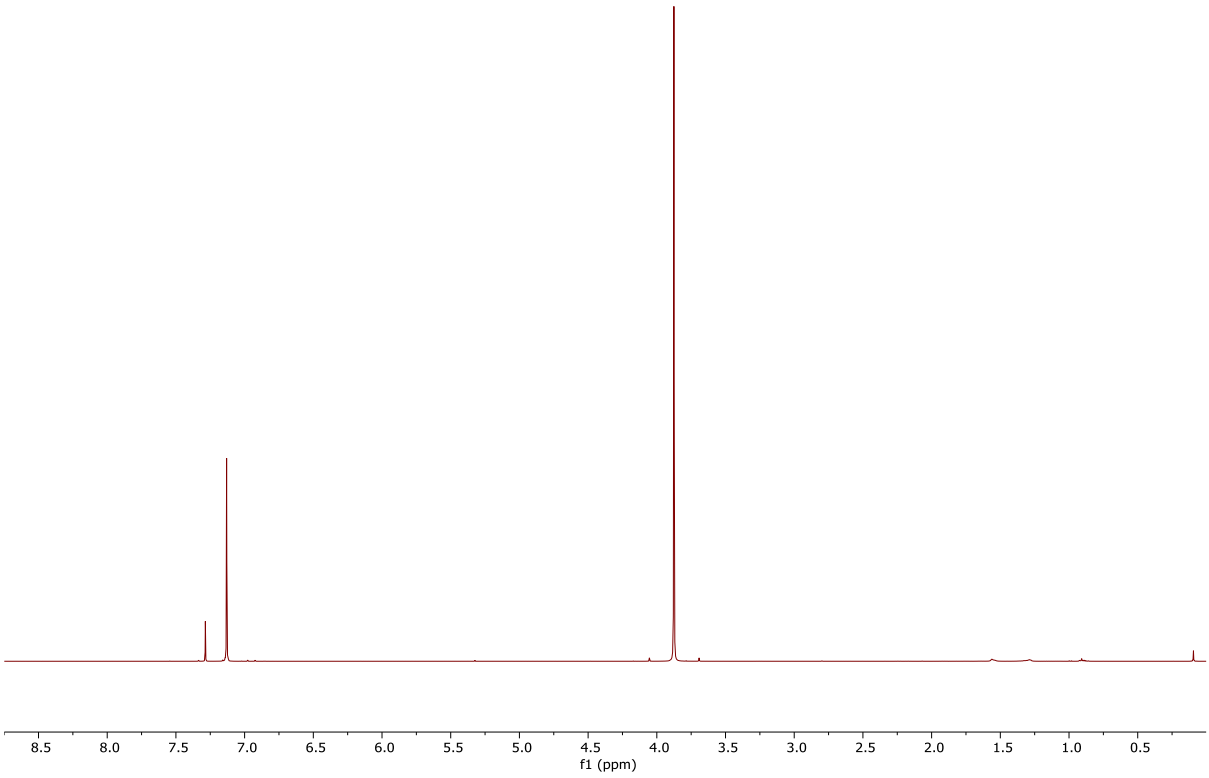

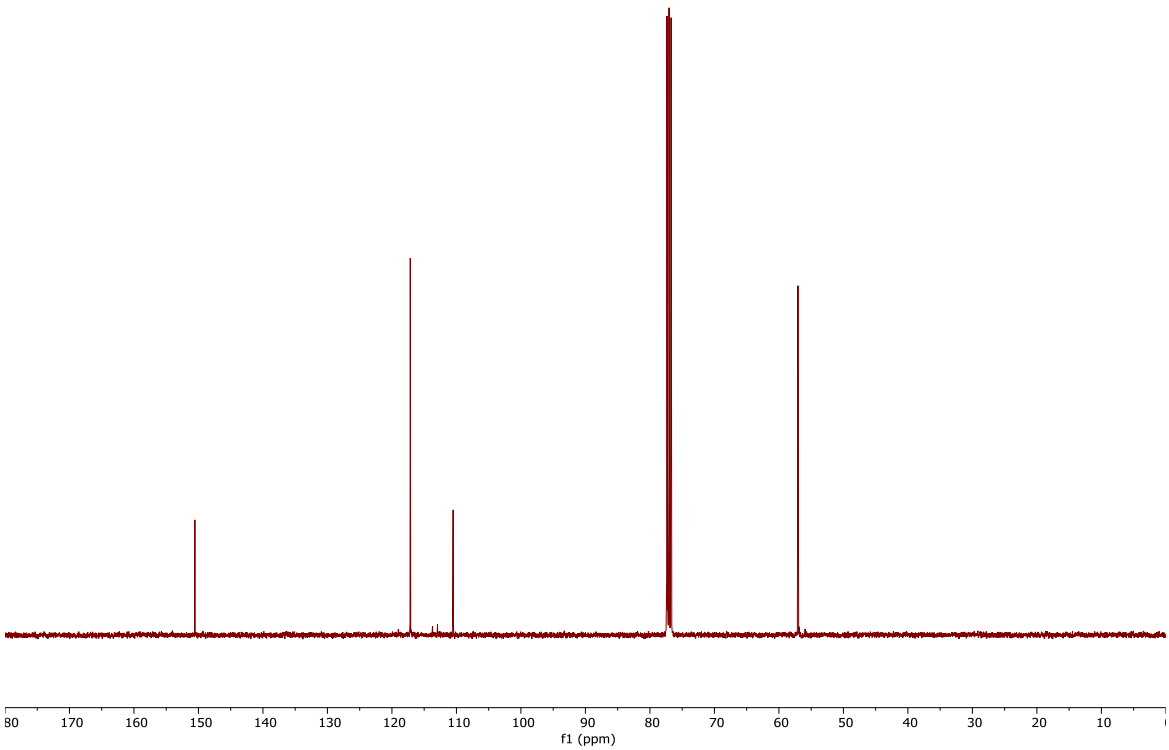

4-(4-bromo-2,5-dimethoxyphenyl)-2-methylbut-3-yn-2-ol (SF-03)

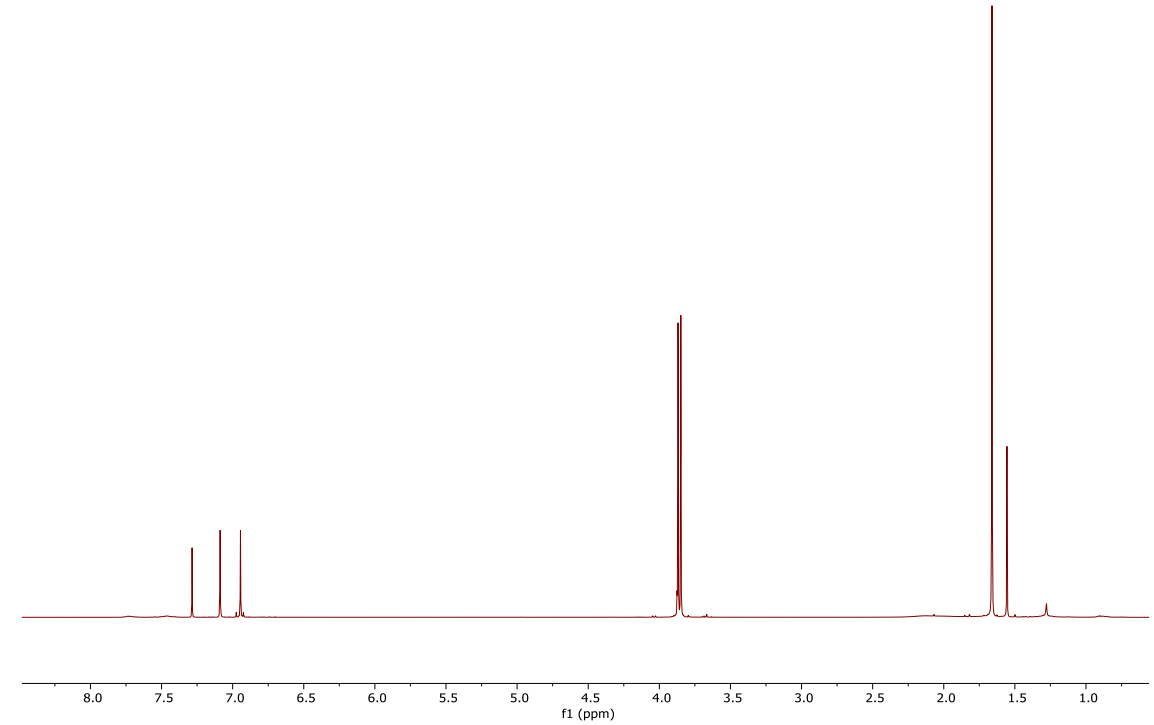

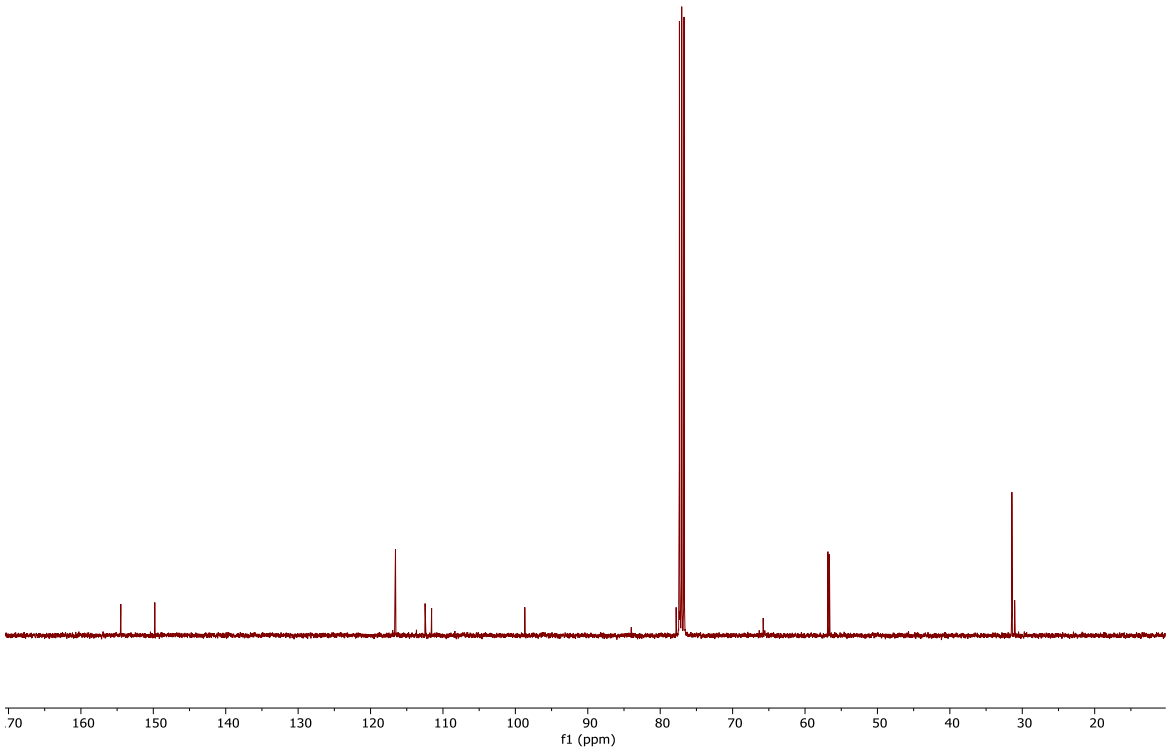

((4-bromo-2,5-dimethoxyphenyl)ethynyl) trimethylsilane (SF 05)

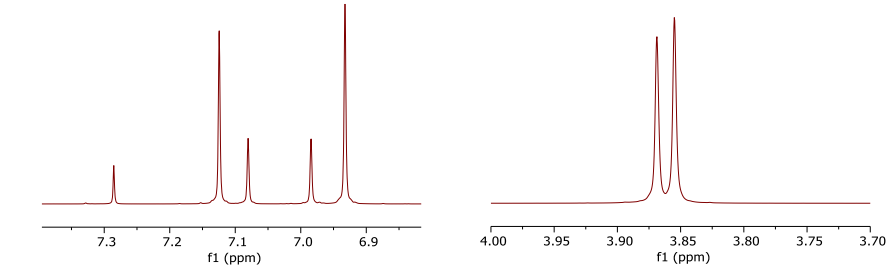

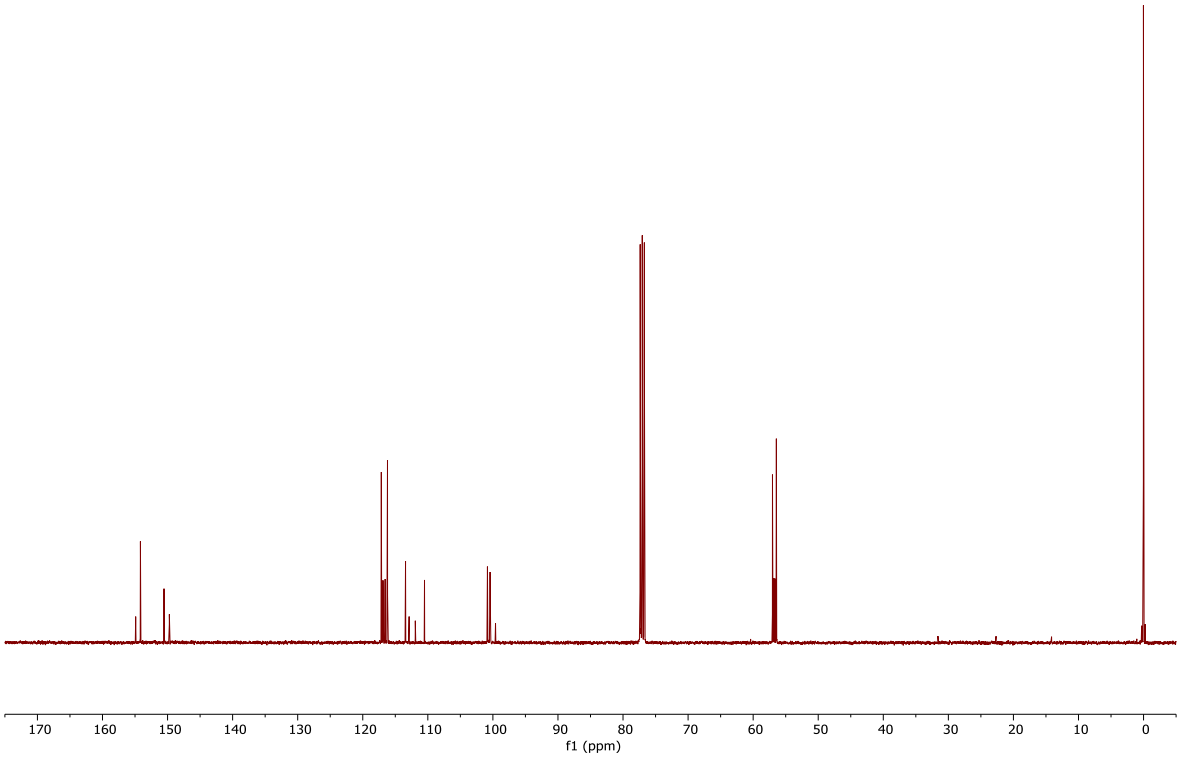

1-bromo-4-ethynyl-2,5-dimethoxybenzene (SF-07)

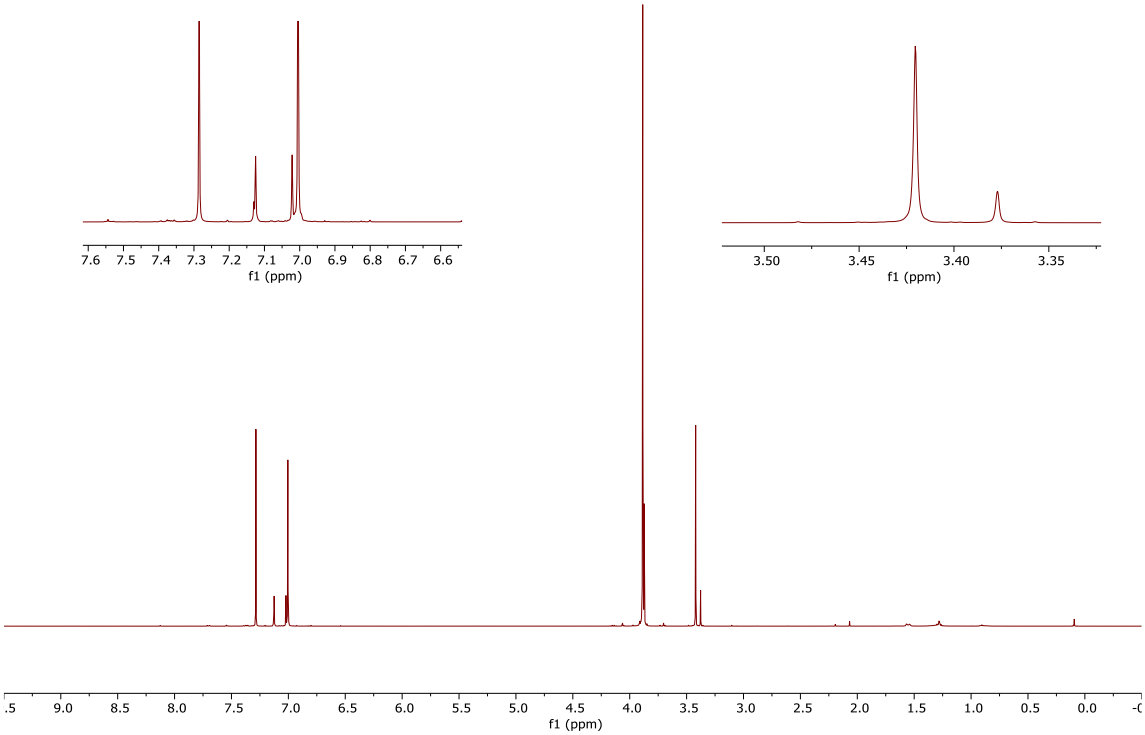

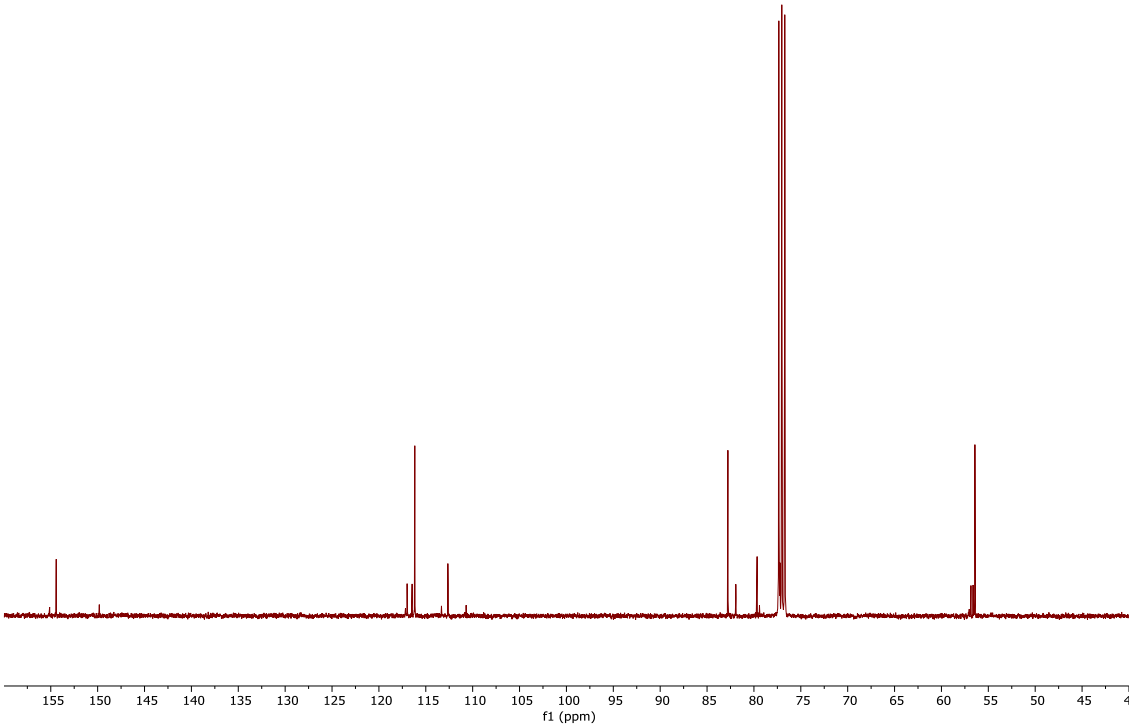

3-(4-bromo-2,5-dimethoxyphenyl)-1,1-diphenylprop-2-yn-1-ol (SF-09)

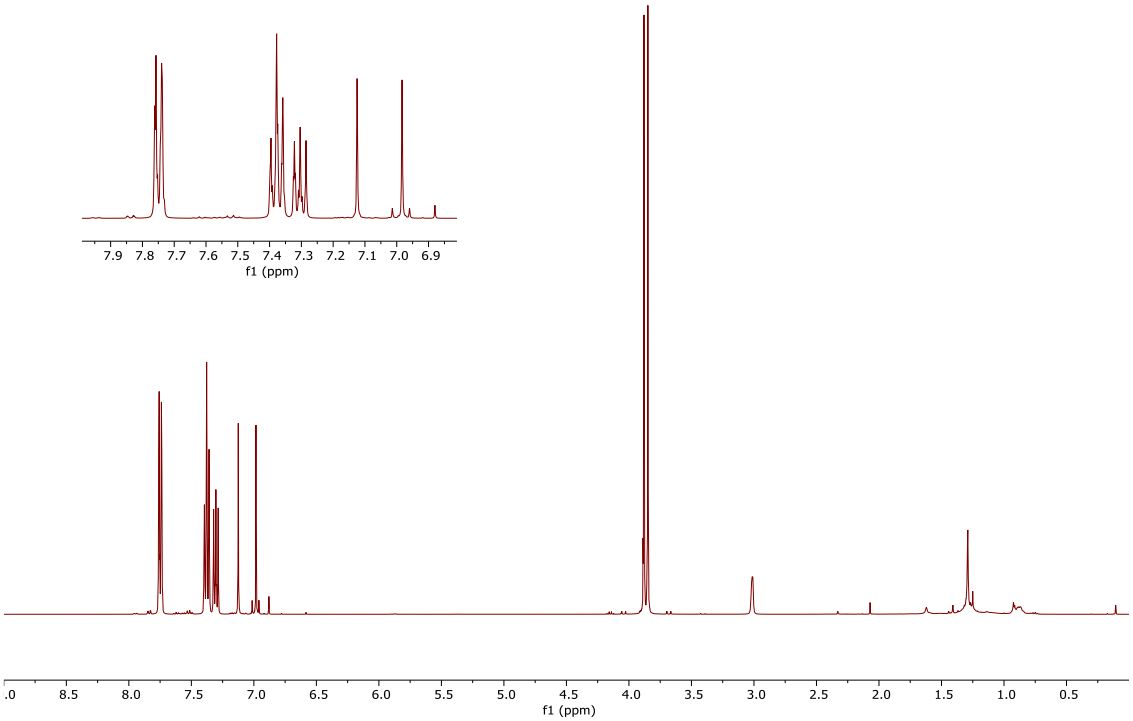

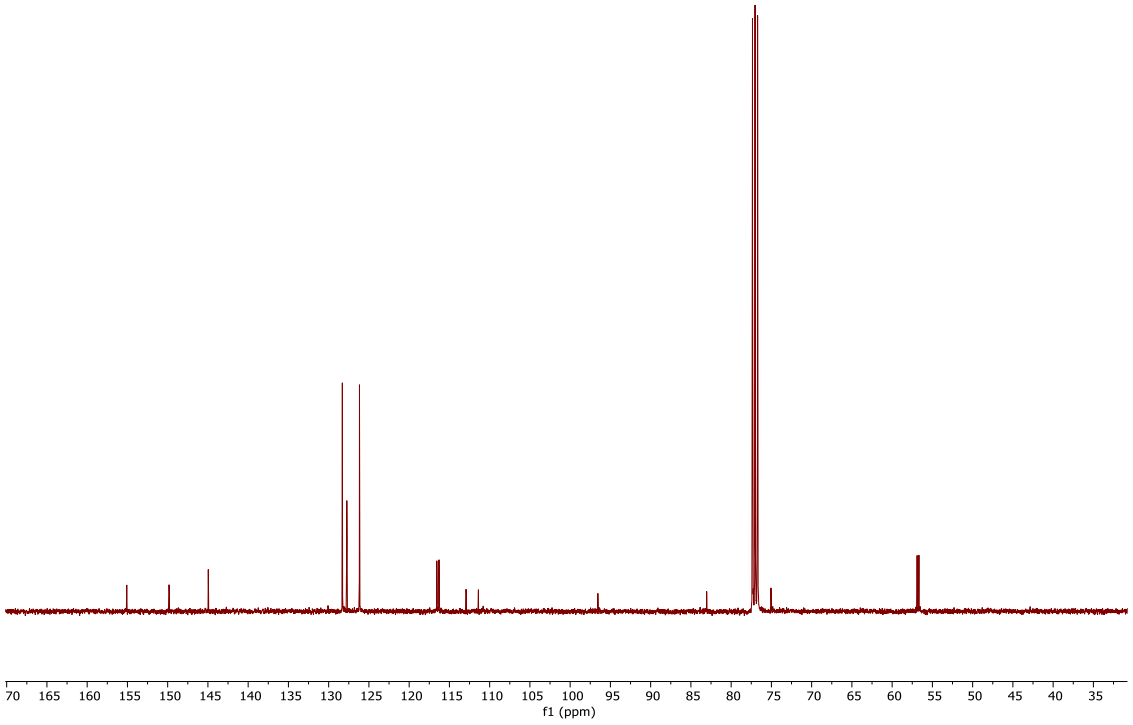

1-bromo-2,5-dimethoxy benzene (SF-12)

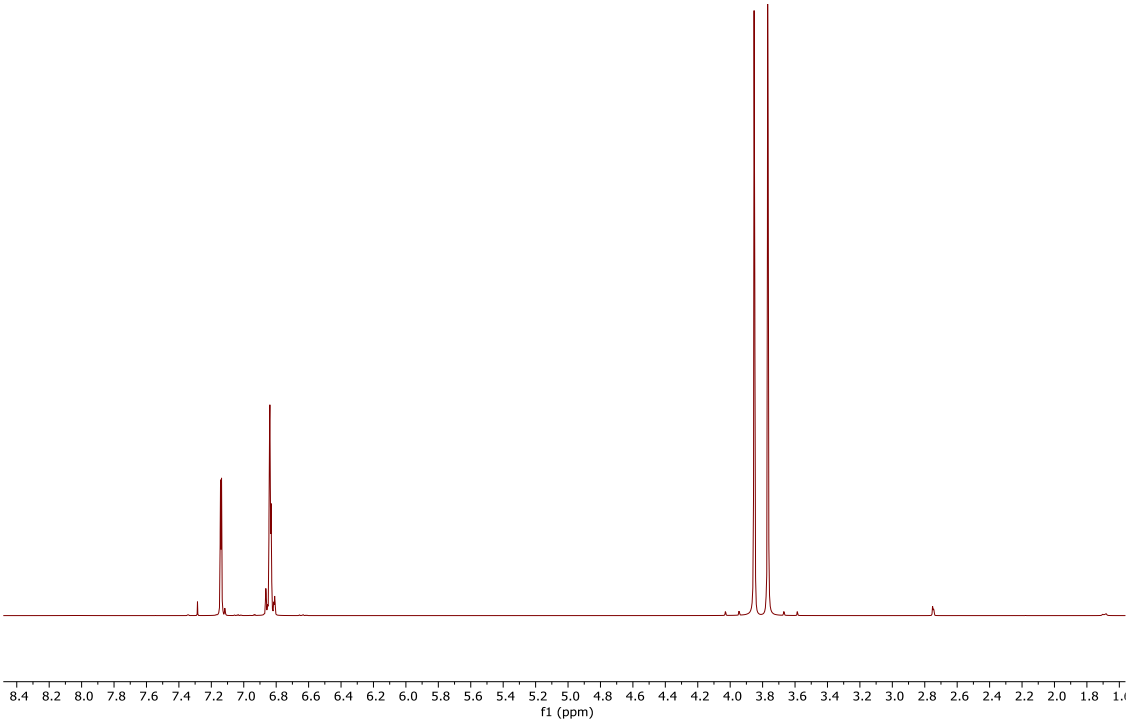

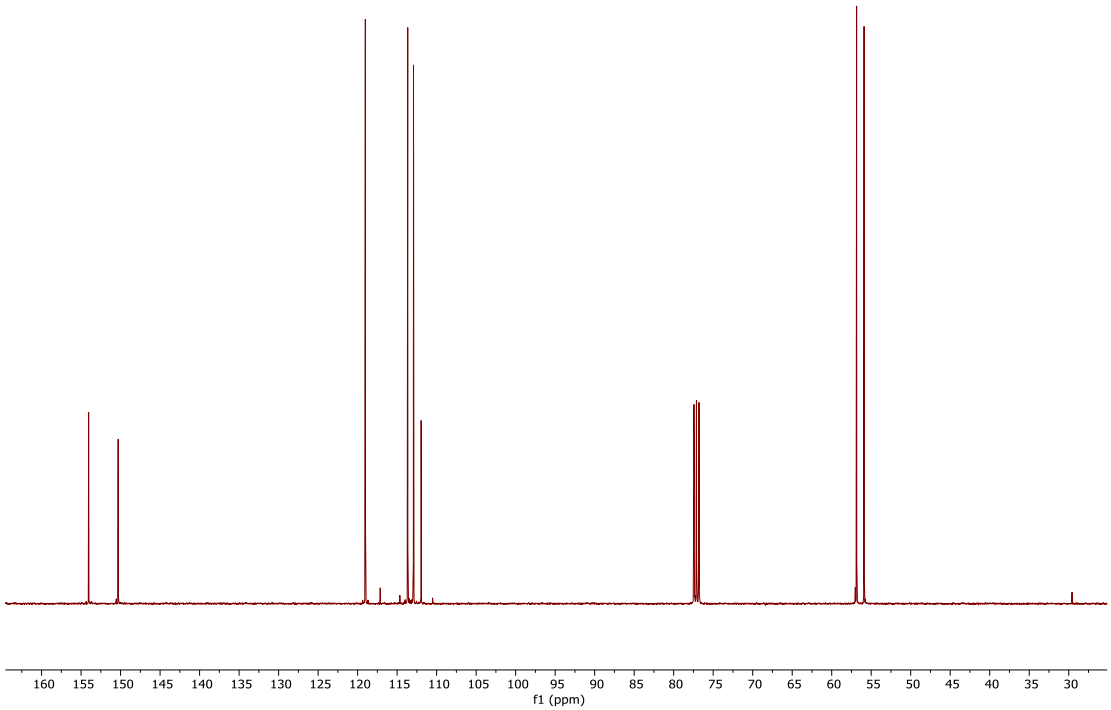

((2,5-dimethoxyphenyl)ethynyl)trimethylsilane (SF-13)

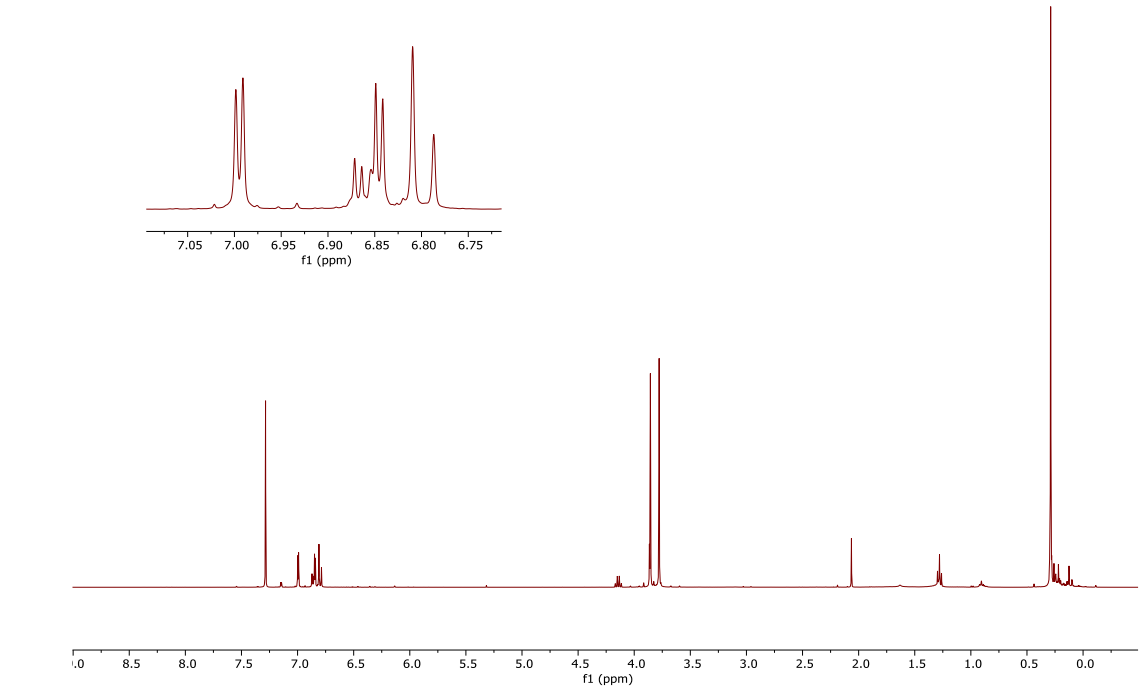

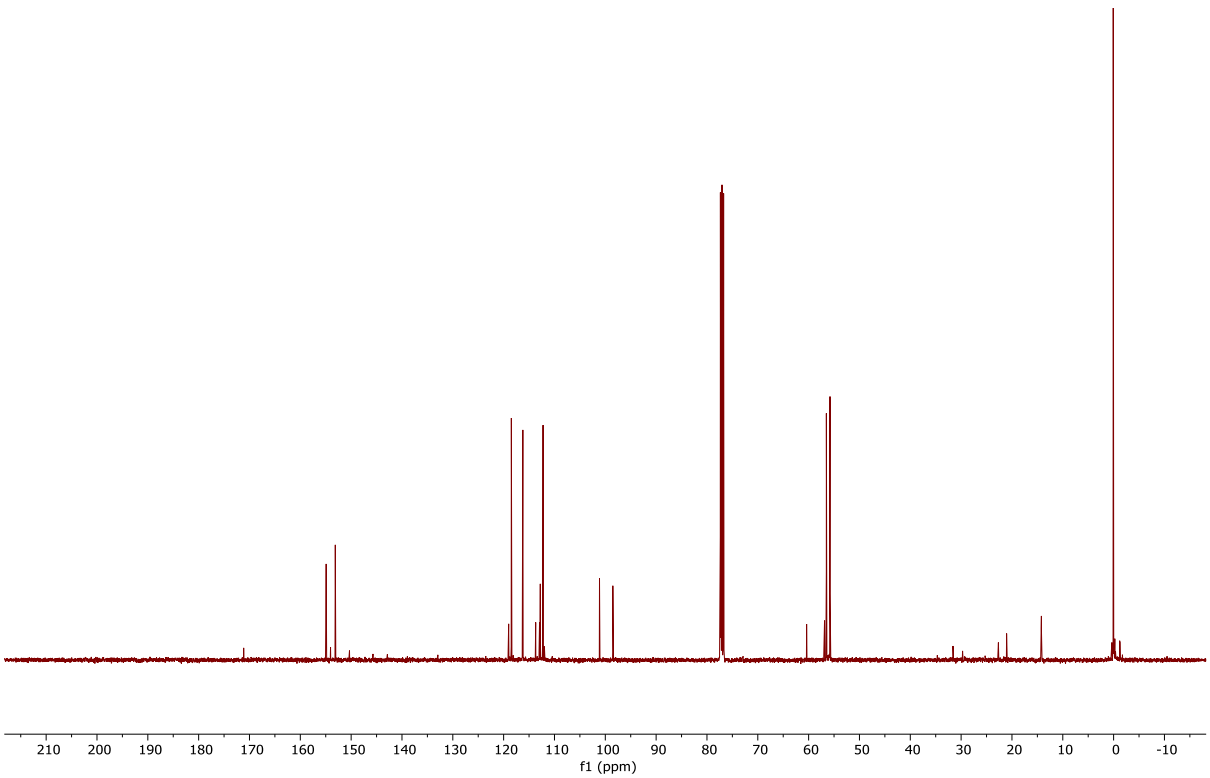

2-ethynyl-1,4-dimethoxybenzene (SF-14)

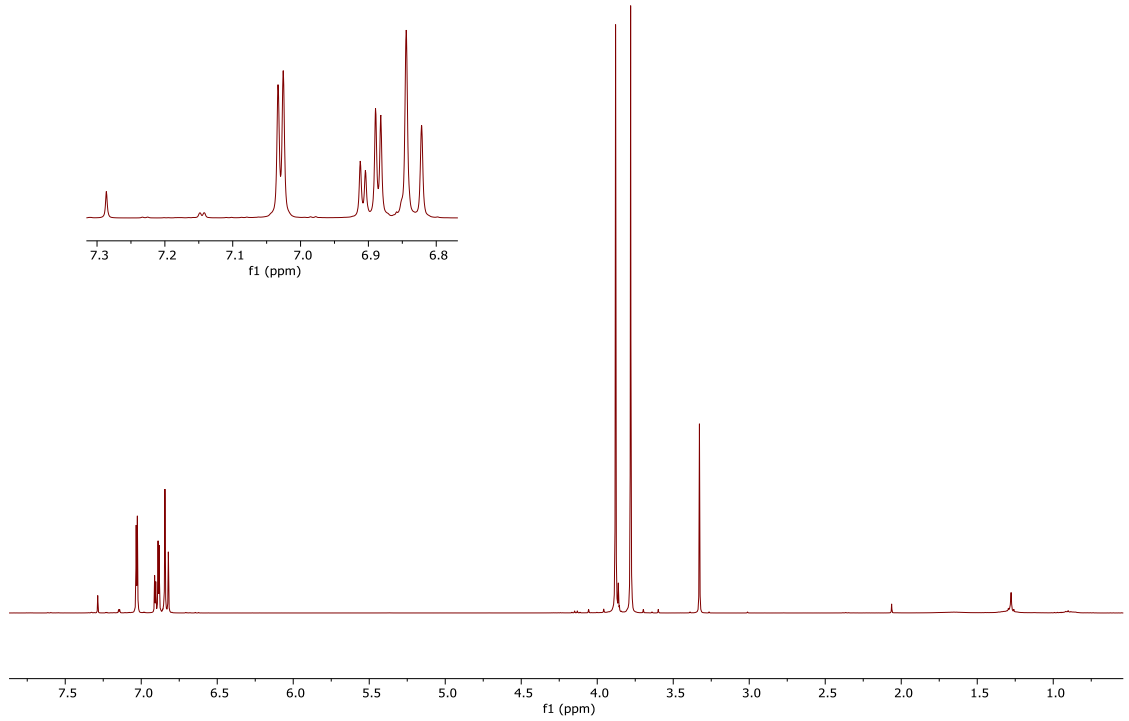

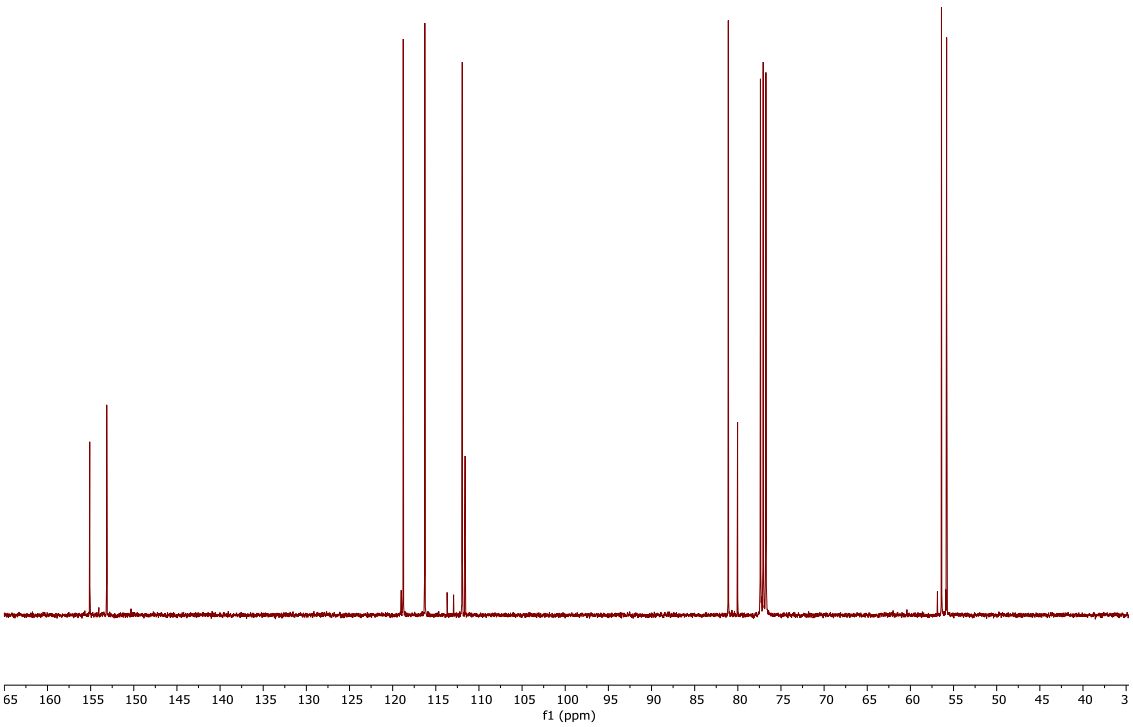

3-(2,5-dimethoxyphenyl)-1,1-diphenylprop-2-yn-1-ol (SF-15)

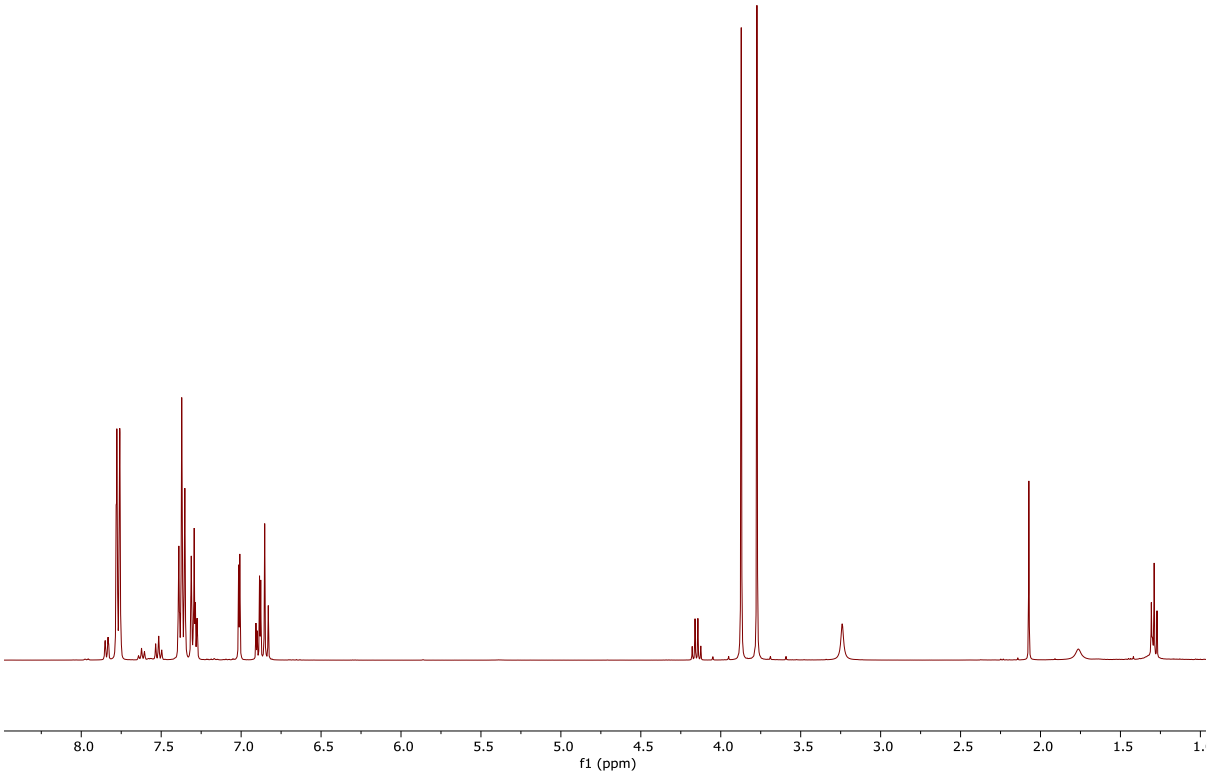

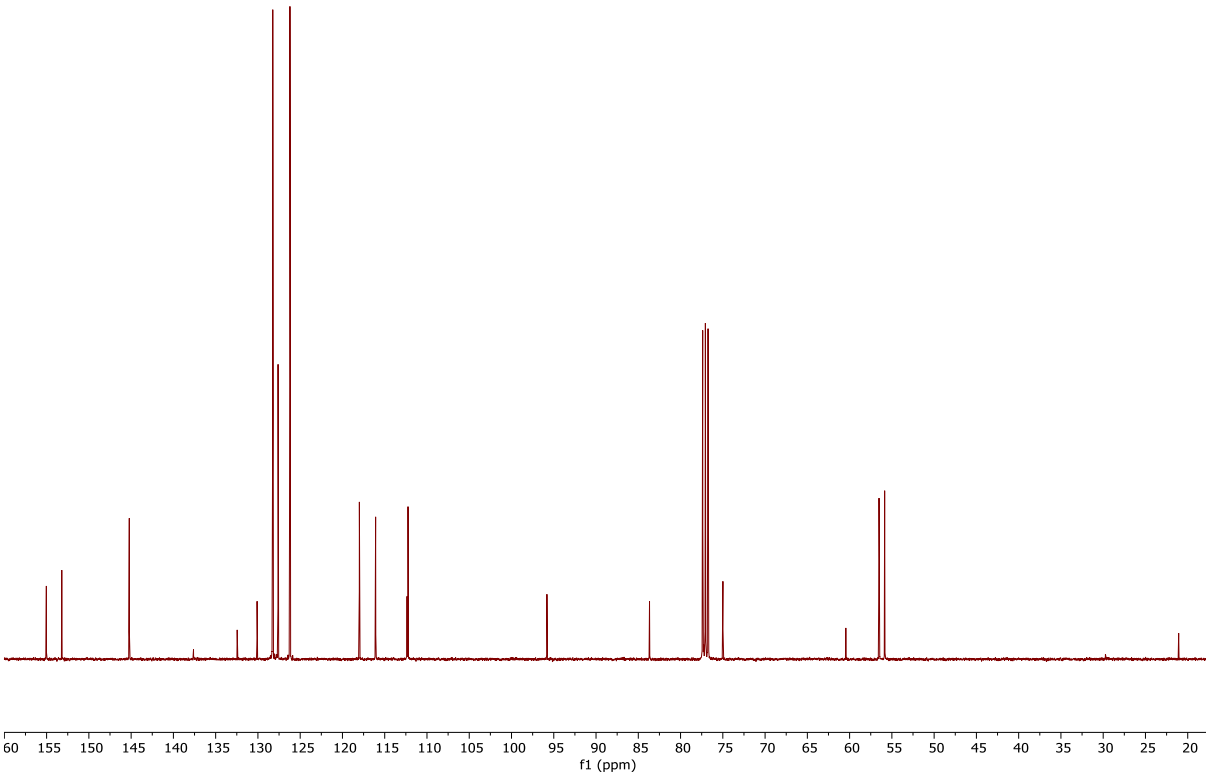

1,1,3-triphenylprop-2-yn-1-ol (SF-17)

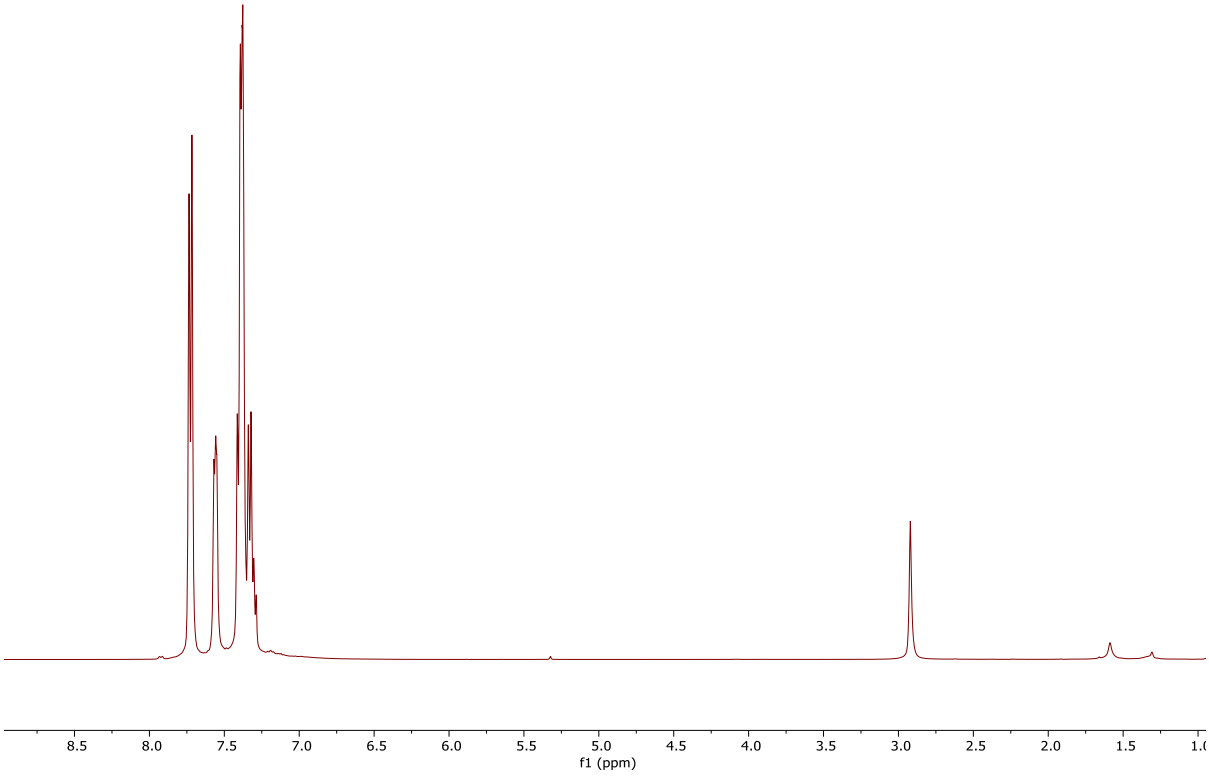
8.5
8.0
7.5
7.0
6.5
6.0
5.5
5.0
4.5
4.0
3.5
3.0
2.5
2.0
1.5
f1 (ppm)

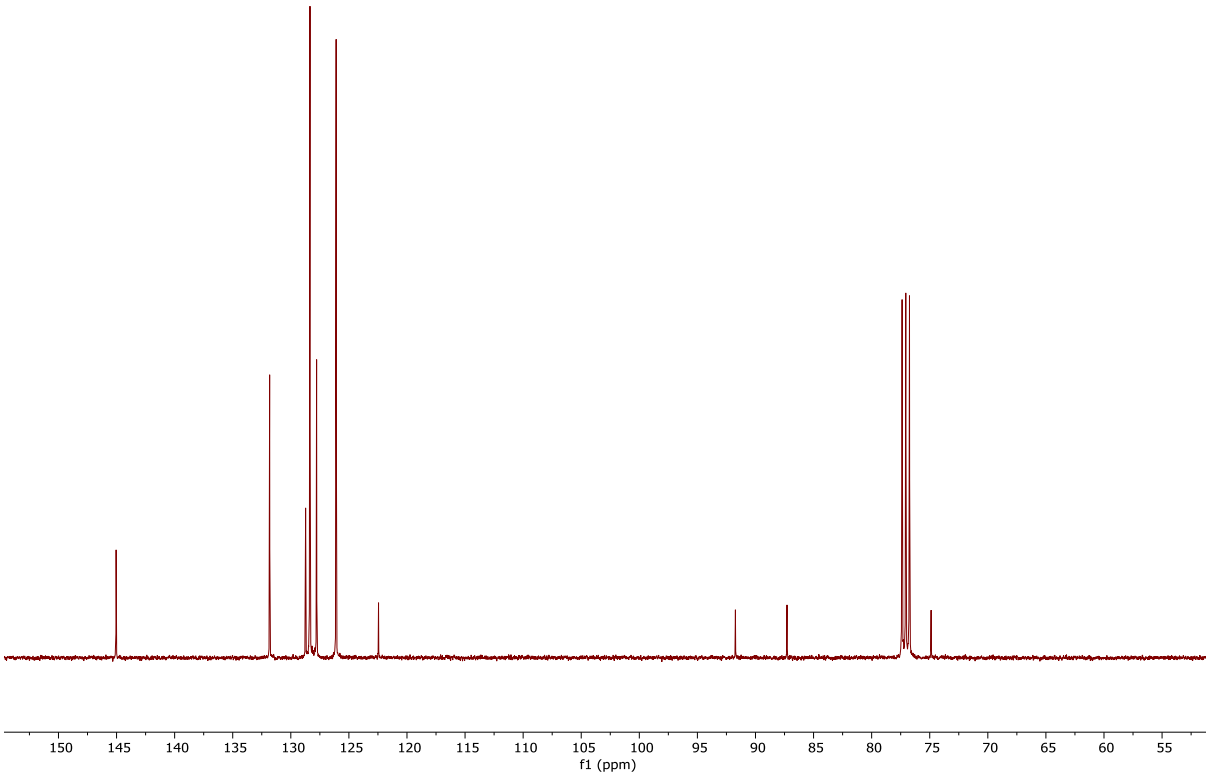
150
145
140
135
130
125
120
115
110
105
100
95
90
85
80
75
70
65
60
55
f1 (ppm)

5,6,11,12-tetraphenyltetracene (SF-18)

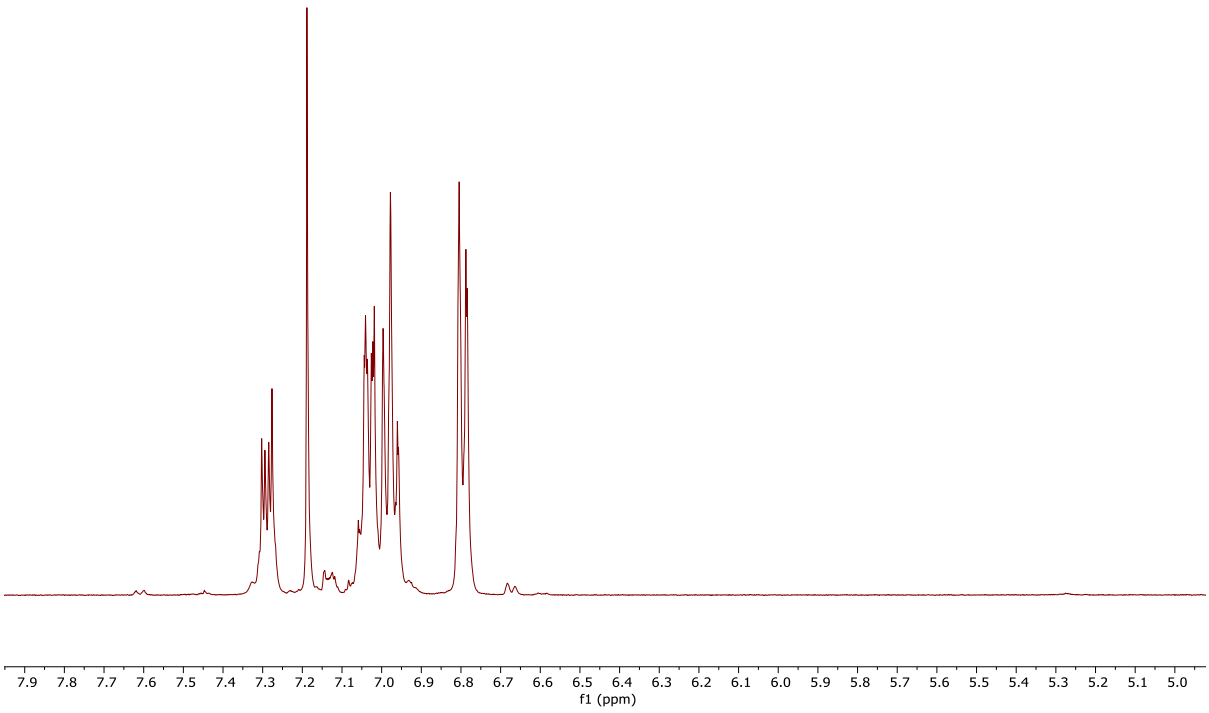

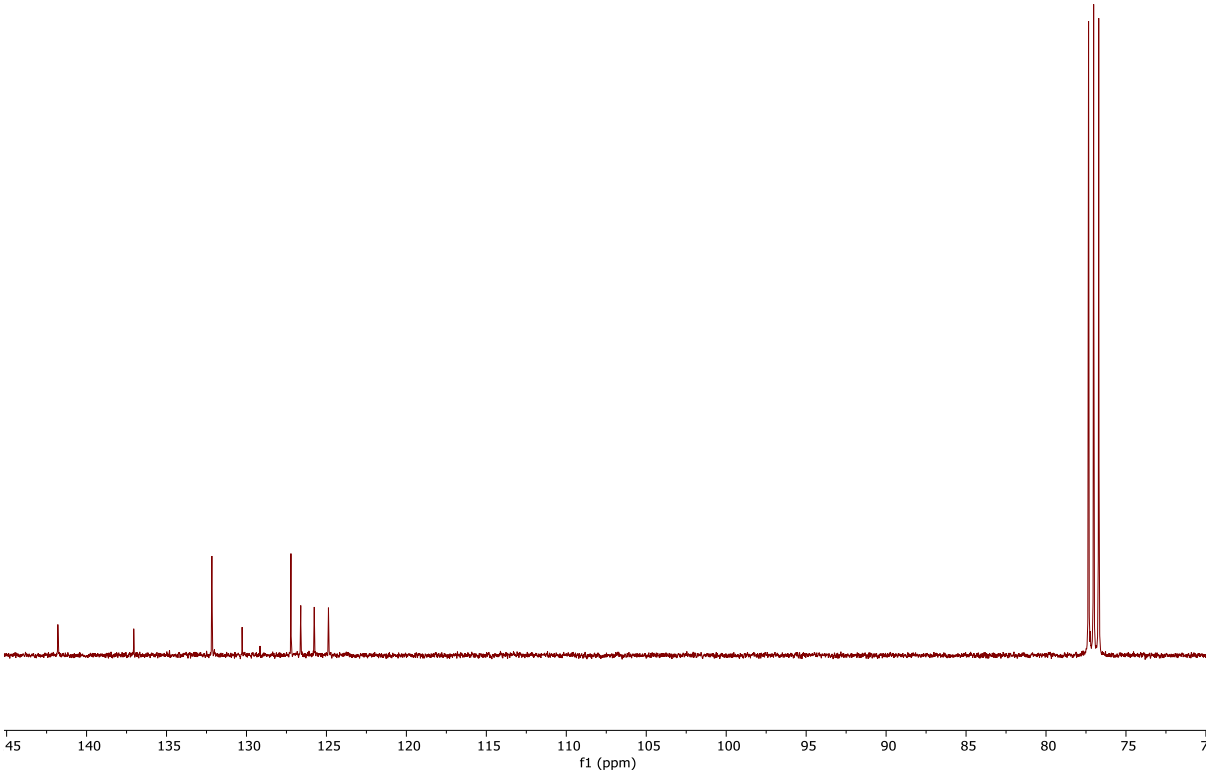

1,4-bis(tetradecyloxy)benzene (SF-27)

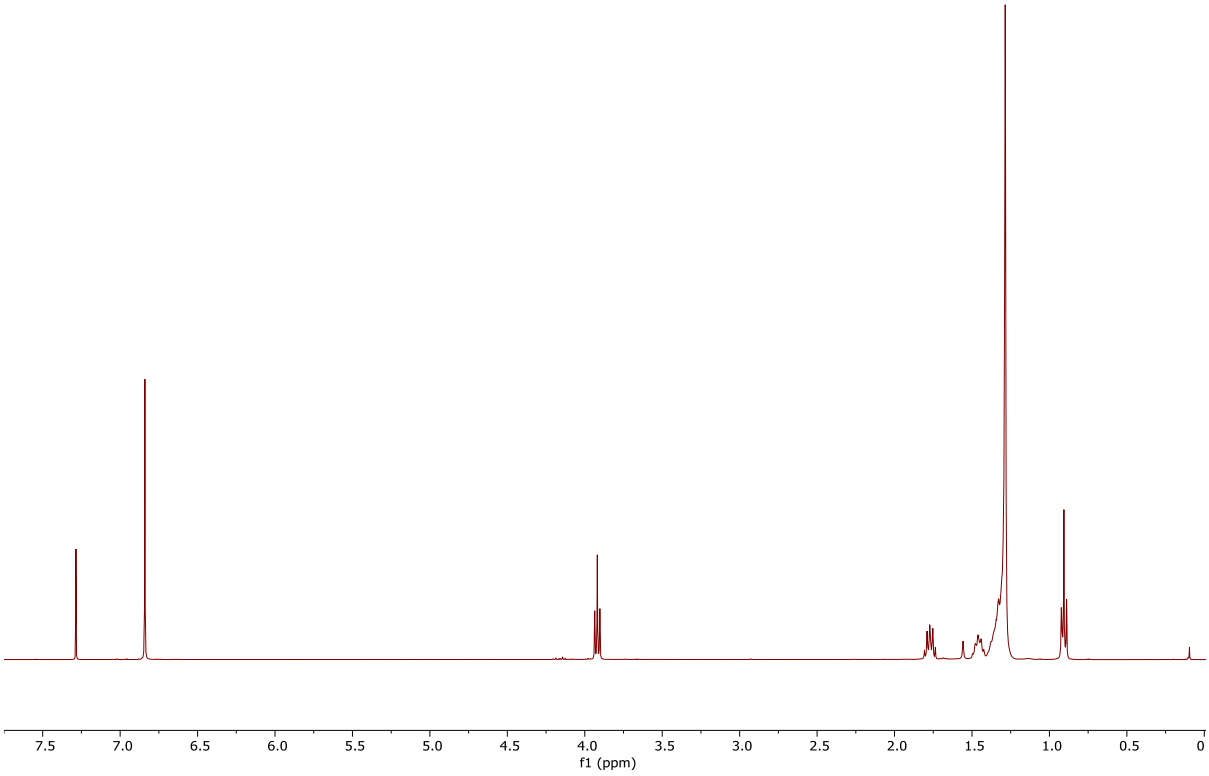
7.5
7.0
6.5
6.0
5.5
5.0
4.5
4.0
3.5
3.0
2.5
2.0
1.5
1.0
0.5
0
f1 (ppm)

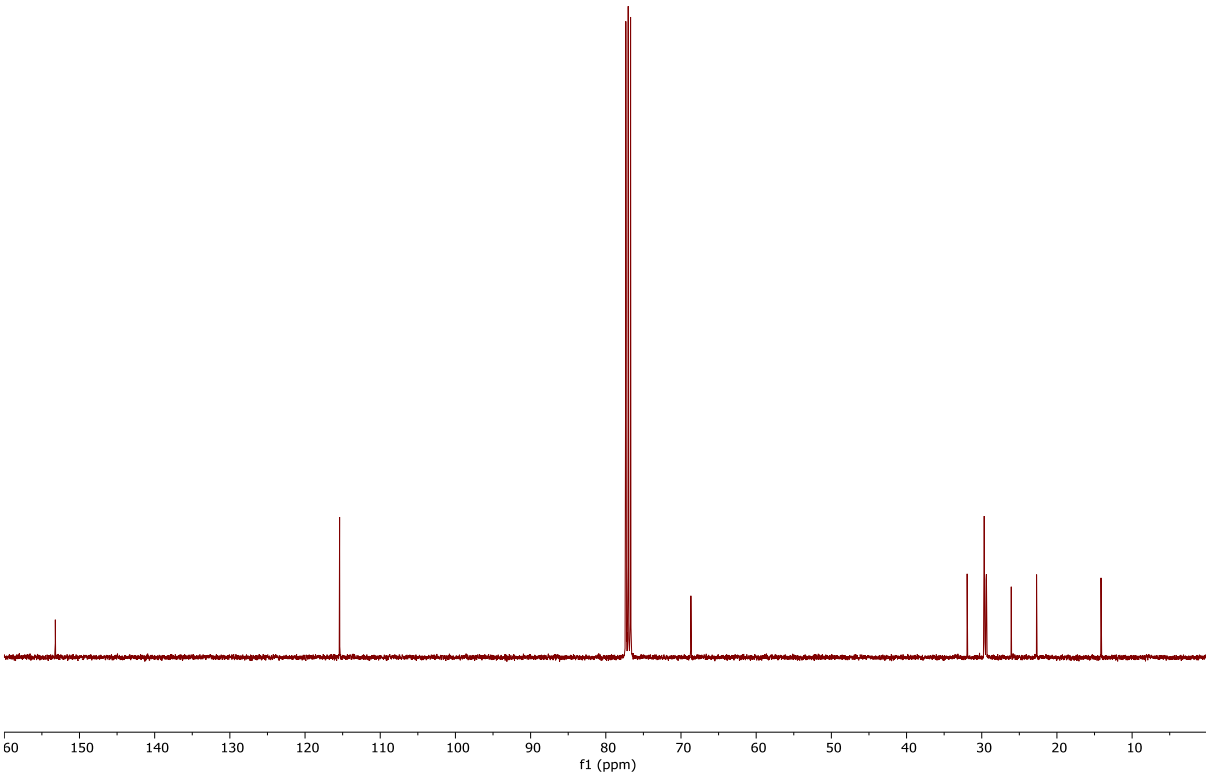
60
150
140
130
120
110
100
90
80
70
60
50
40
30
20
10
f1 (ppm)

1,4-dibromo-2,5-bis(tetradecyloxy)benzene (SF-28)

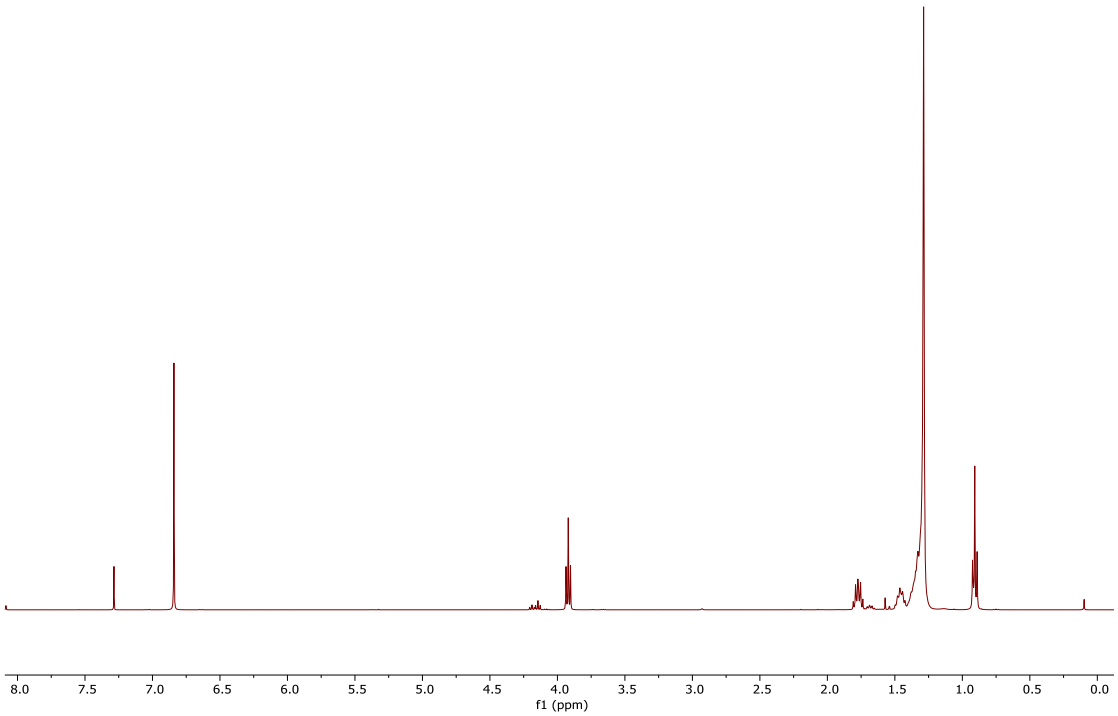

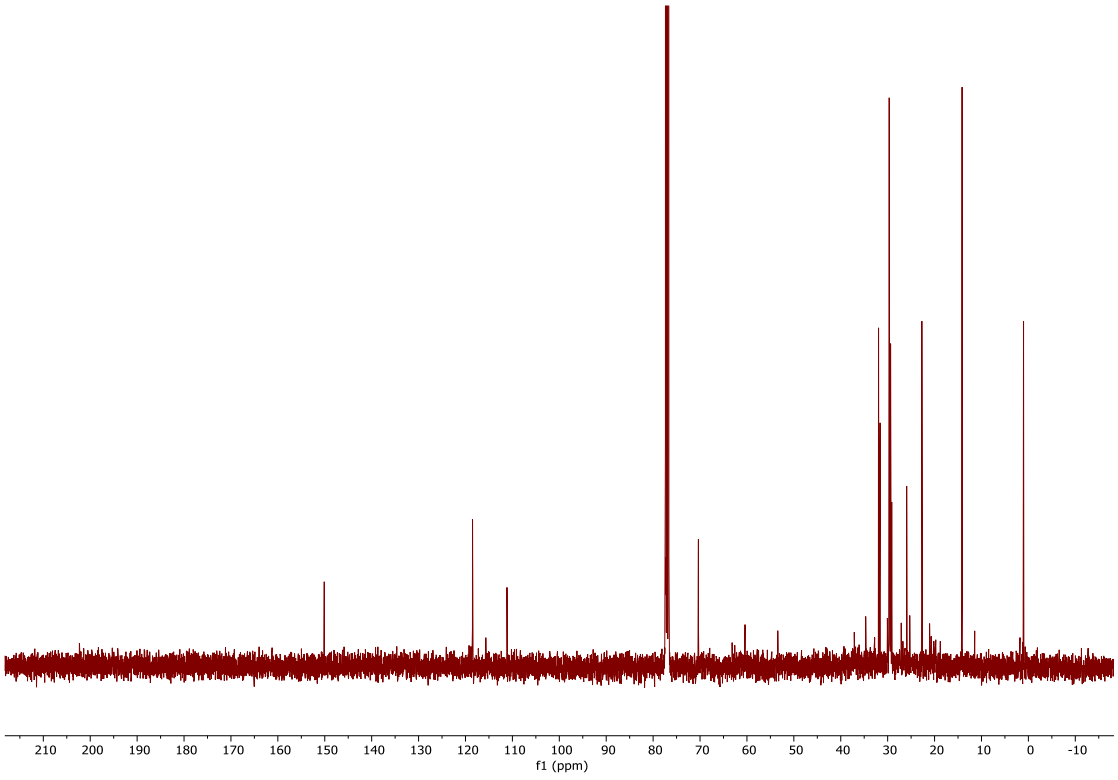

1,4-bis(octyloxy)benzene (SF-29)

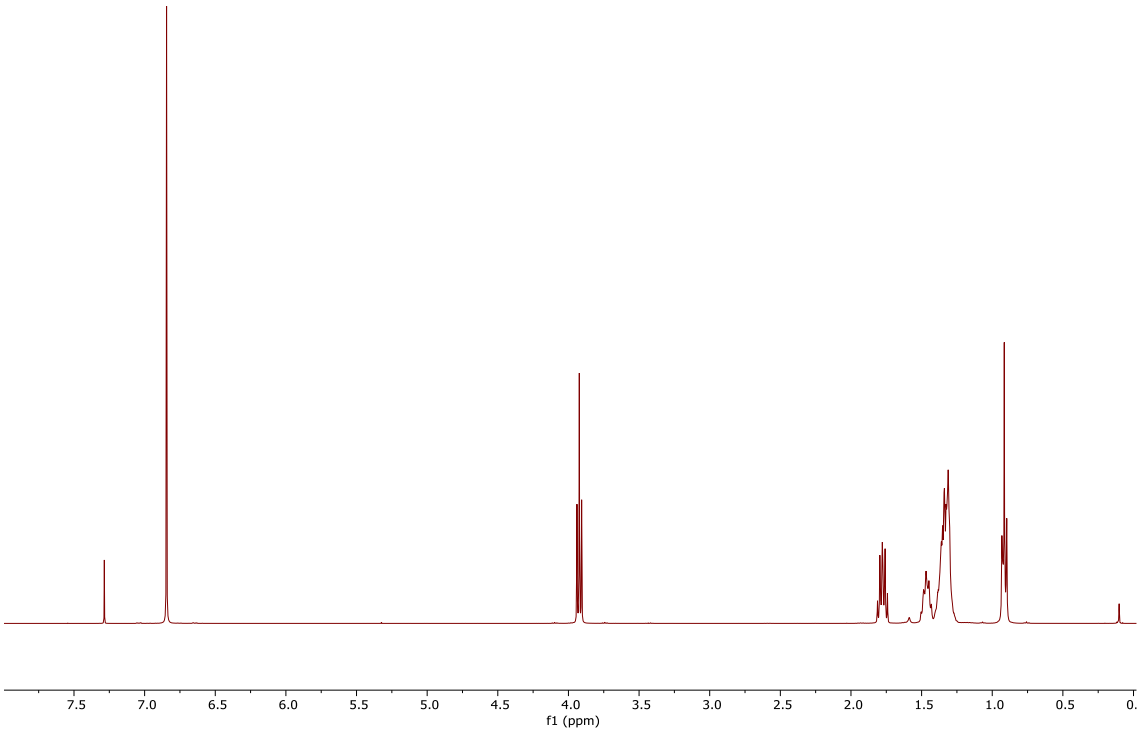

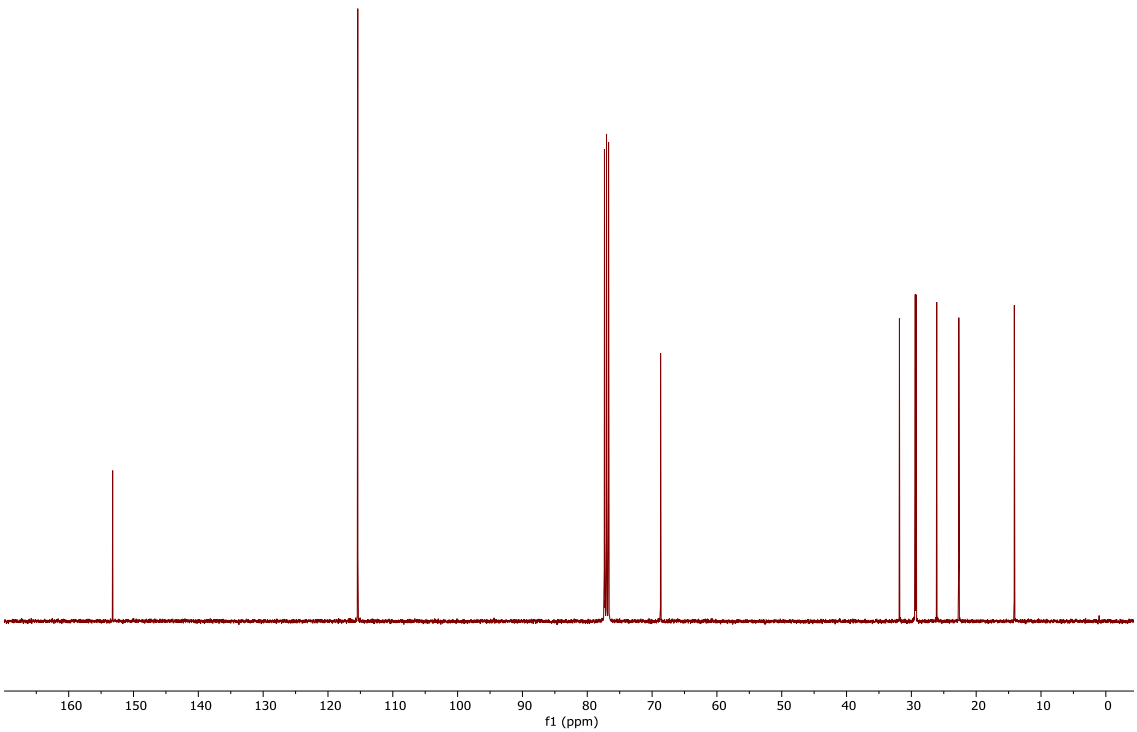

1,4-dibromo-2,5-bis(octyloxy)benzene (SF-30)

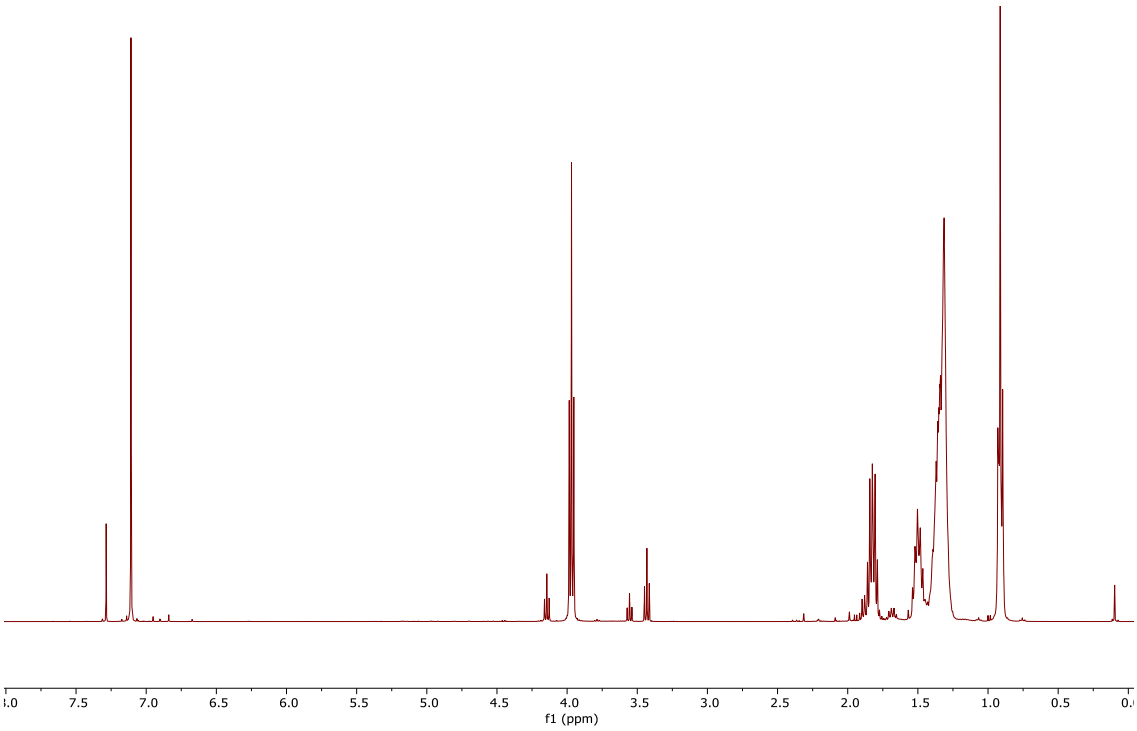

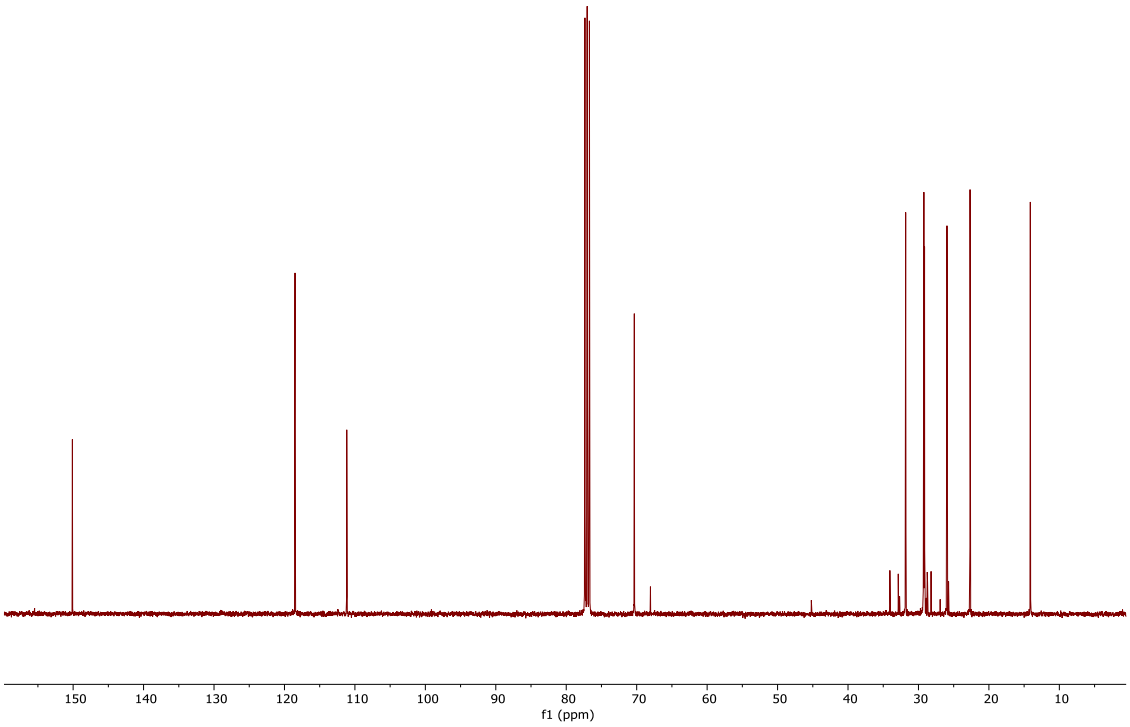

((4-bromo-2,5-bis(octyloxy)phenyl)ethynyl)trimethylsilane (SF-31)

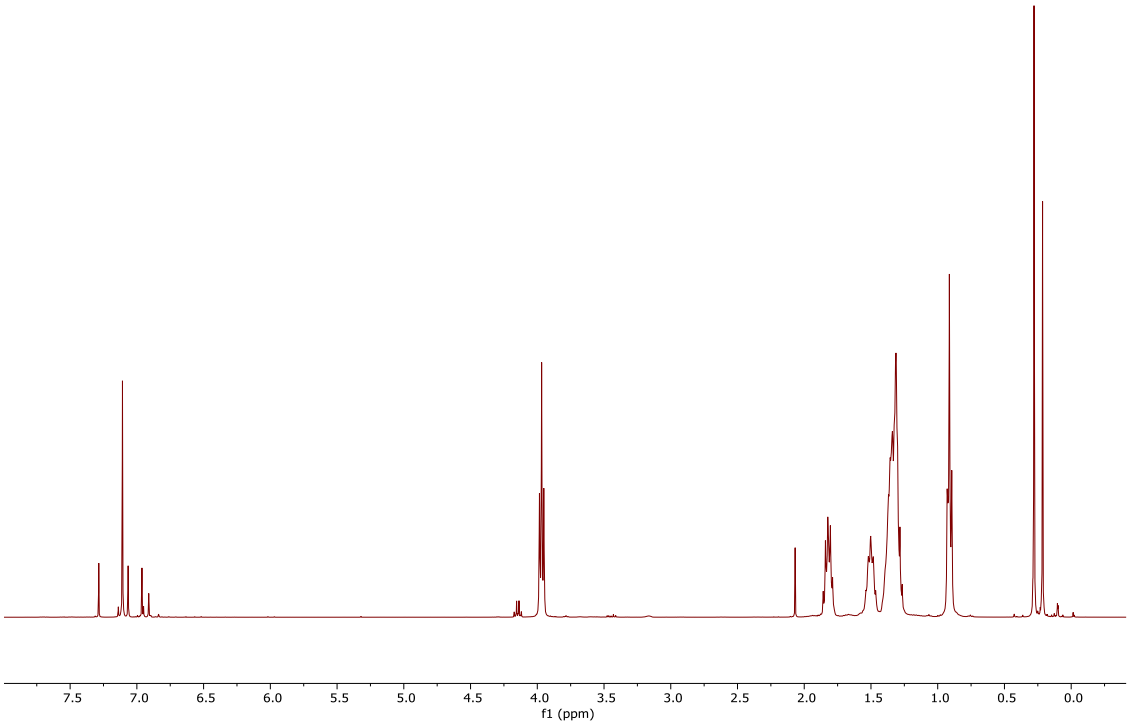

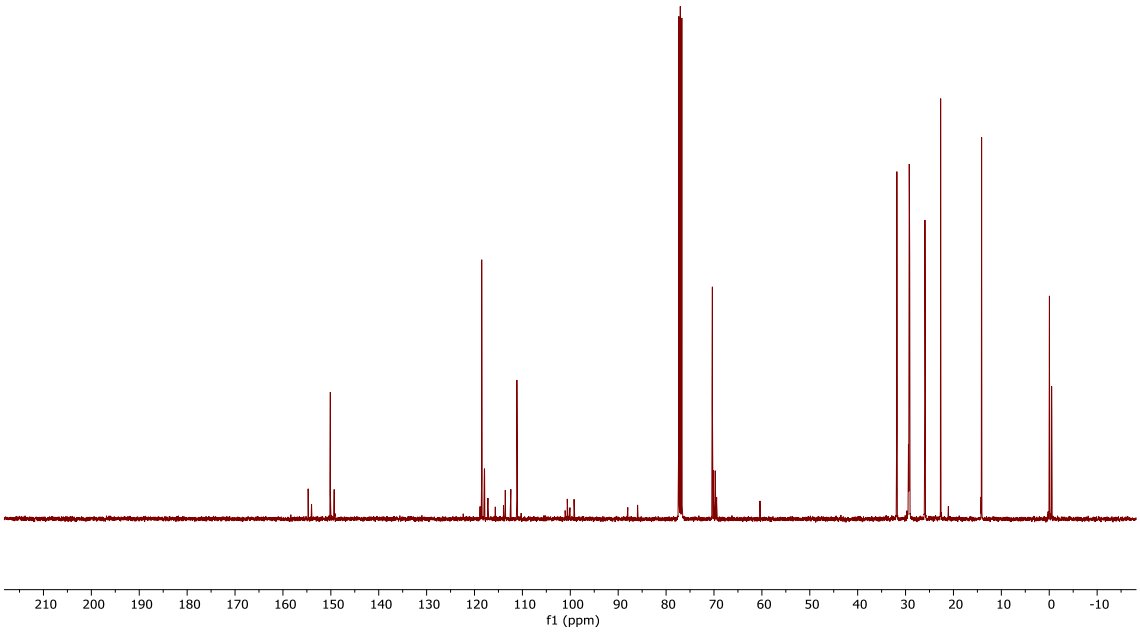

tris(4-bromo-2,5-dimethoxyphenyl)methanol (SF-36)

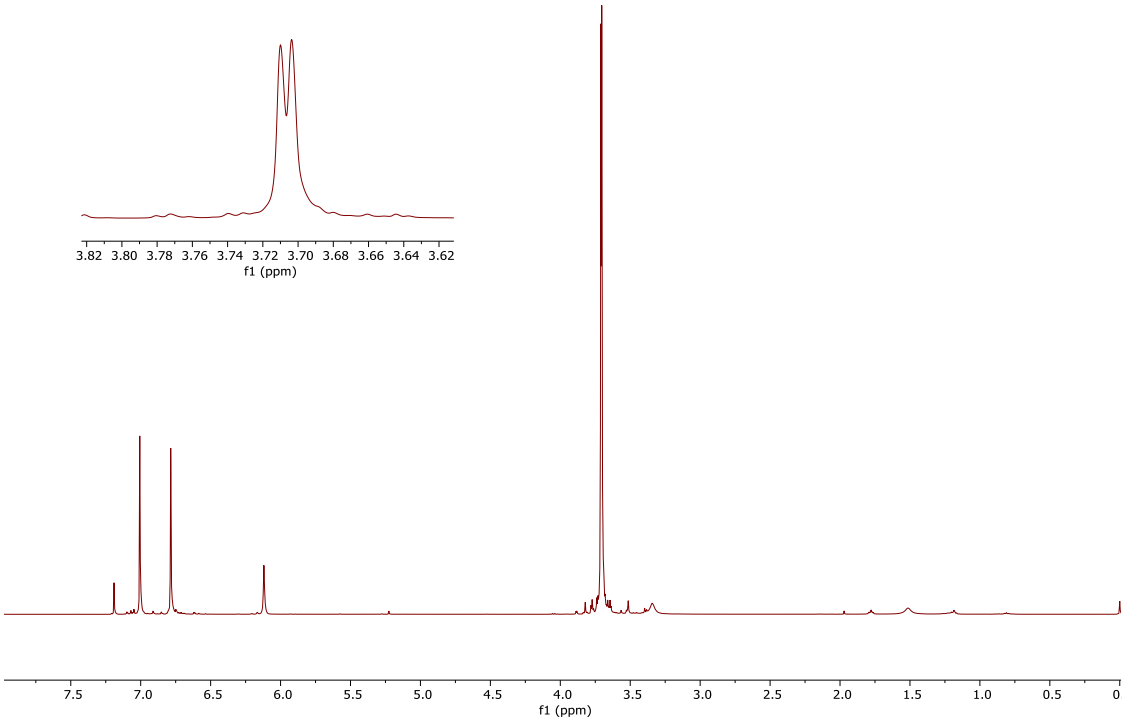

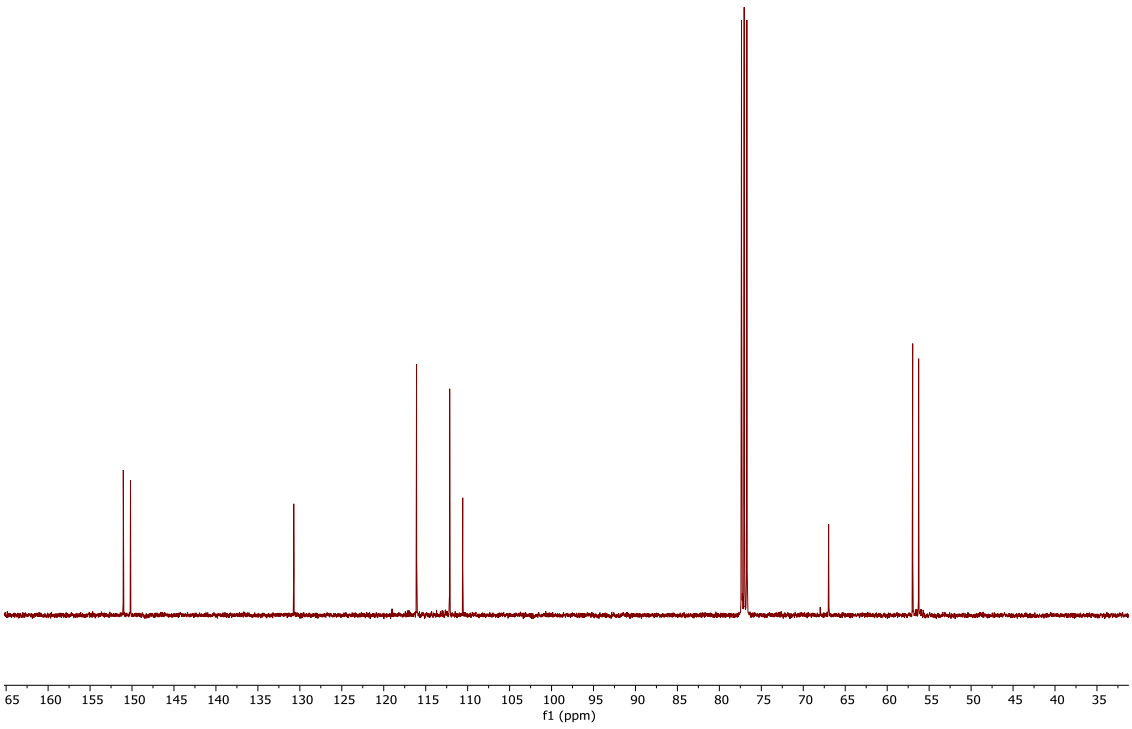

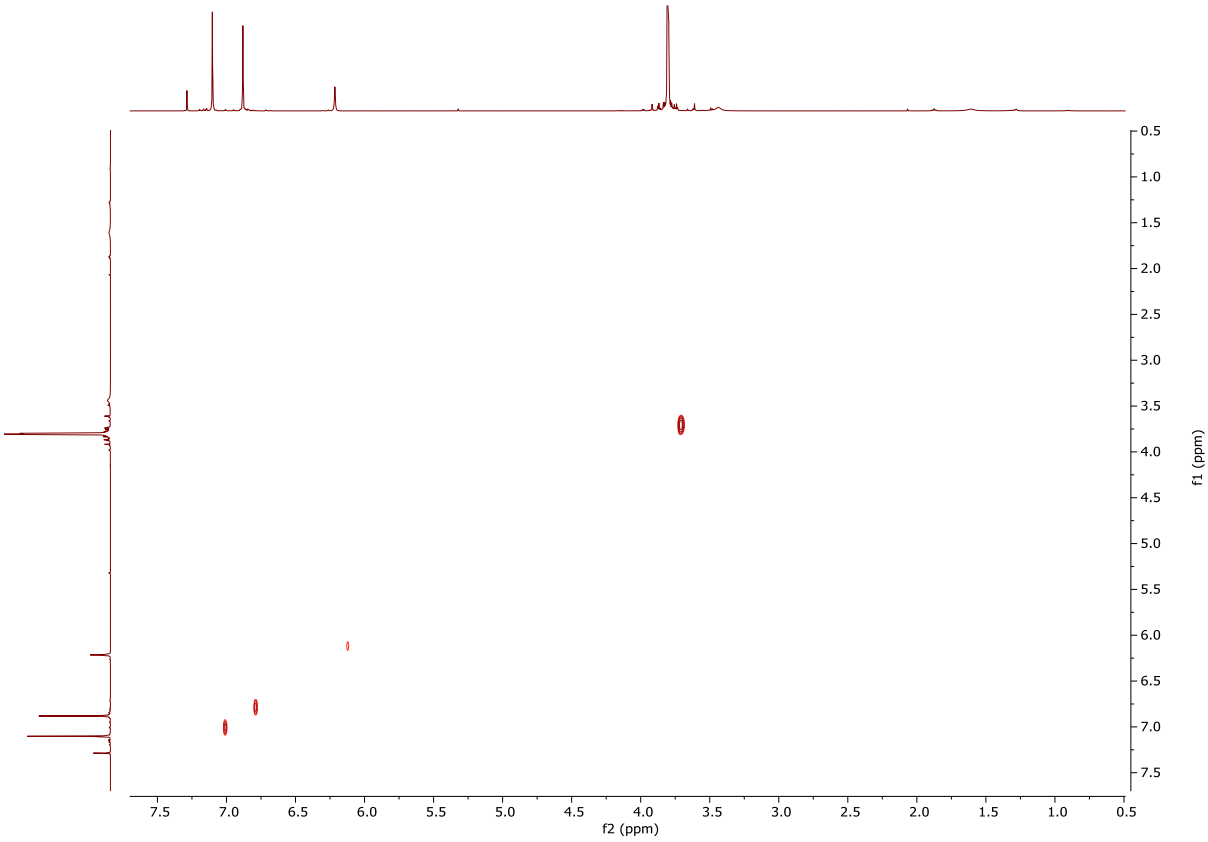
f2 (ppm)
f1 (ppm)

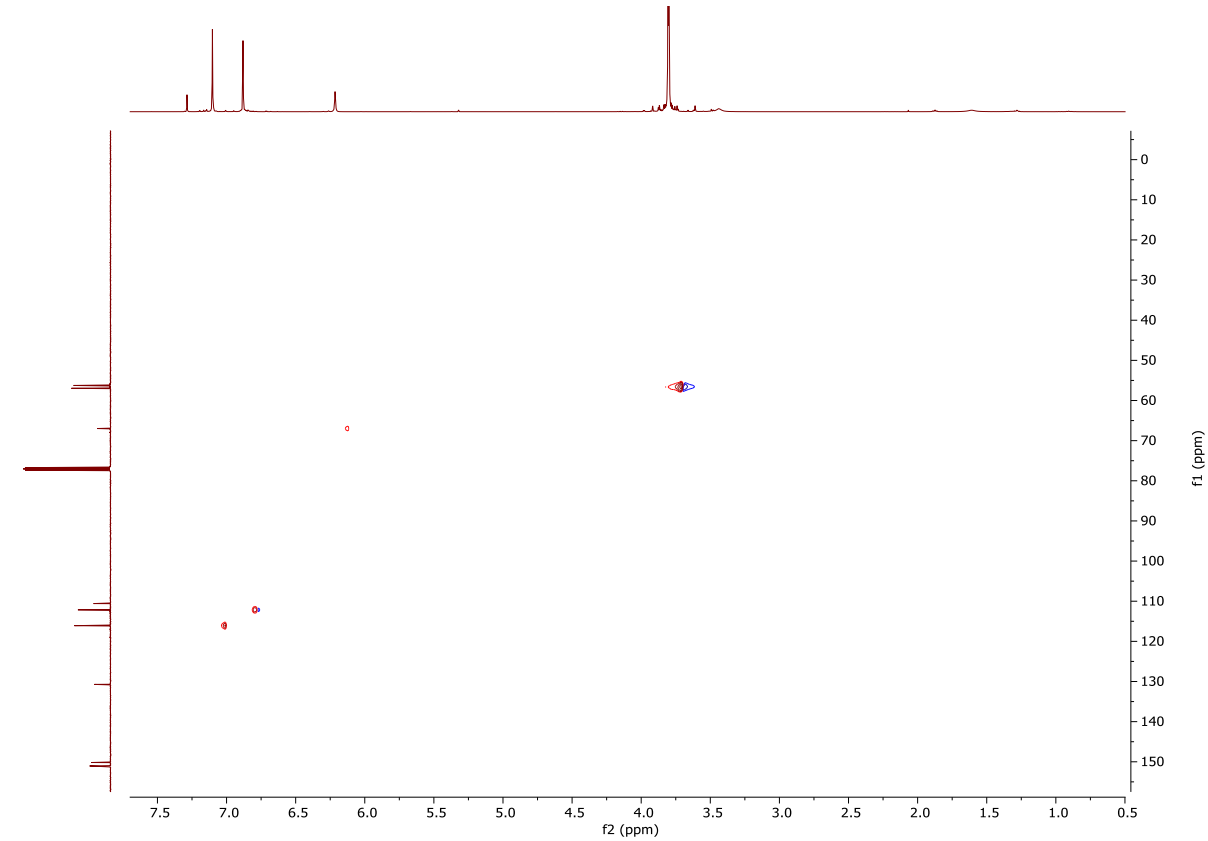
f2 (ppm)
f1 (ppm)

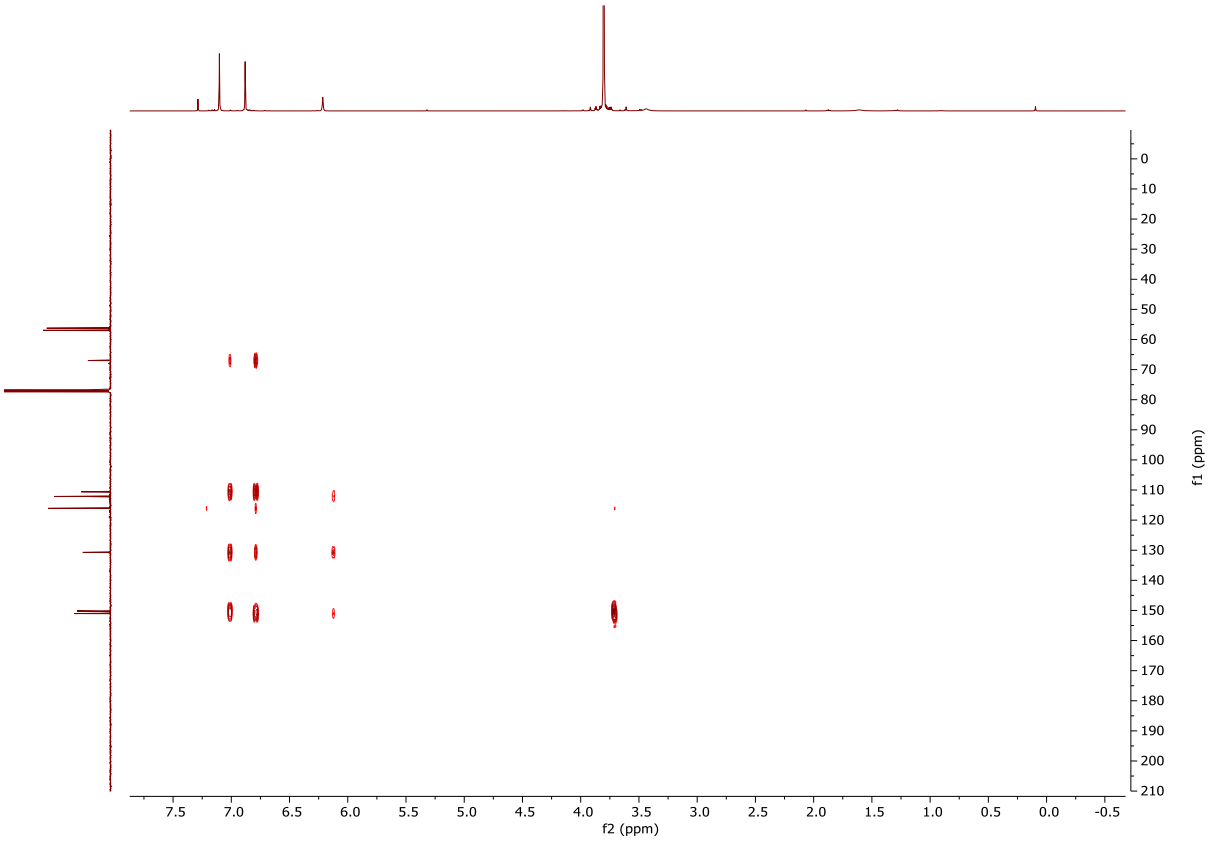

tris(4-bromo-2,5-dimethoxyphenyl)methane (SF-39)

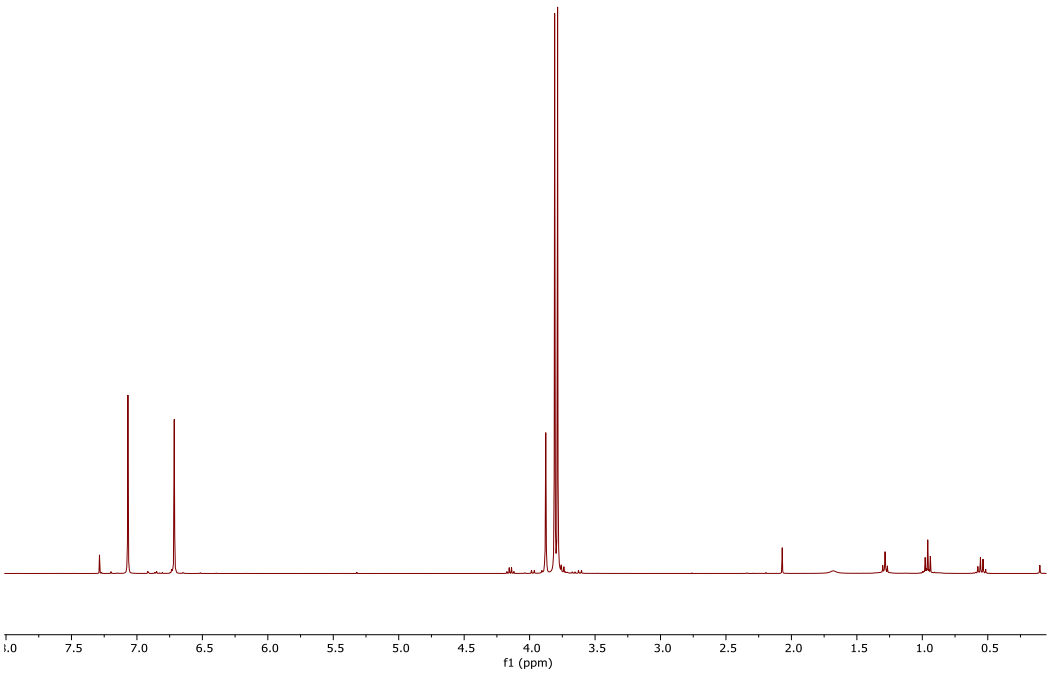

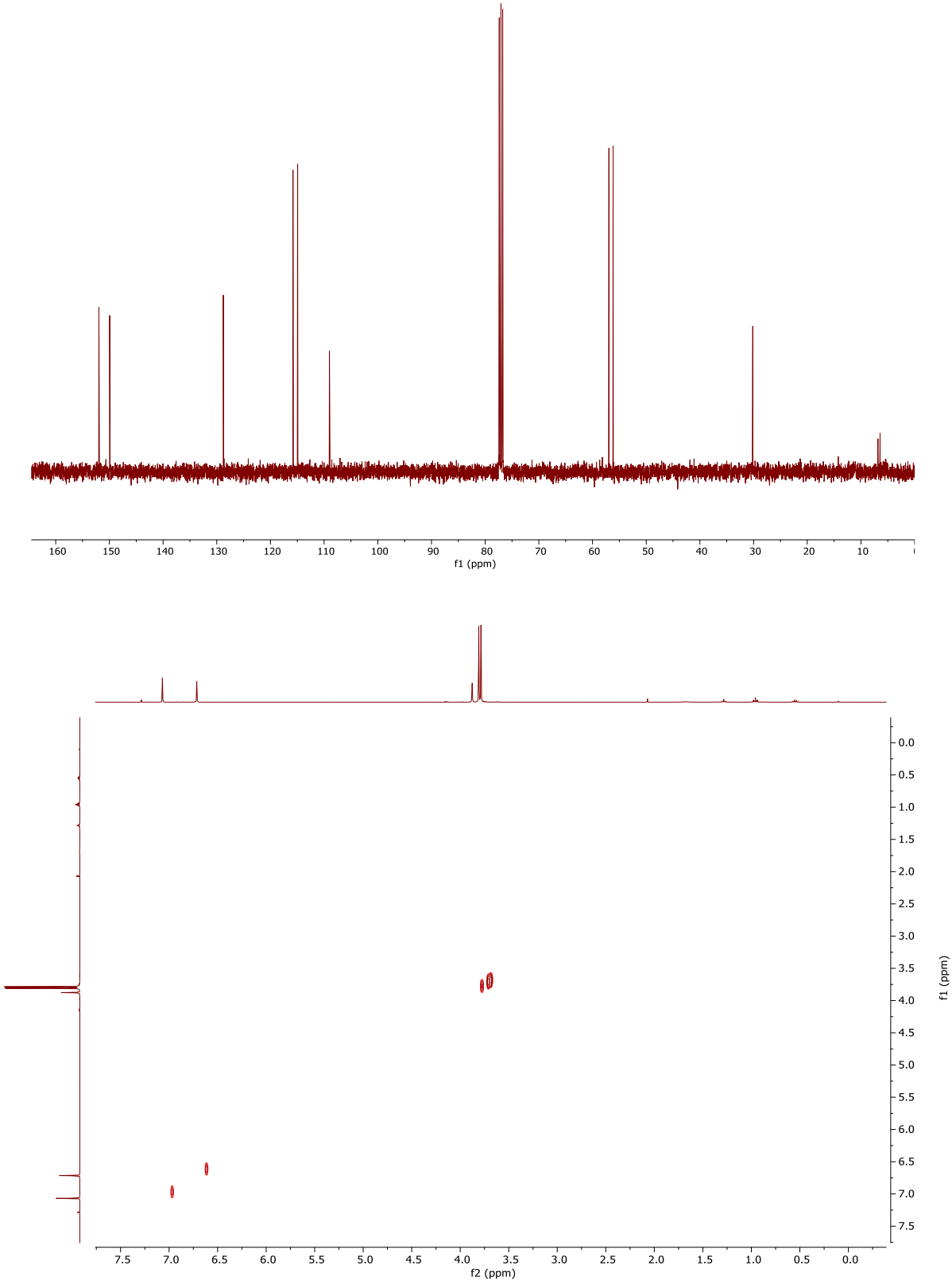
160
150
140
130
120
110
100
90
80
70
60
50
40
30
20
10
f1 (ppm)
7.5
7.0
6.5
6.0
5.5
5.0
4.5
4.0
3.5
3.0
2.5
2.0
1.5
1.0
0.5
0.0
f2 (ppm)
0.0
0.5
1.0
1.5
2.0
2.5
3.0
3.5
4.0
4.5
5.0
5.5
6.0
6.5
7.0
7.5
f1 (ppm)

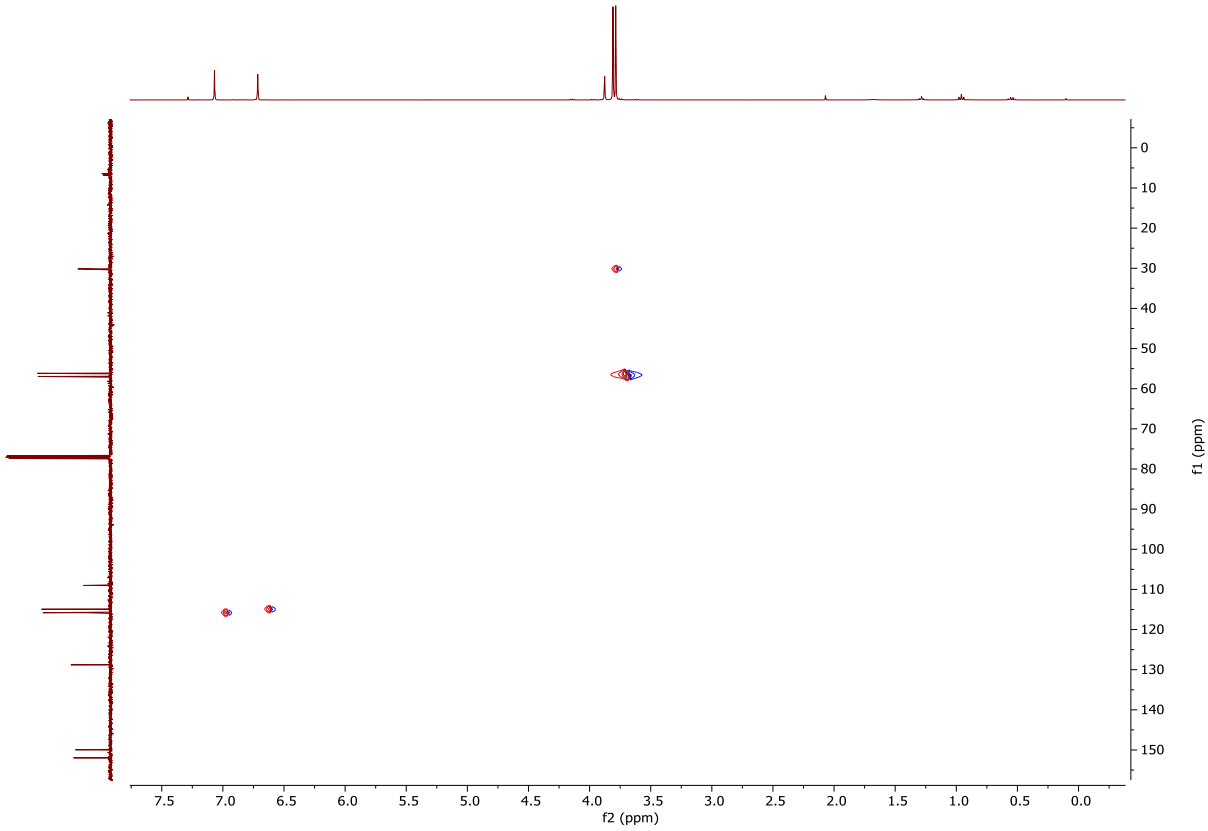
f2 (ppm)
f1 (ppm)

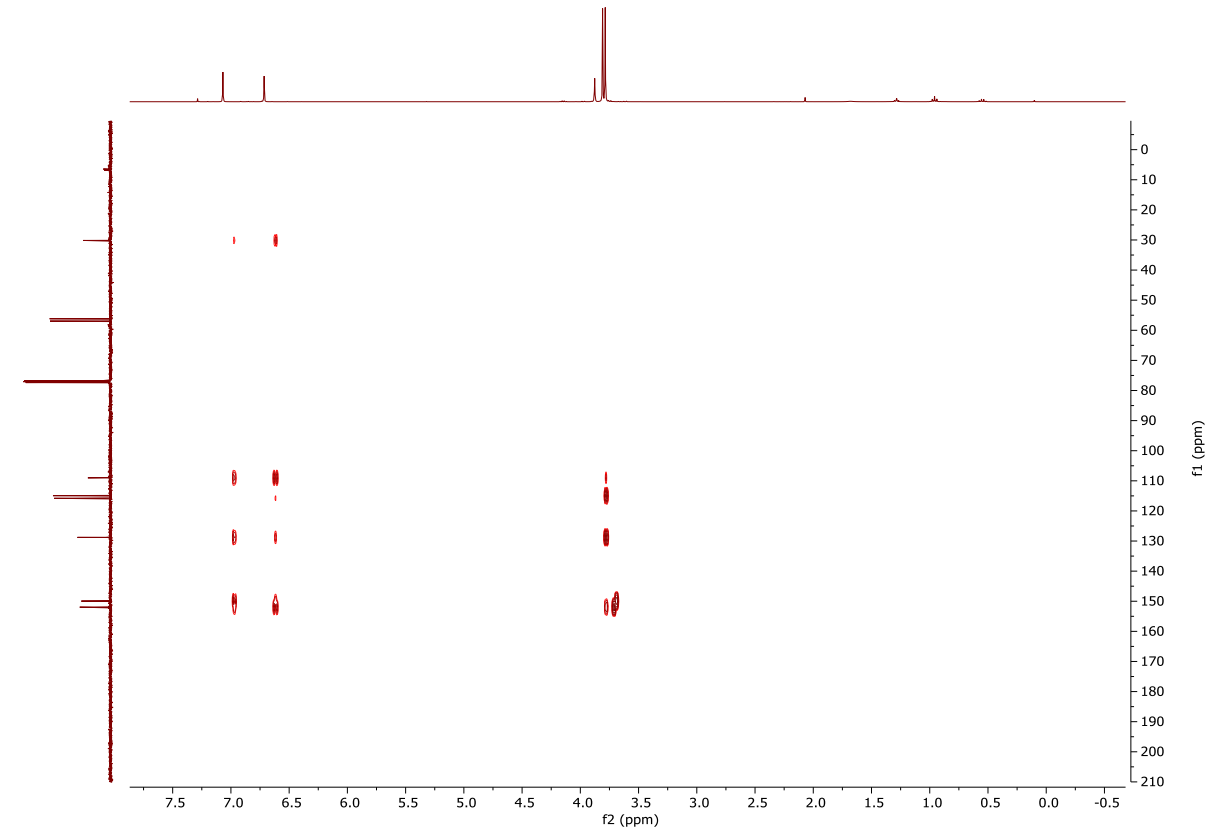
f2 (ppm)
f1 (ppm)

tris(4-bromo-2,5-dimethoxyphenyl)methyl radical (SF-40)